

論文 / 著書情報  
Article / Book Information

題目(和文)	
Title(English)	Design and Synthesis of Thermo-responsive/Photo-reactive Polymers and Their Applications
著者(和文)	PARKSo Jung
Author(English)	So Jung Park
出典(和文)	学位:博士(工学), 学位授与機関:東京工業大学, 報告番号:甲第12110号, 授与年月日:2021年9月24日, 学位の種別:課程博士, 審査員:小畠 英理,金原 数,丸山 厚,堤 浩,三重 正和
Citation(English)	Degree:Doctor (Engineering), Conferring organization: Tokyo Institute of Technology, Report number:甲第12110号, Conferred date:2021/9/24, Degree Type:Course doctor, Examiner:,,,,,
学位種別(和文)	博士論文
Type(English)	Doctoral Thesis

# **Design and Synthesis of Thermo-responsive/Photo-reactive Polymers and Their Applications**

**So Jung Park**

September 2021

# **Design and Synthesis of Thermo-responsive/Photo-Reactive Polymers and Their Applications**

**So Jung Park**

Submitted to the Graduate School of  
Life Science and Technology  
in Partial Fulfillment of the Requirements  
for the Degree of Doctor of Philosophy in  
Engineering

Tokyo Institute of Technology

# Contents

<b>List of abbreviations</b> .....	<b>III</b>
<b>1. General introduction</b> .....	<b>1</b>
1.1 Stimuli responsive polymers .....	2
1.2 Thermo-responsive polymers .....	4
1.2.1 Properties and mechanism of thermo-responsive polymers .....	4
1.2.2 Application: Thermo-responsive system for in-situ hydrogels .....	8
1.3 Photo reactive polymers .....	10
1.3.1 Properties and mechanism of photo reactive polymers .....	10
1.3.2 Application: Photo reactive polymers for antifouling surface .....	12
1.4 Motivation, Objective, and Outline of Study .....	15
1.4.1 Motivation .....	15
1.4.2 Objective and outline .....	17
1.5 References .....	18
<b>2. Thermally induced switch for in-situ gelation using morphological change of thermo-responsive polymer</b> .....	<b>25</b>
2.1 Introduction .....	25
2.2 Materials and methods .....	28
2.2.1 Materials .....	28
2.2.2 Instrumentation .....	29
2.2.3 Synthesis of PBzMA .....	29
2.2.4 Synthesis of diblock copolymers .....	29
2.2.5 Terminal conversion of TR diblock copolymers .....	31
2.2.6 Terminal conversion of PBzMA- <i>b</i> -P(NAS- <i>co</i> -DMAAm) .....	31
2.2.7 Reactivity and stability of the succinimide group on PBzMA- <i>b</i> -P(NAS- <i>co</i> -DMAAm) .....	31
2.2.8 Preparation and characterization of polymeric micelles .....	32
2.2.9 Observation of fluidity change of solution by temperature change .....	34
2.2.10 Rheological measurement .....	34
2.3 Results and discussion .....	35
2.3.1. Characterization of diblock copolymers .....	35
2.3.2. Characterization of nanoparticle .....	41
2.3.3. Thermo-responsive hydrogel formation .....	50

2.4 Conclusions .....	63
2.5 Reference .....	64
<b>3. Photo reactive polymers: PEG-based azide polymer for surface modification .....</b>	<b>67</b>
3.1 Introduction .....	67
3.2. Materials and methods .....	69
3.2.1 Materials .....	69
3.2.2 Instrumentation .....	70
3.2.3 Synthesis of 4-(hydroxymethyl)azidobenzene .....	70
3.2.4 Synthesis of 4-(glycidyloxymethyl)azidobenzene (AzPheEO) .....	70
3.2.5 Polymerization of AzPheEO with ethylene oxide .....	71
3.2.6 Photo-immobilization .....	72
3.2.7 Cell culturing .....	73
3.2.8 Protein adsorption .....	73
3.3 Results and discussion .....	73
3.3.1 Characterization of the photo reactive AzPheEO monomers .....	73
3.3.2 Characterizing AzPEG polymers .....	76
3.3.3 Protein adsorption .....	86
3.3.4 Cell adhesion .....	88
3.4 Conclusions .....	97
3.5 References .....	98
<b>4. Conclusions and future perspective .....</b>	<b>101</b>
4.1 Conclusions .....	101
4.2 Future perspective .....	103
<b>List of publications .....</b>	<b>106</b>
<b>Acknowledgements .....</b>	<b>107</b>

## List of abbreviations

AzPheEO	4-(Glycidyloxymethyl)azidobenzene
AzPEG	Poly(4-azidobenzyl glycidyl ether-co-ethylene oxide)
AIBN	2,2'-Azobisisobutyronitrile
BzMA	Benzyl methacrylate
CPDT	2-Cyano-2-propyl dodecyl trithiocarbonate
DMF	N,N-Dimethylformamide
DLS	Dynamic light scattering
DMAAm	N,N-Dimethylacrylamide
FTIR	Fourier transform infrared
GPC	Gel permeation chromatography
i-Bu <sub>3</sub> Al	Triisobutylaluminium
LCST	Lower critical solution temperature
[MePPh <sub>3</sub> ] <sup>+</sup> Br <sup>-</sup>	Methyltriphenylphosphonium bromide
NAS	N-Succinimidyl acrylate
NIPAAm	N-Isopropylacrylamide
NAPMAAm	N-(3-Aminopropyl) methacrylamide hydrochloride
<sup>1</sup> H NMR	Proton nuclear magnetic resonance
PAA	Polyallylamine
PEG	Poly(ethylene glycol)
PNIPAAm	Poly(N-isopropylacrylamide)
RAFT	Reversible addition fragmentation chain transfer
TABA	Tetrabutylammonium bromide
TR	Thermo-responsive
TCEP	Tris(2-carboxyethyl) phosphine hydrochloride
TEM	Transmission electron microscope
THF	Tetrahydrofuran
UCST	Upper critical solution temperature

---

## Chapter 1

### 1. General introduction

---

Polymers have been playing an important role existing as versatile forms from daily use to high-tech materials and given a great impact on individual lives and our society. Products around you including water bottles, plastic bags, toys, electric cables, automobile, and electronic parts are all made from polymer. Now it is hard to imagine life without it since they have been involving with in form of natural and synthetic polymers. Approximately 80 % of the organic chemical industry is devoted to a production of synthetic polymers and we have taken a lot of advantages of versatility of it in diverse forms of such plastic, textile, resins, oils, and rubbers. Since the first synthetic polymer has been appeared, many pioneer researchers have made groundbreaking advances in polymer chemistry and broaden their applications across interdisciplinary of fields. Conventional polymer is still used a lot in our life and contributed to improve quality of life. With development of modern technology towards smart and intelligent, special functions are required in certain fields, and conventional polymer is not able to serve its full needs there by leading to development of novel polymer. Along with the recent demands and based on the foundational research, a new class of polymers is appeared, called *stimuli-responsive polymer*, which respond to environmental changes and alter their physical and/or chemical properties. These polymers referred to *smart polymers* or *intelligent polymers* as well.

## 1.1 Stimuli responsive polymers

Stimuli responsive polymers have been attracting increasing interest because of their adaptive behavior in response to variations in their surrounding environment. They show a dramatic change in their physical and/or chemical properties upon exposure to external stimuli, which is a unique and interesting property that allows them to be applied in smart and intelligent responsive materials.

In general, stimuli can be classified into three categories: physical, chemical, and biological. Physical stimuli usually alter chain dynamics and include temperature, light, ionic strength, magnetic stress, mechanical stress, and ultrasound. Chemical stimuli such as pH and ionic strength modulate molecular interactions. Some examples of biological stimuli include enzymes, ligands, and receptors.

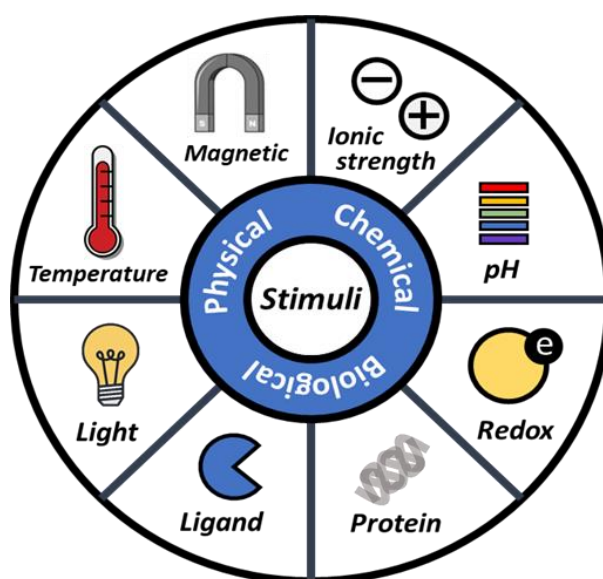


**Figure 1.1** Classification of stimuli based on physical, chemical, and biological triggers

Polymers respond sharply to a given stimulus and this unique properties were used to develop intelligent system.<sup>1</sup> Some polymers can even respond to more than one stimulus, which can be utilized in the development of dual-responsive<sup>2</sup> or multi-responsive system.<sup>3</sup> Some researchers have been reported that simultaneous responsiveness can be accurately and delicately achieved



in complex environments, such as under the physiological condition of human body.<sup>4, 5</sup> Recently, the stimuli-responsive polymers have been attracting increasing interest because they can be used in designing highly sensitive materials and devices for application in complicated systems and technologies.<sup>6-8</sup> The response of stimuli-responsive polymer is sensitive enough to be used for controlling a reaction or the reactivity of a material.<sup>9</sup> Several studies have been reported that the stimuli responsive polymer can be applied to control a drug release reaction<sup>10</sup> or electrostatic interactions.<sup>11</sup> For a chemical reaction to proceed at a reasonable rate, the temperature of the system must be sufficiently high to initiate the reaction or to overcome the energy barrier (i.e., the activation energy). It may be difficult to precisely control the reaction only using 1–2 °C difference. However, thermo-responsive (TR) polymers can respond to thermal stimuli in narrow temperature ranges (within 1–2 °C).<sup>10</sup> When it is reached to the critical solution temperature, polymers show a drastic change in property, altering a hydrophilic/hydrophobic balance, resulting in the aggregation of the polymeric chain.<sup>1</sup> This phenomenon is advantageous for controlling the reaction or reactivity.

Polymer structure is considered as an important factor when the application of responsive system is determined. Stimuli responsive polymer can be assembled into different structures such as block copolymer, star polymer, micelle, dendrimer, hyper-branched, and nano/micro gel.

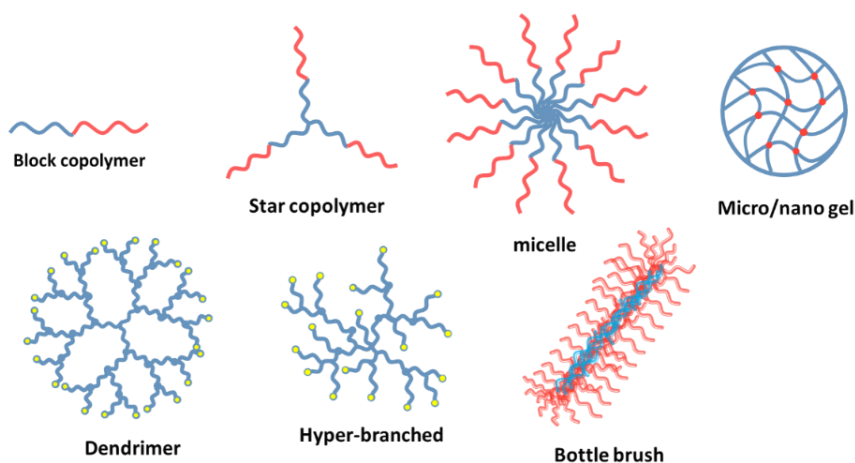


**Figure 1.2** Different assembled structures of stimuli-responsive polymers

Different architectures can be developed based on their various structures. These architectures can then be changed into other forms induced by external stimuli. For example, block copolymers can be assembled into micellar particle and nano/micro gel structures, and hollow particle can be reversed by stimuli.<sup>12-14</sup> Additional changes, including morphological transformation, molecular bond rearrangement, cleavage, and molecular motion can also be performed. They produce not only micro/nanoscale changes in polymer chains but can also induce alternations in their macroscopic properties of material. In other words, a change at molecular level can be reflected into a macroscopic change and then regulate material's properties, including changes in shape, solubility, wettability, and optical properties, etc. The unique property and versatile tailored structures of responsive polymer allow them to be applied in a wide range of fields for various applications, including controlled-drug delivery,<sup>1, 4, 5, 15</sup> in situ hydrogel,<sup>16, 17</sup> smart surface,<sup>6</sup> biosensor,<sup>18, 19</sup> actuator,<sup>20</sup> shape memory materials,<sup>21</sup> and tissue engineering,<sup>22, 23</sup> etc.

## **1.2 Thermo-responsive polymers**

### **1.2.1 Properties and mechanism of thermo-responsive polymers**

Temperature is the most common and well-studied stimulus in the fields of bioengineering and biotechnology. Because the normal human body temperature is always approximately 37 °C, regardless of organs, tissues or cells, the temperature is advantageous to be applied in biomaterial application. In fact, many systems comprising TR polymers have been developed which responds to the body temperature. For example, some researchers have been developed TR micelle which respond to body temperature and become in-situ hydrogel in body.<sup>16, 17</sup> Li and co-workers reported a TR polymeric micelle for chemotherapy.<sup>24</sup> Because cancer cells possess higher metabolic rates compared to normal cells and tissues, the temperature around

tumor is higher of around 40-44 °C. In addition, certain diseases also manifest temperature changes so the temperature system is considered as powerful tool to utilize for such bio-related applications.

TR polymers exhibit a unique property called the critical solution temperature ( $T_c$ ). Typically, there are two critical-solution temperatures: the upper critical-solution temperature (UCST) and the lower critical-solution temperature (LCST). The LCST is the temperature at which a phase separation occurs, while the UCST type polymer shows the phase separation below a critical temperature. (**Figure 1.3**).

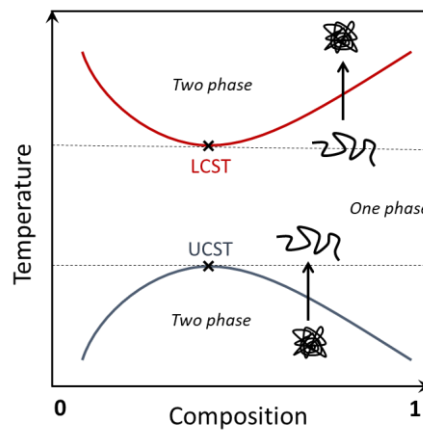


**Figure 1.3** Schematic diagram of phase transition phenomenon for polymer solution of lower critical solution temperature (LCST) behavior and upper critical solution temperature (UCST) behavior.

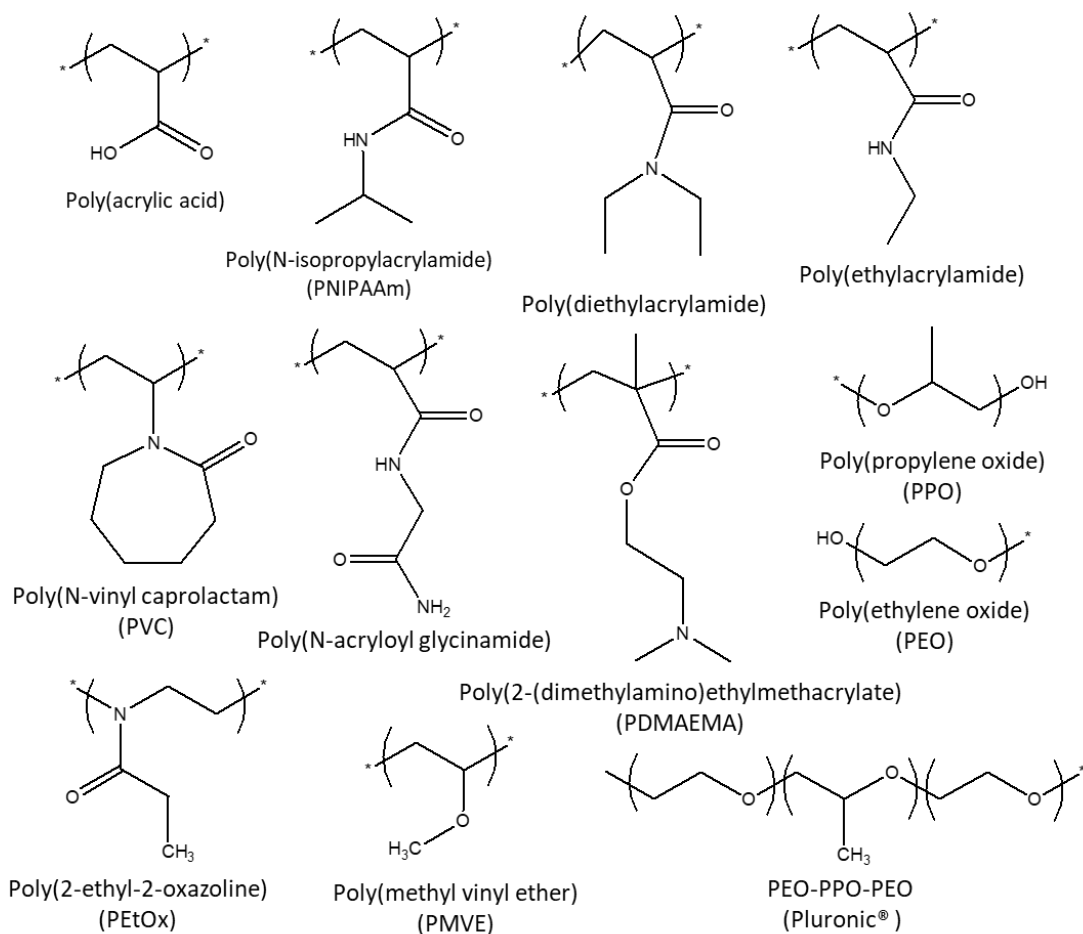
Polymers exhibiting LCST suddenly change their hydrophilicity at a certain temperature, which can be explained based on hydrogen bonding between the polymer chain and the surrounding water molecules. Below a certain temperature, the polymer chains hydrate in aqueous media and mix well with water molecules, forming a homogeneous state and leading to a one-phase system. However, when the temperature is increased, the hydrogen bonds weaken and the polymer chains begin to dehydrate, resulting in the aggregation of polymer chains. This phenomenon can be explained by the free energy of mixing. The weakened hydrogen bonds at higher temperature are a contribution of entropy and enthalpy to the free

energy of mixing. At lower temperature, the polymer chain solvates in water and forms hydrogen bonds with water molecules, resulting in favorable enthalpy of mixing. The solvated polymer enhances ordering and contributes unfavorably to the entropy of mixing. However, as an increase in temperature increases the  $T\Delta S$  value, the entropy term ( $T\Delta S$ ) becomes predominant and the free energy of mixing becomes positive, indicating phase separation. Hence, the LCST phenomenon can be defined as an entropy-driven process. The hydrated polymer chains exhibit a coiled conformation at lower temperatures; however, they reduce their interactions with surrounding water molecules by changing the molecular structure to a globular conformation at high temperatures. This phenomenon is known as the coil-to-globule transition.

Poly(*N*-isopropylacrylamide) (PNIPAAm) exhibits an LCST behavior at 32 °C<sup>25</sup>, poly(2-(dimethylamino)ethyl methacrylate) (PDMAEMA) at 50 °C<sup>26</sup>, and poly(ethylene glycol) (PEG) from 20 to 90 °C<sup>27</sup>, depending on the chain length and the LCST is summarized in **Table 1.1** including some other typical TR polymers. PNIPAAm has been widely studied because its LCST is close to the body temperature.<sup>28-32</sup> The LCST of the PNIPAAm can be adjusted to the target temperature by altering the composition of the co-monomers. For example, the introduction of hydrophilic monomers such as *N,N*-dimethylacrylamide (DMAAm) can increase the LCST.<sup>33</sup> The hydrophilic nature of the comonomer disrupts the alternation of the NIPAAm chains to hydrophobic because it requires more energy to induce a coil-to-globule transition in PNIPAAm. By contrast, introducing a hydrophobic comonomer such as dopamine methacrylamide, can lower the LCST.<sup>34</sup> The adjustable LCST broadens its application in a wide range of biomedical applications, including controlled-release of drugs<sup>1</sup>, colorimetric sensors<sup>35</sup>, and tissue engineering.<sup>16, 22, 36</sup>

**Table 1.1** Critical solution temperature (Tc) of temperature responsive polymer

Temperature responsive polymers	Tc (°C)
Poly( <i>N</i> -isopropylacrylamide) (PNIPAAm)	32
Poly(2-(dimethylamino)ethylmethacrylate) (PDMAEMA)	50
Poly(methyl vinyl ether) (PMVE)	37
Poly( <i>N</i> -ethylacrylamide) (PEA)	82
Poly( <i>N,N</i> -diethylacrylamide)	32-34
Block copolymer of poly(ethylene oxide) and poly(propylene oxide)s	20-90
Poly( <i>N</i> -vinyl piperidone)	67-99
Poly(2-ethyl-2-oxazoline) (PEtOx)	62-65
Poly( <i>N</i> -vinyl caprolactam) (PVC)	35
Poly(pentapeptide) of elastin	28–30

**Figure 1.4** Examples of thermo-responsive polymers

### 1.2.2 Application: Thermo-responsive system for in-situ hydrogels

Conventional hydrogels are commonly prepared beforehand and then surgically implanted in the body. Because the surgical method is invasive, it is associated with a risk of bacterial infections during and after the operation. Recently, in situ hydrogels have been attracting increasing attention owing to their minimal invasiveness and better compliance by patients.<sup>16, 17, 37</sup> An in situ hydrogel, also called an injectable polymer, can be introduced into the body through a syringe in a minimally invasive manner and then solidified at the desired sites in tissues and/or organs. The in-situ gelation system has several other advantages as well. Owing to its flowing nature, the gel precursor can be shaped into its final form and fit into a cavity. Moreover, various therapeutic agents can be incorporated with gel precursors by simple mixing and delivered to the target tissue, organs, or cells.<sup>1, 38</sup> In the past few years, an increasing number of in situ hydrogels have been reported for use in various biomedical applications, including embolization agents<sup>39, 40</sup>, drug delivery<sup>38</sup>, tissue engineering<sup>29, 41, 42</sup>, and cell encapsulation.<sup>43</sup>

Typically, stimuli, including ionic strength, pH, and temperature induce a development of in situ hydrogel. Above all, the temperature stimulus is highly advantageous for in-situ gelation, particularly in biomedical fields because the body temperature can be simply used as a trigger for inducing in situ gelation.<sup>44</sup> In the TR system, the gelling process is attributed to the unique LCST phenomenon from the TR polymer. Temperature induces a change in balance between the hydrophobic and hydrophilic properties of TR polymeric chains, resulting in their aggregation and gelling.

The TR gelling system has been studied for both natural and synthetic polymers. Use of polymers based on polysaccharides such as cellulose derivatives<sup>45</sup>, chitosan<sup>46</sup>, xyloglucan<sup>47</sup>, and gelatin<sup>48</sup> has been extensively investigated. Typical synthetic TR polymer includes

poloxamers (Pluronics®)<sup>49</sup> and PNIPAAm<sup>16</sup>. Poloxamers are of great interest for in situ gelation because their nonionic PEG-*b*-poly(propylene oxide)-*b*-PEG triblock copolymers form a viscous gel at body temperature through the supramolecular interactions of their polymeric blocks. PNIPAAm has also been intensively studied as a synthetic TR polymer because of its LCST, which is very close to the human body temperature. Hydrophilic PEG, in combination with biocompatible polyesters, has been investigated for a longer duration with better biocompatibility and safety.<sup>50</sup> The mechanism of in situ gelation of TR polymers (e.g., poloxamers) involves amphiphilic molecules that maintain the balance between the hydrophobic and hydrophilic properties of their different segments in one polymer chain. When the temperature is increased, the random motion of the copolymer also increases. As a result, the hydrophobic parts of the copolymer self-assemble, resulting in micelle formation. At the critical gelation concentration of the polymer, the micelles are packed closely enough to form a gel structure. The mechanism of the formation of Pluronic systems was proposed by Alexandridis et al.<sup>51</sup> It describes that in the Pluronic systems, the gelation is driven by the reduced polarity of poly(ethylene oxide) and poly(propylene oxide) segments on increasing the temperature and by entropy gain by polymer aggregation.

In situ gelling is achieved using physical or chemical crosslinking structures. If the gel structure is made by physical interaction as described above, it is defined as a *physically crosslinked gel*.<sup>52</sup> In contrast, to fabricate *chemically crosslinked* structures, additional reactions such as coupling reactions or polymerization methods are required.<sup>53</sup> Physically crosslinked gels need only mild conditions without any chemical initiator for their formation. In addition, they undergo rapid gelation once their transition temperature is reached. However, physical gels have weaker interaction in crosslinked structures than the chemically crosslinked gels. As a result, the crosslinked structures of physical gels easily disassociate and go back to sol state. Some studies have investigated gelation using Michael addition reaction for the formation of a

chemical in situ gel.<sup>17</sup> Covalent bond formation strengthens the gel structure, resulting in strong mechanical properties and better stability. However, it is challenging to control the reactivity or regulate gelation. A two-way syringe is generally used to form an in situ chemical gel.<sup>54</sup> An important factor in developing an in situ gel system is the exact timing of gelation at the injected site. For chemical gels, timing is highly important because too slow or too fast reactions can clog the syringe needle or leach out the gel precursor solution from the injected site. A solution state comprising an injectable flowing nature at ambient temperature is the ideal system for the formation of gels at body temperature.

## **1.3 Photo reactive polymers**

### **1.3.1 Properties and mechanism of photo reactive polymers**

Light stimulus is beneficial in polymer chemistry because it can induce various physicochemical changes in polymers. It enables bond formation,<sup>55</sup> degradation, functionalization,<sup>56</sup> and structural change of polymers,<sup>57</sup> photo-crosslinking,<sup>58</sup> and even brings out a response from smart materials.<sup>20</sup> The most distinctive advantage of light stimulus is that it can be applied instantaneously with high accuracy. In addition, temporal control can be achieved by simply switching the light on and off as required. Hence, the photo responsive or photo reactive system is highly advantageous for controlling the reaction. In other words, the photoreaction proceeded by switching on the light stimulus; however, the reaction could immediately stop when the stimuli were removed. In addition, spatial control can also be easily achieved. By simply masking or using patterned lightening, the exposure area can have an exquisite design and be developed in a sophisticated controlled manner. Owing to the distinctive properties imparted by the spatiotemporal control to photo responsive/reactive polymers, the photo reactions are widely used in numerous applications varying from



lithography<sup>59</sup> to optical switching,<sup>60</sup> bioadhesive,<sup>61</sup> self-healing materials,<sup>62</sup> actuations,<sup>63</sup> and data storage<sup>64</sup>. Moreover, because light photons have a much higher energy than thermal energy, the photoreaction can be conducted under more ambient conditions.<sup>65</sup> When the light is given the wavelength at which the photo reactive group absorb, the initiation of reaction immediately starts. The photo responsive molecules absorb only the specific wavelength of the light and do not respond to other wavelengths. This property can be used to develop a more delicate and accurate responsive system. Light is also a noncontact and noninvasive stimulus. Hence, it affords easier accessibility to body parts such as eyes and skin without any contact.

To design photoreactive polymers, a photoreactive functional group must be introduced into polymer chains. Depending on the type of the photoreactive group, the photo responsive system can be classified into reversible or irreversible system. Several photosensitive moieties, such as *o*-nitrobenzylesters,<sup>66</sup> undergo irreversible transformations during irradiation, whereas others can respond reversibly (e.g., azobenzenes).<sup>67</sup> Isomerization is a typical light-induced reversible system based on cis-trans transformation. By altering the absorption wavelength, the structure can be transformed between cis- and trans-forms. This method is commonly used to fabricate photo responsive materials and systems like shape memory materials. For example, chromophores such as azobenzene show reversible cis-trans transformation upon exposure to different wavelengths.<sup>57, 67</sup> Recently, bioinspired light-responsive gating ion channels have been developed by integrating azo molecules into 3D frameworks<sup>68</sup>. In addition, light-induced bond-formation or bond-breaking reactions can be used to develop irreversible systems. A photo-crosslinking reaction is a common bond-forming reaction, which has been used in various fields, including hydrogel,<sup>69</sup> and self-healing materials.<sup>62</sup> Light-induced cleavage, known as a bond-breaking reaction, also occurs, inducing the formation of radical or cationic/anionic intermediates.<sup>70</sup> These reactions have been used to initiate radical polymerization, click chemistry (e.g., thiol-ene and thiol-yne) reactions,<sup>71</sup> and cationic

polymerization. Sometimes, the bond-breaking reactions are used to create a crosslinking structure owing to its ability to transform a monomer to a polymer, typically a crosslinking material.

Recently, Phenylazide groups have gained considerable attention because of their high reactivity.<sup>72, 73</sup> Irradiation of UV light to the phenylazide generates nitrenes and react with various organic materials to form covalent bonds. Highly active nitrene molecules can react with saturated or unsaturated hydrocarbon chains or undergo cycloaddition reactions with alkynes. Hence, the azide groups are useful for application in the fields of chemistry and material science for preparing functionalized surfaces. For example, a methacrylate-based polymer containing a phenylazide group in the side chains was prepared for photo-immobilized surface modification.<sup>73</sup>

### **1.3.2 Application: Photo reactive polymers for antifouling surface**

Fouling is an undesirable adhesion of molecules, living organisms, and suspended particles on a surface. It is a serious issue in many industries, including marine, food, and medical industries, and causes problems such as high energy consumption and maintenance costs. Fouling becomes even more serious for biomedical applications because it can cause our health problems. For example, biofouling causes contaminations in biomaterials or medical devices which lead to infectious diseases. Nonspecific interactions are also an issue because they reduce the sensitivity of biosensors and affect the efficiency of microarray chips and diagnostic systems. In addition, protein adhesion caused by nonspecific interactions between biological components and the device surface is another major problem in the development of blood-contacting biomaterials and medical devices. These issues may result in the formation of thrombus, which leads to platelet formation and ultimately to the failure of the implanted device failures and fatal complications<sup>74</sup>. Because biofouling is mediated by proteins, prevention of

protein adsorption has been proposed as an effective solution to biofouling. Many antifouling strategies have been developed, which can be categorized into three groups: fouling-resistant, fouling-release, and fouling-degrading/killing biofoulants. Initially, antifouling systems were designed to have antimicrobial properties, which can be explained as a fouling-degrading mechanism.<sup>75</sup> It uses biocides or antibacterial materials, such as silver nanoparticles or quaternary ammonium compounds, which can directly kill microorganisms. Hydrophobic surfaces such as those of poly(dimethylsiloxane) (PDMS) are known to show good fouling-release.<sup>76</sup> Non-polar hydrophobic surfaces have a high interfacial energy with water; however, low surface energy make the protein or other adhered organisms to easily detach from the surface. Poly(ethylene glycol)-coated hydrophilic surface—the most common example of a fouling-resistant surface—shows strong resistance to protein adsorption because of the low interfacial energy between the polymer and water.<sup>73</sup> The ethylene glycol repeating unit in the PEG chain can strongly bind to water molecules and form a water layer that hinders the

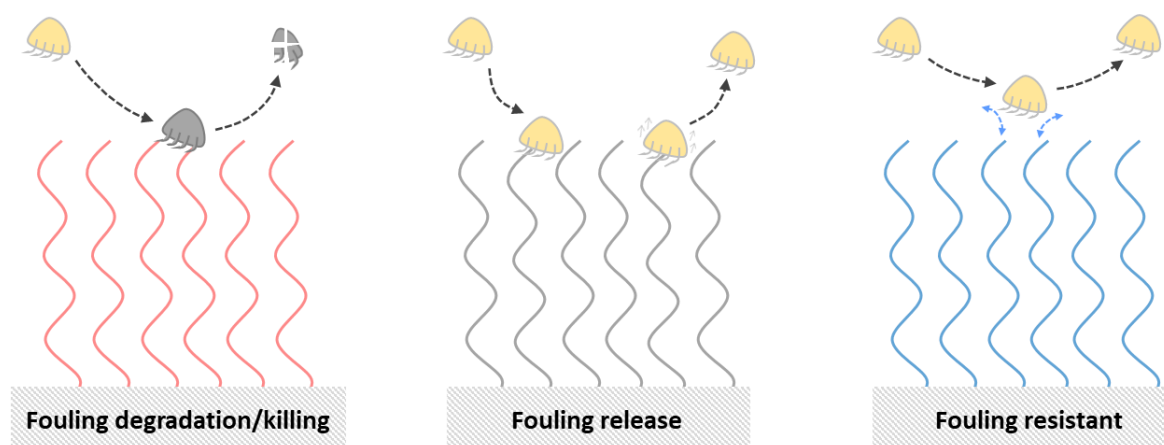


**Figure 1.5** Schematic illustration of antifouling strategies depending on different mechanisms

approaching protein and other biomolecules. When a protein approaches the highly hydrated layer, the compression of the layer decreases the entropy of the polymer chains, resulting in the repulsion of the approaching proteins. The high mobility of the PEG chain also contributes to the overall antifouling properties.

Advanced polymer synthesis methods and self-assembly technologies have enabled the development of several polymer-coating methods to fabricate antifouling surfaces. Antifouling coating modifies the surface chemistry to prevent unwanted adhesion. Polymer coating is considered a useful method for developing antifouling surfaces and other such functionalized surfaces. Because polymer is cheap, non-toxic, biocompatible, and easy to process and modify. Hence, it easily tunes the interfacial properties. Surface coating using PEG has been widely used to prevent biofouling in medical devices and implants. Surface modification, immobilization, and functionalization can be achieved using either “grafting-from”<sup>77</sup> or “grafting-to” methods.<sup>78</sup> The “grafting-from” is a method of polymerization from the surface, and therefore, it requires specific functional groups for the initiation process. In contrast, the “grafting-to” method uses a pre-synthesized polymer to adhere onto the surface. However, anchoring pre-synthesized PEG to immobilize on the surface requires extensive chemical modification and affords limited density control. Photo reaction is considered an effective method to prepare a polymer-coated surface through grafting. The photo reactive polymer can be initiated by the light stimuli and can easily and covalently immobilize various types of organic molecules and biomolecules on the surface. Photo immobilization enables random immobilization to all reactive molecules; hence, the activity/reactivity of polymer which is immobilized on the surface can be considered an average.

The methacrylate-based polymer containing PEG and photoreactive phenylazide group has been synthesized and applied for photo immobilization.<sup>73</sup> And photoreactive poly(vinyl alcohol) (PVA) had prepared by conjugation with azidophenyl groups<sup>56</sup> and it was applied as antifouling polymers in wide applications including ship hull, biosensors, microarray chips, and drug delivery systems.

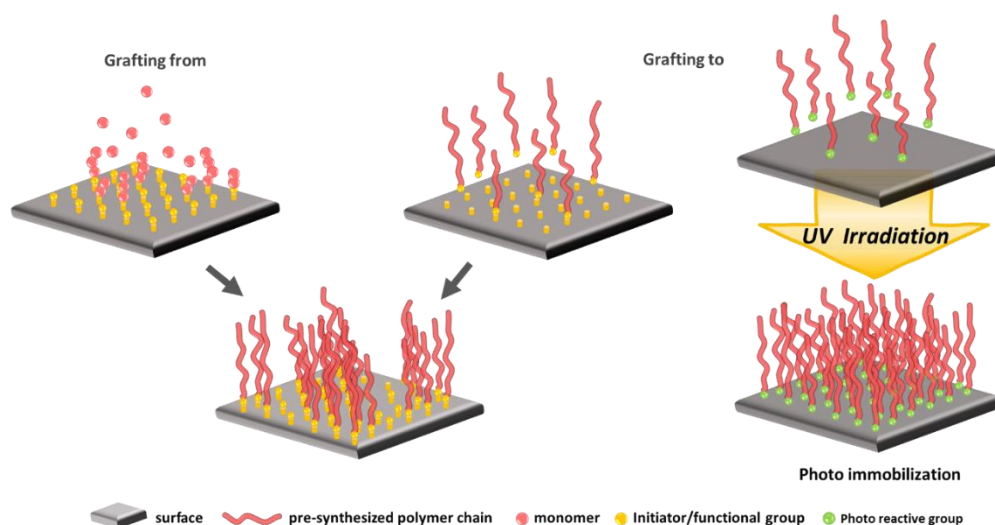


**Figure 1.6** Schematic illustration of grafting method of polymer onto surface

## 1.4 Motivation, Objective, and Outline of This Study

### 1.4.1 Motivation

Recently, polymeric materials have gained significant momentum in highly developed industries such as biomaterials, automobiles, electronics, aerospace, and construction. Technology has been continuously developing toward smart, intelligent, autonomous, nanoscale, sophisticated, integrated and more complicated systems in recent times. As the technology is rapidly developed, the industries have confronted the challenges with a reliability, sensitivity, and efficiency issues. In addition, conventional materials or technologies is no longer provide good solution for difficulties and problems that we have are facing with. In this regard, the demand for smart and intelligent materials, has been continuously increasing. Polymers having well-controlled properties which can be responded by minor environmental variations have great potential in the development of innovative systems to resolve the current technological limitations. The stimuli-responsive polymer is a powerful tool to overcome the current limitations and the challenges. Autonomous adaptive behavior of the stimuli responsive

polymers is highly beneficial to develop smart materials, mimicking biological intelligence which is observed in nature. Moreover, such stimuli responsive or reactive polymers are highly versatile, and can be tailored-made depending on the target application, such as for developing intelligent biomaterials and smart drug-delivery systems. Combining appropriate stimuli, structures, and architectures, the system can be engineered into diverse polymeric materials and broaden applications. Especially, thermal and light stimuli are highly beneficial owing to the distinctive properties. Because the normal human body temperature is always approximately 37 °C, so it is advantageous to be applied in biomaterial application using body temperature as a trigger. Recently, thermal-induced in situ gelling achieved by chemical crosslinking networks have gained great attention. It is highly useful for embolization therapy due to its strong and stable structure however, it is difficult to control the reactivity or regulate the gelation. Therefore, a new method is required to control such reaction and thermal induced system can provide a platform for developing reactivity control switch in the body. On the other hand, photo reaction is highly useful for preparing polymer coated surface. The conventional method using a physical adsorption or chemical coupling reaction showed the limitations regarding instability, functional groups, and controlling density. Integrating with photo reactive system, the polymer coating surface can be easily developed by UV exposure. Light stimulus is highly useful for surface immobilization owing to the distinctive feature for reaction controlling. Temporal and spatial controls can simply achieve by switching a light on and off and by using a photo mask/patterned lightening. Hence, it is easy to develop an exquisite surface in a sophisticated controlled manner. Phenylazide-PEG polymer have been used for antifouling coatings, however, has limitation in hydrophilicity due to the hydrophobic property of phenylazide groups. To improve the hydrophilicity of phenylazide photo reactive polymer, a new design of the polymer is necessary.

It is expected to solve the current technological problems or limitations by applying well-controlled polymers. In this dissertation, we describe stimuli-responsive and stimuli-reactive polymers, preparation of polymeric materials, and their potential applications especially focusing on thermal and light system.

### **1.4.2 Objective and outline**

The objectives of this study were to design and synthesize stimuli induced responsive or reactive polymers which can provide a platform for the development of new functional polymeric materials. For this purpose, temperature-responsive and photoreactive polymers were designed and synthesized, and their properties were evaluated for potential applications.

Chapter 2 describes about the design and synthesis of TR polymer and their applications. It discusses the preparation of TR polymers in detail, followed by the development of TR reactive nanoparticles using the prepared TR polymers. The thermal properties of nanoparticles and the controllable reactivity of the particles and hydrogel were discussed. The chapter also discusses the evaluation and the measurement of sol-gel behavior using a rheometer to confirm viscosity changes depending on temperature stimuli.

Chapter 3 describes the design and synthesis of photo-induced reactive polymers and their applications. It details the design of polyethylene glycol-based photo reactive polymers. The prepared photoreactive polymer was used to develop a polymer-coated surface using various materials by photo-irradiation and then the surface properties were evaluated through protein adsorption and cell adhesion experiments. In addition, improvements in the solubility of the polymer and increased hydrophilicity have also been described and compared with those of the conventional phenylazide photoreactive polymer.

Chapter 4 concludes this dissertation and discusses future perspectives.

## 1.5 References

1. Chung, J. E.; Yokoyama, M.; Yamato, M.; Aoyagi, T.; Sakurai, Y.; Okano, T., Thermo-responsive drug delivery from polymeric micelles constructed using block copolymers of poly(N-isopropylacrylamide) and poly(butylmethacrylate). *Journal of Controlled Release* **1999**, *62* (1), 115-127.
2. Stoffelen, C.; Voskuhl, J.; Jonkheijm, P.; Huskens, J., Dual stimuli-responsive self-assembled supramolecular nanoparticles. *Angewandte Chemie International Edition* **2014**, *53* (13), 3400-3404.
3. Dong, Y.; Wang, J.; Guo, X.; Yang, S.; Ozen, M. O.; Chen, P.; Liu, X.; Du, W.; Xiao, F.; Demirci, U.; Liu, B.-F., Multi-stimuli-responsive programmable biomimetic actuator. *Nature Communications* **2019**, *10* (1), 4087.
4. Tiwari, A. P.; Hwang, T. I.; Oh, J.-M.; Maharjan, B.; Chun, S.; Kim, B. S.; Joshi, M. K.; Park, C. H.; Kim, C. S., pH/NIR-Responsive Polypyrrole-Functionalized Fibrous Localized Drug-Delivery Platform for Synergistic Cancer Therapy. *ACS Applied Materials & Interfaces* **2018**, *10* (24), 20256-20270.
5. Ang, C. Y.; Tan, S. Y.; Teh, C.; Lee, J. M.; Wong, M. F. E.; Qu, Q.; Poh, L. Q.; Li, M.; Zhang, Y.; Korzh, V.; Zhao, Y., Redox and pH Dual Responsive Polymer Based Nanoparticles for In Vivo Drug Delivery. *Small* **2017**, *13* (7), 1602379.
6. Nath, N.; Chilkoti, A., Creating "Smart" Surfaces Using Stimuli Responsive Polymers. *Advanced Materials* **2002**, *14* (17), 1243-1247.
7. Nakamitsu, M.; Oyama, K.; Imai, H.; Fujii, S.; Oaki, Y., Ultrahigh-Sensitive Compression-Stress Sensor Using Integrated Stimuli-Responsive Materials. *Advanced Materials* **2021**, *33* (14), 2008755.
8. Chu, L.-Y.; Yamaguchi, T.; Nakao, S., A Molecular-Recognition Microcapsule for Environmental Stimuli-Responsive Controlled Release. *Advanced Materials* **2002**, *14* (5), 386-389.
9. Akimoto, J.; Tamate, R.; Okazawa, S.; Akimoto, A. M.; Onoda, M.; Yoshida, R.; Ito, Y., Reactivity Control of Polymer Functional Groups by Altering the Structure of Thermoresponsive Triblock Copolymers. *ACS Omega* **2019**, *4* (15), 16344-16351.
10. Akimoto, J.; Ito, Y.; Okano, T.; Nakayama, M., Controlled aggregation behavior of thermoresponsive polymeric micelles by introducing hydrophilic segments as corona components. *Journal of Polymer Science Part A: Polymer Chemistry*. **2018**, *56* (15), 1695-1704.
11. Akimoto, J.; Lin, H.-P.; Li, Y.-K.; Ito, Y., Controlling the electrostatic interaction using a thermal signal to structurally change thermoresponsive nanoparticles. *Colloids and Surfaces A: Physicochemical and Engineering Aspects* **2019**, *577*, 27-33.



12. Clara-Rahola, J.; Fernandez-Nieves, A.; Sierra-Martin, B.; South, A. B.; Lyon, L. A.; Kohlbrecher, J.; Barbero, A. F., Structural properties of thermoresponsive poly(N-isopropylacrylamide)-poly(ethyleneglycol) microgels. *The Journal of Chemical Physics* **2012**, *136* (21), 214903.
13. Can, A.; Zhang, Q.; Rudolph, T.; Schacher, F. H.; Gohy, J.-F.; Schubert, U. S.; Hoogenboom, R., Schizophrenic thermoresponsive block copolymer micelles based on LCST and UCST behavior in ethanol–water mixtures. *European Polymer Journal* **2015**, *69*, 460-471.
14. Bütün, V.; Sönmez, Ş.; Yarlğan, S.; Taktak, F. F.; Atay, A.; Bütün, S., Micelles and 'reverse micelles' with a novel water-soluble diblock copolymer. *Polymer* **2008**, *49* (19), 4057-4065.
15. Nakayama, M.; Okano, T., Multi-targeting cancer chemotherapy using temperature-responsive drug carrier systems. *Reactive and Functional Polymers* **2011**, *71* (3), 235-244.
16. Lee, B. H.; West, B.; McLemore, R.; Pauken, C.; Vernon, B. L., In-situ injectable physically and chemically gelling NIPAAm-based copolymer system for embolization. *Biomacromolecules* **2006**, *7* (6), 2059-2064.
17. Censi, R.; Fieten, P. J.; Di Martino, P.; Hennink, W. E.; Vermonden, T., In-situ forming hydrogels by simultaneous thermal gelling and Michael addition reaction between methacrylate bearing thermosensitive triblock copolymers and thiolated hyaluronan. *Journal of Controlled Release* **2010**, *148* (1), e28-e29.
18. Cai, Q.; Zeng, K.; Ruan, C.; Desai, T. A.; Grimes, C. A., A Wireless, Remote Query Glucose Biosensor Based on a pH-Sensitive Polymer. *Analytical Chemistry* **2004**, *76* (14), 4038-4043.
19. Zhang, K.; Liang, Y.; Liu, D.; Liu, H., An on–off biosensor based on multistimuli-responsive polymer films with a binary architecture and bioelectrocatalysis. *Sensors and Actuators B: Chemical* **2012**, *173*, 367-376.
20. Li, X.; Yin, R.; Cheng, F.; Yu, Y., *Light-responsive actuation materials based on azo-containing liquid-crystalline polymers*. SPIE: 2011; Vol. 7955.
21. Iqbal, D.; Samiullah, M. H., Photo-Responsive Shape-Memory and Shape-Changing Liquid-Crystal Polymer Networks. *Materials* **2013**, *6* (1), 116-142.
22. Kumashiro, Y.; Yamato, M.; Okano, T., Cell Attachment–Detachment Control on Temperature-Responsive Thin Surfaces for Novel Tissue Engineering. *Annals of Biomedical Engineering* **2010**, *38* (6), 1977-1988.

23. Tang, Z.; Akiyama, Y.; Okano, T., Temperature-Responsive Polymer Modified Surface for Cell Sheet Engineering. *Polymers* **2012**, *4* (3), 1478-1498.
24. Li, J.; Wang, B.; Liu, P., Possibility of active targeting to tumor by local hyperthermia with temperature-sensitive nanoparticles. *Medical Hypotheses* **2008**, *71* (2), 249-251.
25. Fujishige, S.; Kubota, K.; Ando, I., Phase transition of aqueous solutions of poly(N-isopropylacrylamide) and poly(N-isopropylmethacrylamide). *The Journal of Physical Chemistry* **1989**, *93* (8), 3311-3313.
26. Yuk, S. H.; Cho, S. H.; Lee, S. H., pH/Temperature-Responsive Polymer Composed of Poly((N,N-dimethylamino)ethyl methacrylate-co-ethylacrylamide). *Macromolecules* **1997**, *30* (22), 6856-6859.
27. Becer, C. R.; Hahn, S.; Fijten, M. W. M.; Thijs, H. M. L.; Hoogenboom, R.; Schubert, U. S., Libraries of methacrylic acid and oligo(ethylene glycol) methacrylate copolymers with LCST behavior. *Journal of Polymer Science Part A: Polymer Chemistry* **2008**, *46* (21), 7138-7147.
28. Schild, H. G., Poly(N-isopropylacrylamide): experiment, theory and application. *Progress in Polymer Science* **1992**, *17* (2), 163-249.
29. Stile, R. A.; Burghardt, W. R.; Healy, K. E., Synthesis and Characterization of Injectable Poly(N-isopropylacrylamide)-Based Hydrogels That Support Tissue Formation in Vitro. *Macromolecules* **1999**, *32* (22), 7370-7379.
30. Mou, F.; Chen, C.; Zhong, Q.; Yin, Y.; Ma, H.; Guan, J., Autonomous Motion and Temperature-Controlled Drug Delivery of Mg/Pt-Poly(N-isopropylacrylamide) Janus Micromotors Driven by Simulated Body Fluid and Blood Plasma. *ACS Applied Materials & Interfaces* **2014**, *6* (12), 9897-9903.
31. Lanzalaco, S.; Armelin, E., Poly(N-isopropylacrylamide) and Copolymers: A Review on Recent Progresses in Biomedical Applications. *Gels* **2017**, *3* (4), 36.
32. Hsiue, G.-H.; Hsu, S.-h.; Yang, C.-C.; Lee, S.-H.; Yang, I. K., Preparation of controlled release ophthalmic drops, for glaucoma therapy using thermosensitive poly-N-isopropylacrylamide. *Biomaterials* **2002**, *23* (2), 457-462.
33. Hu, Y.; Darcos, V.; Monge, S.; Li, S.; Zhou, Y.; Su, F., Tunable thermo-responsive P(NIPAAm-co-DMAAm)-b-PLLA-b-P(NIPAAm-co-DMAAm) triblock copolymer micelles as drug carriers. *Journal of Materials Chemistry B* **2014**, *2* (18), 2738-2748.
34. García-Peñas, A.; Biswas, C. S.; Liang, W.; Wang, Y.; Yang, P.; Stadler, F. J., Effect of Hydrophobic Interactions on Lower Critical Solution Temperature for Poly(N-

isopropylacrylamide-co-dopamine Methacrylamide) Copolymers. *Polymers* **2019**, *11* (6), 991.

35. Liu, X.-Y.; Cheng, F.; Liu, Y.; Li, W.-G.; Chen, Y.; Pan, H.; Liu, H.-J., Thermoresponsive gold nanoparticles with adjustable lower critical solution temperature as colorimetric sensors for temperature, pH and salt concentration. *Journal of Materials Chemistry* **2010**, *20* (2), 278-284.

36. Yoshida, Y.; Kawahara, K.; Inamoto, K.; Mitsumune, S.; Ichikawa, S.; Kuzuya, A.; Ohya, Y., Biodegradable injectable polymer systems exhibiting temperature-responsive irreversible sol-to-gel transition by covalent bond formation. *ACS Biomater. Sci. Eng.* **2017**, *3* (1), 56-67.

37. Diryak, R.; Kontogiorgos, V.; Ghorri, M. U.; Bills, P.; Tawfik, A.; Morris, G. A.; Smith, A. M., Behavior of in situ cross-linked hydrogels with rapid gelation kinetics on contact with physiological fluids. *Macromol. Chem. Phys.* **2018**, *219* (8), 1700584.

38. Cao, Y.; Zhang, C.; Shen, W.; Cheng, Z.; Yu, L.; Ping, Q., Poly(N-isopropylacrylamide)-chitosan as thermosensitive in situ gel-forming system for ocular drug delivery. *Journal of Controlled Release* **2007**, *120* (3), 186-194.

39. Avery, R. K.; Albadawi, H.; Akbari, M.; Zhang, Y. S.; Duggan, M. J.; Sahani, D. V.; Olsen, B. D.; Khademhosseini, A.; Oklu, R., An injectable shear-thinning biomaterial for endovascular embolization. *Sci. Transl. Med* **2016**, *8* (365), 365ra156.

40. Hu, J.; Albadawi, H.; Chong, B. W.; Deipolyi, A. R.; Sheth, R. A.; Khademhosseini, A.; Oklu, R., Advances in Biomaterials and Technologies for Vascular Embolization. *Advanced Materials* **2019**, *31* (33), 1901071.

41. Fitzpatrick, S. D.; Jafar Mazumder, M. A.; Lasowski, F.; Fitzpatrick, L. E.; Sheardown, H., PNIPAAm-Grafted-Collagen as an Injectable, In Situ Gelling, Bioactive Cell Delivery Scaffold. *Biomacromolecules* **2010**, *11* (9), 2261-2267.

42. Gan, T.; Zhang, Y.; Guan, Y., In Situ Gelation of P(NIPAM-HEMA) Microgel Dispersion and Its Applications as Injectable 3D Cell Scaffold. *Biomacromolecules* **2009**, *10* (6), 1410-1415.

43. Zhan, H.; de Jong, H.; Löwik, D. W. P. M., Comparison of Bioorthogonally Cross-Linked Hydrogels for in Situ Cell Encapsulation. *ACS Applied Bio Materials* **2019**, *2* (7), 2862-2871.

44. Zhao, Y.; Zheng, C.; Wang, Q.; Fang, J.; Zhou, G.; Zhao, H.; Yang, Y.; Xu, H.; Feng, G.; Yang, X., Permanent and Peripheral Embolization: Temperature-Sensitive p(N-Isopropylacrylamide-co-butyl Methacrylate) Nanogel as a Novel Blood-Vessel-Embolic Material in the Interventional Therapy of Liver Tumors. *Advanced Functional Materials* **2011**, *21* (11), 2035-2042.

45. Thermo-Responsive Methylcellulose Hydrogels: From Design to Applications as Smart Biomaterials. *Tissue Engineering Part B: Reviews*
46. Ahsan, A.; Farooq, M. A.; Parveen, A., Thermosensitive Chitosan-Based Injectable Hydrogel as an Efficient Anticancer Drug Carrier. *ACS Omega* **2020**, *5* (32), 20450-20460.
47. Brun-Graeppe, A. K. A. S.; Richard, C.; Bessodes, M.; Scherman, D.; Narita, T.; Ducouret, G.; Merten, O.-W., Study on the sol-gel transition of xyloglucan hydrogels. *Carbohydrate Polymers* **2010**, *80* (2), 555-562.
48. Zheng, Y.; Liang, Y.; Zhang, D.; Sun, X.; Liang, L.; Li, J.; Liu, Y.-N., Gelatin-Based Hydrogels Blended with Gellan as an Injectable Wound Dressing. *ACS Omega* **2018**, *3* (5), 4766-4775.
49. Al Khateb, K.; Ozhmukhametova, E. K.; Mussin, M. N.; Seilkhanov, S. K.; Rakhypbekov, T. K.; Lau, W. M.; Khutoryanskiy, V. V., In situ gelling systems based on Pluronic F127/Pluronic F68 formulations for ocular drug delivery. *International Journal of Pharmaceutics* **2016**, *502* (1), 70-79.
50. Gong, C.-Y.; Shi, S.; Peng, X.-Y.; Kan, B.; Yang, L.; Huang, M.-J.; Luo, F.; Zhao, X.; Wei, Y.-Q.; Qian, Z.-Y., Biodegradable thermosensitive injectable PEG-PCL-PEG hydrogel for bFGF antigen delivery to improve humoral immunity. *Growth Factors* **2009**, *27* (6), 377-383.
51. Alexandridis, P.; Nivaggioli, T.; Hatton, T. A., Temperature Effects on Structural Properties of Pluronic P104 and F108 PEO-PPO-PEO Block Copolymer Solutions. *Langmuir* **1995**, *11* (5), 1468-1476.
52. Song, G.; Zhang, L.; He, C.; Fang, D.-C.; Whitten, P. G.; Wang, H., Facile Fabrication of Tough Hydrogels Physically Cross-Linked by Strong Cooperative Hydrogen Bonding. *Macromolecules* **2013**, *46* (18), 7423-7435.
53. Liu, F.; Seuring, J.; Agarwal, S., A Non-ionic Thermophilic Hydrogel with Positive Thermosensitivity in Water and Electrolyte Solution. *Macromolecular Chemistry and Physics* **2014**, *215* (15), 1466-1472.
54. Au - Sivakumaran, D.; Au - Bakaic, E.; Au - Campbell, S. B.; Au - Xu, F.; Au - Mueller, E.; Au - Hoare, T., Fabricating Degradable Thermoresponsive Hydrogels on Multiple Length Scales via Reactive Extrusion, Microfluidics, Self-assembly, and Electrospinning. *JoVE* **2018**, (134), e54502.
55. Kalayci, K.; Frisch, H.; Truong, V. X.; Barner-Kowollik, C., Green light triggered [2+2] cycloaddition of halochromic styrylquinoxaline—controlling photoreactivity by pH. *Nature Communications* **2020**, *11* (1), 4193.

56. Krishnan, S.; Weinman, C. J.; Ober, C. K., Advances in polymers for anti-biofouling surfaces. *Journal of Materials Chemistry* **2008**, *18* (29), 3405-3413.
57. Müller, K.; Knebel, A.; Zhao, F.; Bléger, D.; Caro, J.; Heinke, L., Switching Thin Films of Azobenzene-Containing Metal–Organic Frameworks with Visible Light. *Chemistry – A European Journal* **2017**, *23* (23), 5434-5438.
58. Albuszis, M.; Roth, P. J.; Pauer, W.; Moritz, H.-U., Two in one: use of azide functionality for controlled photo-crosslinking and click-modification of polymer microspheres. *Polymer Chemistry* **2016**, *7* (34), 5414-5425.
59. Kravchenko, A.; Shevchenko, A.; Grahm, P.; Ovchinnikov, V.; Kaivola, M., Photolithographic periodic patterning of gold using azobenzene-functionalized polymers. *Thin Solid Films* **2013**, *540*, 162-167.
60. Huck, N. P. M.; Jager, W. F.; de Lange, B.; Feringa, B. L., Dynamic Control and Amplification of Molecular Chirality by Circular Polarized Light. *Science* **1996**, *273* (5282), 1686-1688.
61. Wang, J.; Karami, P.; Ataman, N. C.; Pioletti, D. P.; Steele, T. W. J.; Klok, H.-A., Light-Activated, Bioadhesive, Poly(2-hydroxyethyl methacrylate) Brush Coatings. *Biomacromolecules* **2020**, *21* (1), 240-249.
62. Ji, S.; Cao, W.; Yu, Y.; Xu, H., Visible-Light-Induced Self-Healing Diselenide-Containing Polyurethane Elastomer. *Advanced Materials* **2015**, *27* (47), 7740-7745.
63. Lv, J.-a.; Liu, Y.; Wei, J.; Chen, E.; Qin, L.; Yu, Y., Photocontrol of fluid slugs in liquid crystal polymer microactuators. *Nature* **2016**, *537* (7619), 179-184.
64. Zhuang, Y.; Ren, X.; Che, X.; Liu, S.; Huang, W.; Zhao, Q., Organic photoresponsive materials for information storage: a review. *Advanced Photonics* **2020**, *3* (1), 014001.
65. Chatani, S.; Kloxin, C. J.; Bowman, C. N., The power of light in polymer science: photochemical processes to manipulate polymer formation, structure, and properties. *Polymer Chemistry* **2014**, *5* (7), 2187-2201.
66. Tajmoradi, Z.; Roghani-Mamaqani, H.; Salami-Kalajahi, M., Stimuli-transition of hydrophobicity/hydrophilicity in o-nitrobenzyl ester-containing multi-responsive copolymers: Application in patterning and droplet stabilization in heterogeneous media. *Polymer* **2020**, *205*, 122859.
67. Jochum, F. D.; zur Borg, L.; Roth, P. J.; Theato, P., Thermo- and Light-Responsive Polymers Containing Photoswitchable Azobenzene End Groups. *Macromolecules* **2009**, *42* (20), 7854-7862.

68. Qian, T.; Zhang, H.; Li, X.; Hou, J.; Zhao, C.; Gu, Q.; Wang, H., Efficient Gating of Ion Transport in Three-Dimensional Metal–Organic Framework Sub-Nanochannels with Confined Light-Responsive Azobenzene Molecules. *Angewandte Chemie International Edition* **2020**, *59* (31), 13051-13056.
69. Son, T. I.; Sakuragi, M.; Takahashi, S.; Obuse, S.; Kang, J.; Fujishiro, M.; Matsushita, H.; Gong, J.; Shimizu, S.; Tajima, Y., Visible light-induced crosslinkable gelatin. *Acta biomater.* **2010**, *6* (10), 4005-4010.
70. Byambaa, B.; Konno, T.; Ishihara, K., Cell adhesion control on photoreactive phospholipid polymer surfaces. *Colloids and Surfaces B: Biointerfaces* **2012**, *99*, 1-6.
71. Hoyle, C. E.; Lowe, A. B.; Bowman, C. N., Thiol-click chemistry: a multifaceted toolbox for small molecule and polymer synthesis. *Chemical Society Reviews* **2010**, *39* (4), 1355-1387.
72. Na, H.-N.; Kim, K.-I.; Han, J.-H.; Lee, J.-G.; Son, T.-I.; Han, D.-K.; Ito, Y.; Song, K.-S.; Jang, E.-C., Synthesis of O-carboxylated low molecular chitosan with azido phenyl group: Its application for adhesion prevention. *Macromolecular Research* **2010**, *18* (10), 1001-1007.
73. Ito, Y.; Hasuda, H.; Sakuragi, M.; Tsuzuki, S., Surface modification of plastic, glass and titanium by photoimmobilization of polyethylene glycol for antibiofouling. *Acta Biomater.* **2007**, *3* (6), 1024-1032.
74. Damodaran, V. B.; Murthy, N. S., Bio-inspired strategies for designing antifouling biomaterials. *Biomater Res* **2016**, *20*, 18.
75. Yang, W.; Li, J.; Zhou, P.; Zhu, L.; Tang, H., Superhydrophobic copper coating: Switchable wettability, on-demand oil-water separation, and antifouling. *Chemical Engineering Journal* **2017**, *327*, 849-854.
76. Wynne, K. J.; Swain, G. W.; Fox, R. B.; Bullock, S.; Uilk, J., Two silicone nontoxic fouling release coatings: Hydrosilation cured PDMS and CaCO<sub>3</sub> filled, ethoxysiloxane cured RTV11. *Biofouling* **2000**, *16* (2-4), 277-288.
77. Prucker, O.; R  he, J., Polymer Layers through Self-Assembled Monolayers of Initiators. *Langmuir* **1998**, *14* (24), 6893-6898.
78. Akiyama, Y.; Mori, T.; Katayama, Y.; Niidome, T., The effects of PEG grafting level and injection dose on gold nanorod biodistribution in the tumor-bearing mice. *Journal of Controlled Release* **2009**, *139* (1), 81-84.
79. Brighenti, R.; Li, Y.; Vernerey, F. J., Smart Polymers for Advanced Applications: A Mechanical Perspective Review. *Frontiers in Materials* **2020**, *7* (196).

---

## Chapter 2

### 2. Thermally induced switch for in-situ gelation using morphological change of thermo-responsive polymer

---

#### 2.1 Introduction

In situ forming hydrogels have been received great attention as one of effective approaches in biomedical fields especially for embolization agent because of their easy administration and minimal invasiveness which enhance patient's compliances.<sup>1-4</sup> In situ hydrogel can be formed using either physical or chemical interactions<sup>5, 6</sup>. The chemical gel is advantageous under physiological conditions because of its stable crosslinking structure which comes from the covalent bond.<sup>6</sup> Typical chemical crosslinking is achieved either by polymerization<sup>7</sup> or a reaction between complementary groups such as activated esters and primary amine for amide bonds,<sup>8</sup> aldehyde and amine for imine bond.<sup>9</sup>

Although the chemical crosslinking gel improves stability, controlling the crosslinking reaction still remains as a difficult challenge because it is developed through chemical reaction. Moreover, the chemical reaction has limitations such as low yield, prolonged reaction times, and an extreme reaction condition, which is undesirable when forming in situ hydrogel in body.<sup>10-12</sup> In situ gel using in biomedical field must meet basic requirements, such as forming under physiological conditions, rapid crosslinking, and biocompatibility.<sup>13-15</sup> However, the significant aspect for in situ chemical crosslinking gel is obviously an appropriate timing of crosslinking reaction.<sup>16</sup>

For example, a two-solution mixing syringe is typically used to control the reaction for preparing in situ gel.<sup>17</sup> If the reaction rate is too rapid, it leads a clogging in syringe, resulting difficulty in injection.<sup>18</sup> In contrast, a slow reaction may lead to gelation, leaching out from the injected site. These problems are caused by passive and rapid chemical reaction, resulting difficulty in controlling crosslinking reaction precisely. Controlling the reaction is considered as prerequisite to achieve in situ gel with desired property which is enabled by given exact gelation timing immediately after the gel flows and fills a cavity or defect area, leading to better therapeutic expectations as an implanted material.

For the chemical reactions to proceed, the temperature is needed to be increased.<sup>19</sup> However, it is extremely difficult to control the rate of the chemical reaction with a slight temperature difference, especially under limited conditions in the body. Conversely, responsive polymer changes their physicochemical properties in response to even a slight difference.<sup>20</sup> The crosslinking structure can be formed by utilizing stimuli-responsive polymers that change physicochemical properties in response to changes of external environment.<sup>21, 22</sup> With such susceptible responsiveness, the crosslinking reaction can also be controlled by introducing the responsive system. In particular, temperature is facile stimulus to physically apply from the outside and is suitable for biomedical applications in terms of safety and accessibility of a variety of thermal treatment devices.<sup>23, 24</sup>

Recently, there have been several independent reports on ABA triblock copolymer based systems developing gels using covalent bonds in response to thermal stimuli.<sup>8, 25</sup> These methods utilize the phase transition of TR segments in polymer assembly structure to control the formation of hydrogel. By changing the structure of the polymer assembly, the polymeric nanoparticle controlled the reactivity with the external substrate by thermal signal. A previous study focused on examining the controlling duration time of gel states by changing the molar



ration of each particle.<sup>8</sup> Yet, controlling the reactivity between two functional groups during gel formation was not investigated extensively.

In this study, we designed a hetero-armed TR nanoparticle using simple diblock copolymers, which can be used to control the reactivity of functional groups through the changes in the excluded volume of the extended armed TR polymer induced by phase transition of the TR segment. This is a strategy of our TR system, and it is depicted in **Figure 2.1**. Poly(*N*-isopropylacrylamide) (PNIPAAm) and its copolymers, are a well-known TR polymer which shows phase transition across the lower critical solution temperature (LCST).<sup>20</sup> The polymer extends below the LCST and shrinks by the dehydration above the LCST. By introducing TR polymer to outer shell component of the core-shell micelle, the morphology of the outer shell can be rapidly changed in response to temperature.<sup>26,27</sup> Therefore, the morphological changing of shell forming TR polymer controls the interaction with external molecules.<sup>25,28</sup>

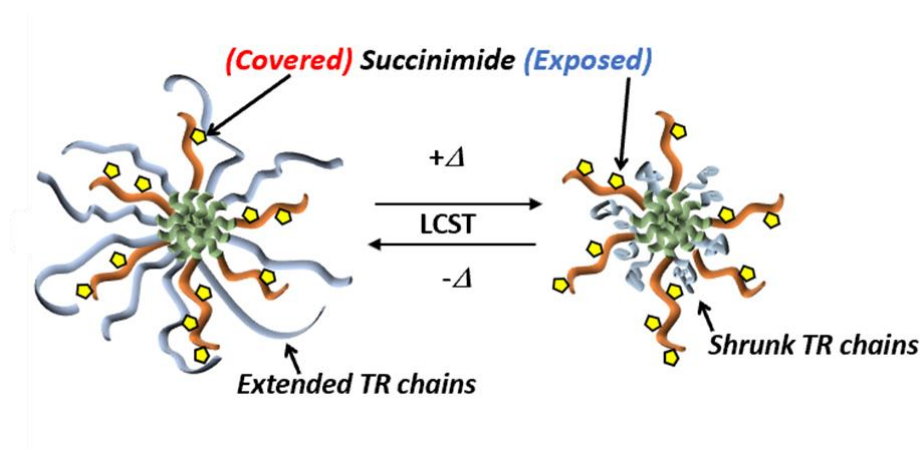


**Figure 2.1** Schematic illustration of structural change of hetero-armed responsive particle by temperature

Specifically, the hetero-armed TR nanoparticle was prepared simply by co-assembly of two different kinds of amphiphilic block copolymers, possessing TR segment and hydrophilic segment with succinimide group as reactive functional group. Here, we investigated the critical

switch effect of TR nanoparticle on the controlling chemical reaction. By using sharp response of TR polymer to slight temperature changes which induced extended/shrink TR polymers, the coupling reaction between succinimide group on hetero-armed TR nanoparticle and external primary amine on another nanoparticle was well-controlled. Moreover, we used high concentration particle solutions to investigate the critical controlling effect of TR nanoparticle system on gelation behavior in by temperature. The fundamental study of viscoelastic property changes in response to the thermal stimulus was carried out to examine this system as potential method for injectable in-situ chemical hydrogel.

## 2.2 Materials and methods

### 2.2.1 Materials

*N*-isopropylacrylamide (NIPAAm) was provided by KJ chemicals (Tokyo, Japan) and purified twice by recrystallization from *n*-hexane. Benzyl methacrylate (BzMA) and *N,N*-dimethylacrylamide (DMAAm) were purchased from Fuji Film Wako Pure chemicals (Tokyo, Japan) and distilled under reduced pressure before use. Ethanolamine, 2,2'-azobisisobutyronitrile (AIBN), 1,4-dioxane, *n*-hexane, acetone, and tetrahydrofuran (THF) were purchased from Fuji Film Wako Pure chemicals. *N*-(3-Aminopropyl) methacrylamide hydrochloride, (NAPMAAm) (Polyscience, Warrington, PA, USA), 2-cyano-2-propyl dodecyl trithiocarbonate (CPDT) (Sigma-Aldrich, St. Louis, MO, USA), *N*-succinimidyl acrylate (NAS) (Tokyo Chemical Industry, Tokyo, Japan), tris(2-carboxyethyl) phosphine hydrochloride (TCEP) (Tokyo Chemical Industry), and diethyl ether (Junsei Chemical, Tokyo, Japan) were used as received. Polyallylamine (M 133 n: 150 kDa, 40 wt % solution) was provided by Nittobo Medical (Tokyo, Japan).

### 2.2.2 Instrumentation

Proton nuclear magnetic resonance ( $^1\text{H}$  NMR) was measured using a JNM-ECZ400R spectrometer (400 Mhz, JEOL, Tokyo, Japan). Hydrodynamic diameters of polymeric micelles were measured by dynamic light scattering (DLS) using an ELSZ-2PL (Otsuka Electronics, Osaka, Japan). Optical transmittance of the polymeric micelles (5.0 mg/mL) in Milli-Q at various temperatures (heating rate was 0.2 °C/min) was measured by a UV-vis spectrophotometer ( $\lambda=600$  nm, V-530, JASCO, Tokyo, Japan). Fluorescent spectra were measured using an FP6500 ( $\lambda_{\text{ex}}=490$  nm, JASCO). Viscoelastic properties of hydrogel were measured using an AR-G2 rheometer (TA instruments, USA). A transmission electron microscope (TEM) was carried out using a JEM1230 (JEOL, Tokyo, Japan). Infrared (IR) spectra were recorded using a Fourier transform infrared (FTIR) spectrophotometer (FTIR 4100, JASCO, Tokyo, Japan). Gel permeation chromatography (GPC) analysis was performed by a GPC system (Tosoh, Tokyo) with three columns (Shoedex KD802, KD804 and KD-806M) (Showa Denko, Tokyo, Japan) at 45 °C using *N,N*-dimethylformamide (DMF) containing 10 mmol/L lithium bromide as an eluent with a flow rate of 0.6 mL/min.

### 2.2.3 Synthesis of PBzMA

BzMA (25 mmol), CPDT (0.5 mmol), and AIBN (0.1 mmol) were dissolved in 50 mL of 1,4-dioxane and bubbled with nitrogen gas for 30 min at 25 °C. Polymerization was performed at 80 °C for 48 h. After the reaction, the solution was precipitated in an excess amount of *n*-hexane 3 times and then dried under vacuum at room temperature for 2 h.

### 2.2.4 Synthesis of diblock copolymers

To prepare TR diblock copolymers of PBzMA-*b*-P(NIPAAm-*co*-DMAAm) diblock copolymers, NIPAAm, DMAAm and AIBN were dissolved in 1,4-dioxane (5mL). The mixture solution was bubbled with nitrogen gas for 20 min and then allowed to react at 80 °C for 24 h

under an N<sub>2</sub> atmosphere. Polymer was recovered by precipitation in an excess amount of hexane and then dried under vacuum at room temperature for 2 h. PBzMA-*b*-P(NAS-*co*-DMAAm) and PBzMA-*b*-P(NAPMAAm-*co*-DMAAm) were prepared by the same procedure using NAS and NAPMAAm instead of NIPAAm, respectively.

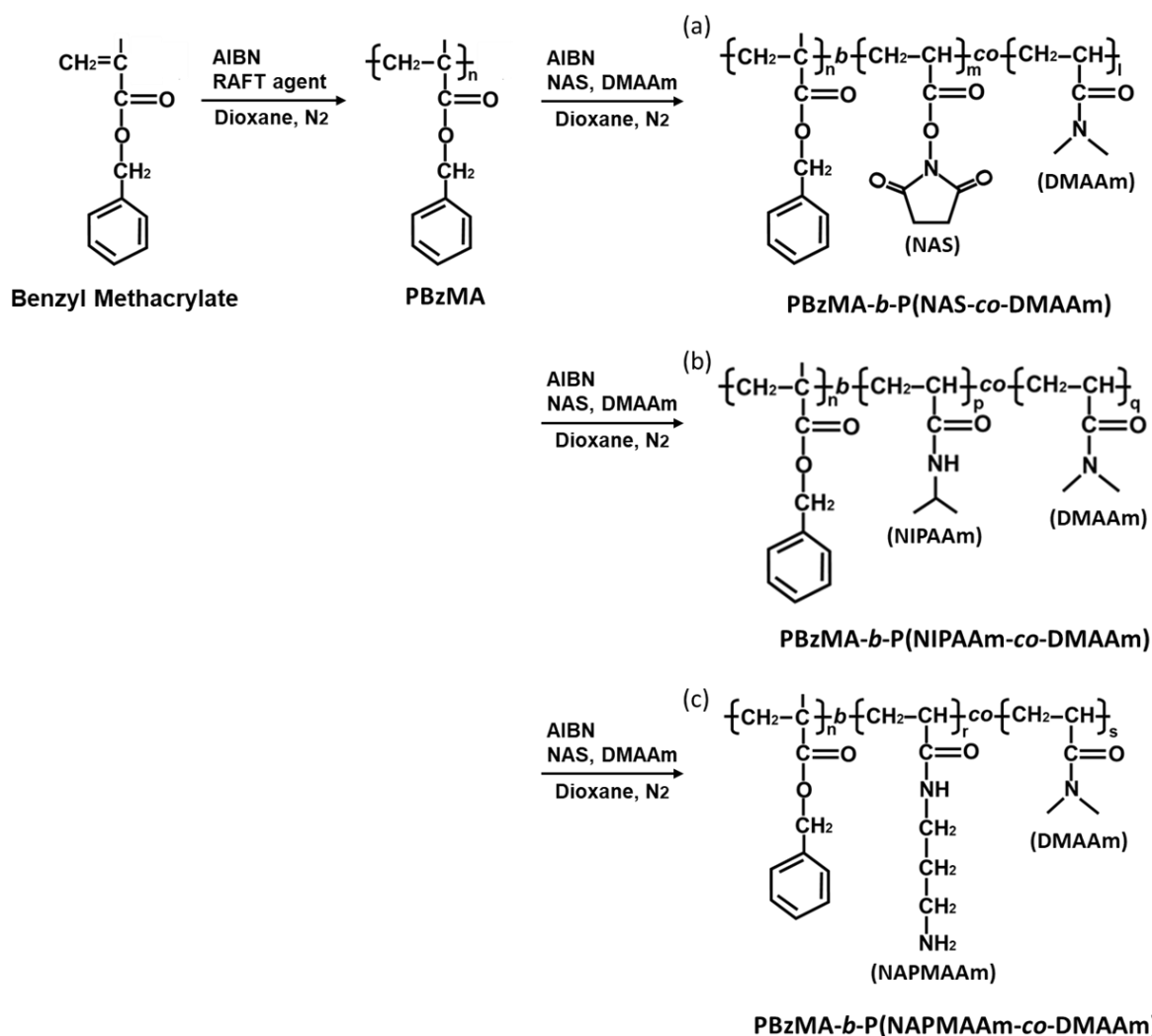


**Figure 2.2** Synthesis of block copolymers (a)PBzMA-*b*-P(NAS-*co*-DMAAm), (b)PBzMA-*b*-P(NIPAAm-*co*-DMAAm), and (c)PBzMA-*b*-P(NAPMAAm-*co*-DMAAm).

### 2.2.5 Terminal conversion of TR diblock copolymers

PBzMA-*b*-P(NIPAAm-*co*-DMAAm), NIPAAm (20 molar equivalents of polymer), and TCEP were dissolved in 1,4-dioxane (5mL). And then, 2-aminoethanol (20 molar equivalents of polymer) was slowly added to the solution and allowed to react at 25 °C for 24 h. After the reaction, the polymer solution was dialyzed against Milli-Q for 48 h using a dialysis membrane (Spectra/Por 6, MWCO 1000, Spectrum Laboratories, Rancho Dominguez, CA) and then polymers were obtained by freeze drying.

### 2.2.6 Terminal conversion of PBzMA-*b*-P(NAS-*co*-DMAAm)

Trithiododecyl terminal group on PBzMA-*b*-P(NAS-*co*-DMAAm) was substituted by radical substitution reaction using AIBN. PBzMA-*b*-P(NAS-*co*-DMAAm) (200mg) and AIBN (60 mol times against polymer) were dissolved in 1,4-dioxane and then bubbled with nitrogen gas for 20 min. The reaction was performed at 80 °C for 4 h. Polymer was recovered by precipitation in excess amount of hexane, followed by drying in vacuum.

### 2.2.7 Reactivity and stability of the succinimide group on PBzMA-*b*-P(NAS-*co*-DMAAm)

PBzMA-*b*-P(NAS-*co*-DMAAm) was dissolved in acetone and 5-aminofluorescein was dissolved in co-solvent of DMSO/H<sub>2</sub>O (1:1). Subsequently, both solutions were mixed together and then allowed to be reacted for 1 day at room temperature. After the reaction, unreacted 5-aminofluorescein was removed dialysis using a dialysis membrane (MWCO 3500). Fluorescent spectra ( $\lambda_{\text{ex}}$ =490 nm) was recorded at 25 °C.

The stability of the succinimide group on the polymer was investigated. In brief, PBzMA-*b*-P(NAS-*co*-DMAAm) was dissolved in acetone and dialyzed against water. The polymer solution was then freeze-dried, and its <sup>1</sup>H NMR spectra using chloroform-*d* as the solvent

were recorded. The amount of the remaining succinimide groups on the polymer was calculated from the protons of succinimide (4H, 2.9 ppm).

## 2.2.8 Preparation and characterization of polymeric micelles

Polymeric micelles were prepared using a cosolvent evaporation method. PBzMA-*b*-P(NAS-*co*-DMAAm) and PBzMA-*b*-P(NIPAAm-*co*-DMAAm) were dissolved in 1 mL of acetone in different mole ratio (30/70, 50/50 and 70/30). Subsequently, 1 mL of water was added to the polymer solution. Acetone was completely removed by vacuum at 25 °C using a rotary evaporator (100 mmHg). The obtained micelle was coded as M(TR/NAS)[A/B] (A and B represent the ratio of weight percentage of PBzMA-*b*-P(NAS-*co*-DMAAm) and PBzMA-*b*-P(NIPAAm-*co*-DMAAm). The PBzMA-*b*-P(NAPMAAm-*co*-DMAAm) micelle was also prepared by the same protocol as above using methanol and tetrahydrofuran, instead of acetone. The prepared aminated polymeric micelle was coded as M(NH<sub>2</sub>) (**Table 2.1**).

**Table 2.1** polymer composition of particle

Code	Composition of polymer		
	Reactive polymer	Thermo-responsive polymer	Amine polymer
M(TR/NAS)[30/70]	3	7	-
M(TR/NAS)[50/50]	5	5	-
M(TR/NAS)[30/70]	7	3	-
M(NH <sub>2</sub> )	-	-	10

For the DLS study, M(TR/NAS)[30/70] and M(NH<sub>2</sub>) solutions were diluted to 0.025–0.1 mg/mL, and equal volumes of the solutions were mixed prior to performing measurements between 25 and 60 °C. To measure optical transmittance change, the M(TR/NAS) solution was diluted to 5 mg/mL, and the measurement was performed with and without M(NH<sub>2</sub>) (1

mg/mL) at various temperatures. For TEM observation, the micellar solutions of M(TR/NAS)[70/30] and M(NH<sub>2</sub>) were prepared at various diluted concentrations (0.001 – 0.05 mg/mL). Samples were prepared by mixing respective concentrations of both solutions and then kept at 25 or 50 °C for 10 min. Subsequently, a drop of the sample was mounted on a carbon-coated TEM grid (COL-C10, 100 μm grid pitch, Okenshoji, Tokyo, Japan). All the samples were negatively stained with 2% samarium acetate, and excess liquid was removed with a filter paper. The samples were dried for 1 h and observed by TEM.

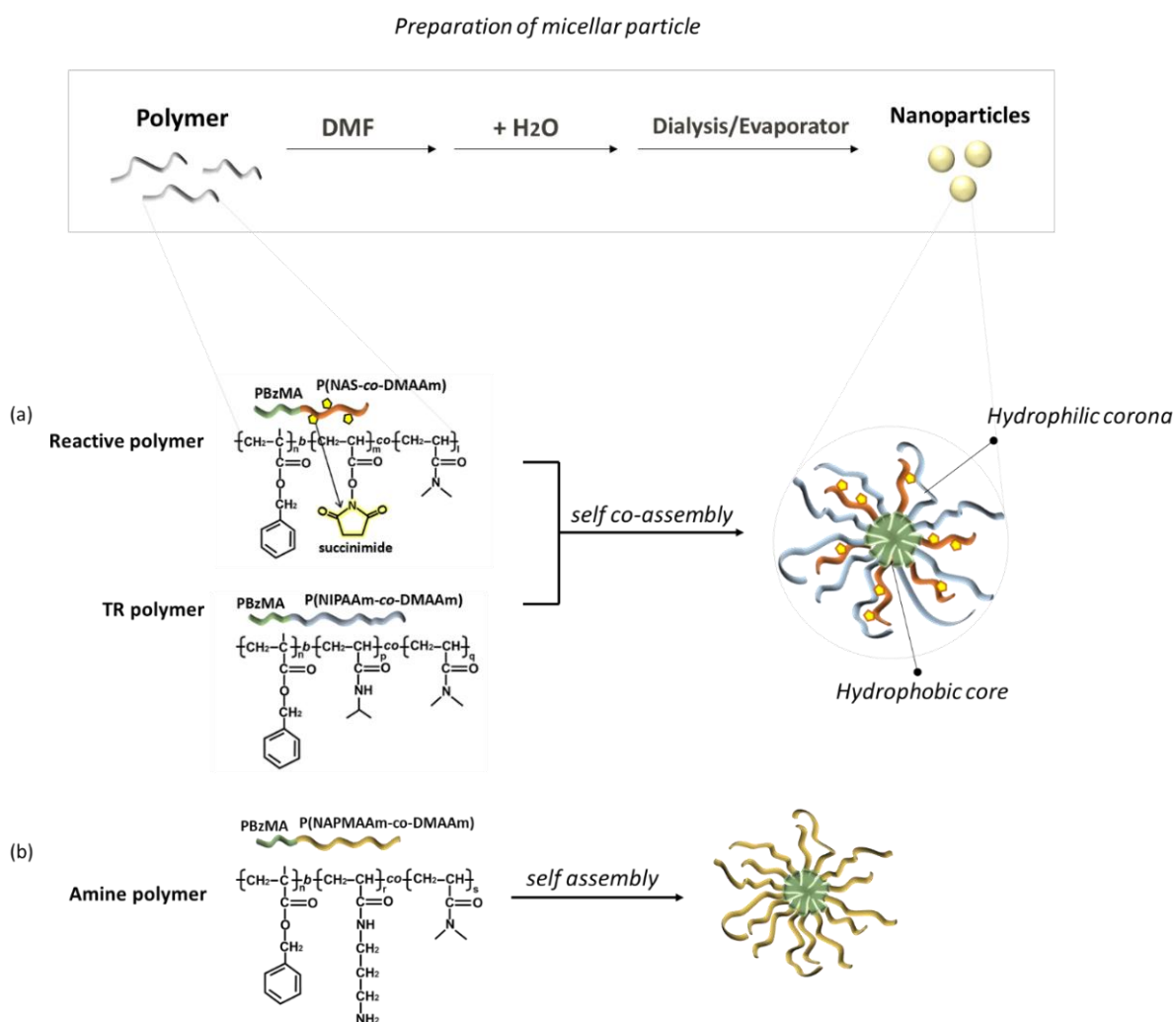


**Figure 2.3** Preparation of (a)hetero-armed thermo-responsive particle and (b) amino group possessing particle

### 2.2.9 Observation of fluidity change of solution by temperature change

The fluidity of the mixture of M(TR/NAS) and M(NH<sub>2</sub>) was observed by changing temperature at 25 and 50 °C. Briefly, 0.1 mL of M(TR/NAS) solutions (5–13 wt%) was poured into 2 mL vial and adjust pH in 8 using NaOH. Then, the equal volume of M(NH<sub>2</sub>) solutions (10 wt%) was added and gently mixed via pipetting. The fluidity change was observed by inverting the vial. The fluidity was evaluated as follows. The mixture showing high fluidity after inverting the vial was recorded as F. The mixture showing no fluidity and becoming a gel in the inverted vial was recorded as S.

### 2.2.10 Rheological measurement

The viscoelastic change of micellar solution was measured using the rheometer. The mixture of M(TR/NAS) and M(NH<sub>2</sub>) was placed on the rheometer plate. The solution was covered with silicon oil to avoid evaporation of water, and then the time sweep measurement was performed under the fixed frequency ( $\omega = 1$  Hz) and strain ( $\gamma = 1\%$ ). The measurement was proceeded at 25 °C for the first 20 min and then increased to 50 °C for another 20 min. The complex shear modulus,  $G^*$ , were calculated by following equation:

$$G^* = G' + iG'' \quad (1)$$

where  $G'$  and  $G''$  indicates storage and loss moduli, respectively.



## 2.3 Results and discussion

### 2.3.1. Characterization of diblock copolymers

The TR block copolymer (PBzMA-*b*-P(NIPAAm-*co*-DMAAm)), succinimide group introduced reactive block copolymer (PBzMA-*b*-P(NAS-*co*-DMAAm)), and primary amine introduced block copolymer (PBzMA-*b*-P(NAPMAAm-*co*-DMAAm)) were synthesized by RAFT polymerization. Firstly, hydrophobic PBzMA was synthesized using a RAFT agent of CPDT. Subsequently, functional segment of diblock copolymer was connected to  $\omega$ -terminal of PBzMA by RAFT polymerization using PBzMA as a macro-RAFT agent. The number-averaged molecular weight of PBzMA was 5380 g/mol, which was determined from the UV absorbance of the trithiocarbonate unit at 310 nm ( $\epsilon = 11,000$  L/mol/cm). The composition of the functional segment was determined by the monomer consumption determined by  $^1\text{H}$  NMR (**Figure 2.4**). The consumed monomer was determined by comparing the proton intensity of vinylic protons of monomers in the reaction solution before and after the reaction. The monomer unit ratio in the polymers was almost the same as that in the feed. In addition, number averaged molecular weight ( $M_n$ ) of diblock copolymers was calculated from monomer conversion. The monomer units of TR and reactive functional diblock copolymers were 195 (IPAAm/DMAAm=145/50) and 80 (NAS/DMAAm=8/72), respectively. Thus, chain length of TR polymer was more than two times longer than that of functional one.

The terminal dodecyltrithiocarbonate group on PBzMA-*b*-P(NIPAAm-*co*-DMAAm) and PBzMA-*b*-P(NAPMAAm-*co*-DMAAm) was converted into NIPAAm or DMAAm moieties by Michael addition reaction after aminolysis of dodecyltrithiocarbonate group. For the PBzMA-*b*-P(NAS-*co*-DMAAm), terminal conversion was performed by radical substituted reaction using AIBN to avoid the aminolysis of succinimide group by 2-ethanolamine. The terminal conversion was confirmed by the UV absorbance change of trithiocarbonate group at 310 nm

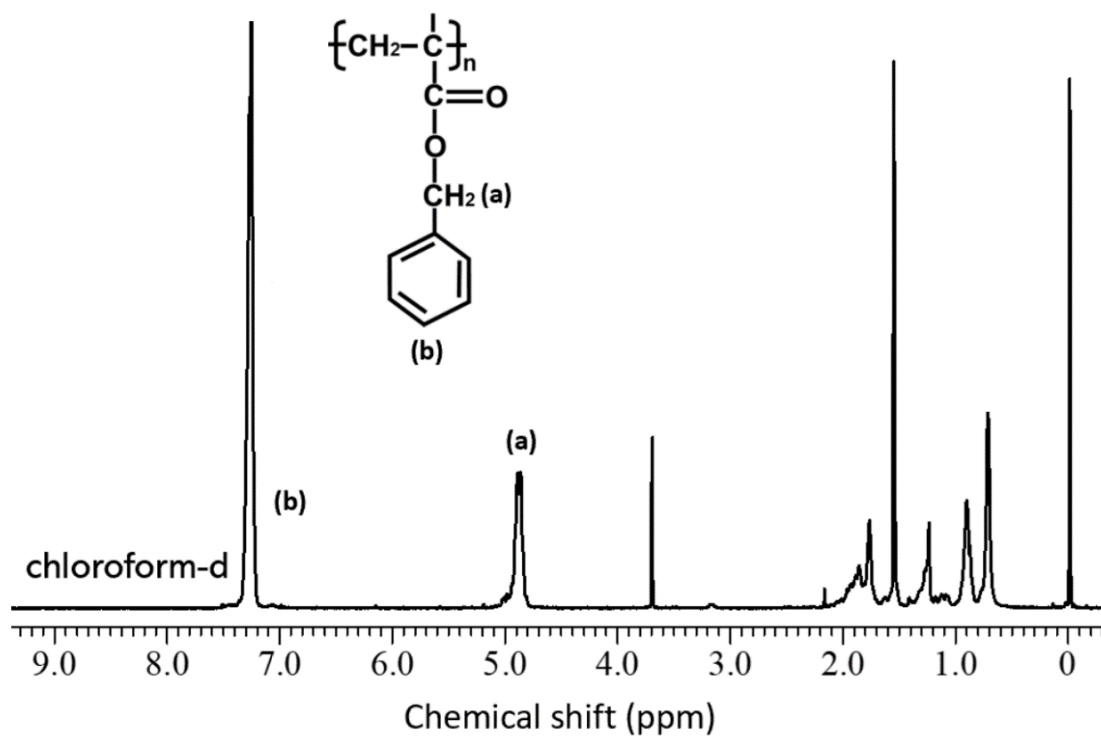
and the absorbance was completely disappeared after the reactions. Finally,  $^1\text{H}$  NMR of terminal converted polymers were measured and phenyl (5H, 7.26 ppm) and methylene (2H, 4.9 ppm) on BzMA, methylene (4H, 2.9 ppm) on NAS, methyne (1H, 4.0 ppm) and methyl (6H, 1.0 ppm) on NIPAAm, methyl (6H, 2.9ppm) on DMAAm, and methylene (4H, 2.8–3.0ppm) on NAPMAAm were respectively assigned (**Figure 2.5-2.7**). The characterization results of the obtained polymers are summarized in **Table 2.2**.

**Table 2.2** Characterization of composition of polymer and molecular weights.

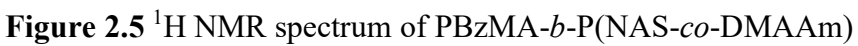
Code	BzMA <sup>a</sup>	DMAAm <sup>a</sup>	NAS <sup>a</sup>	NIPAAm <sup>a</sup>	NAPMAAm <sup>a</sup>	M <sub>n</sub> <sup>b</sup>
PBzMA- <i>b</i> -P(NAS- <i>co</i> -DMAAm)	28	72	8	-	-	13700
PBzMA- <i>b</i> -P(NIPAAm- <i>co</i> -DMAAm)	28	50	-	145	-	28500
PBzMA- <i>b</i> -P(NAPMAAm- <i>co</i> -DMAAm)	28	131	-	-	30	23600

<sup>a</sup>Degree of polymerization and number molecular weight was calculated by  $^1\text{H}$  NMR

<sup>b</sup>Calculated from monomer units determined by  $^1\text{H}$  NMR



**Figure 2.4**  $^1\text{H}$  NMR spectrum of PBzMA



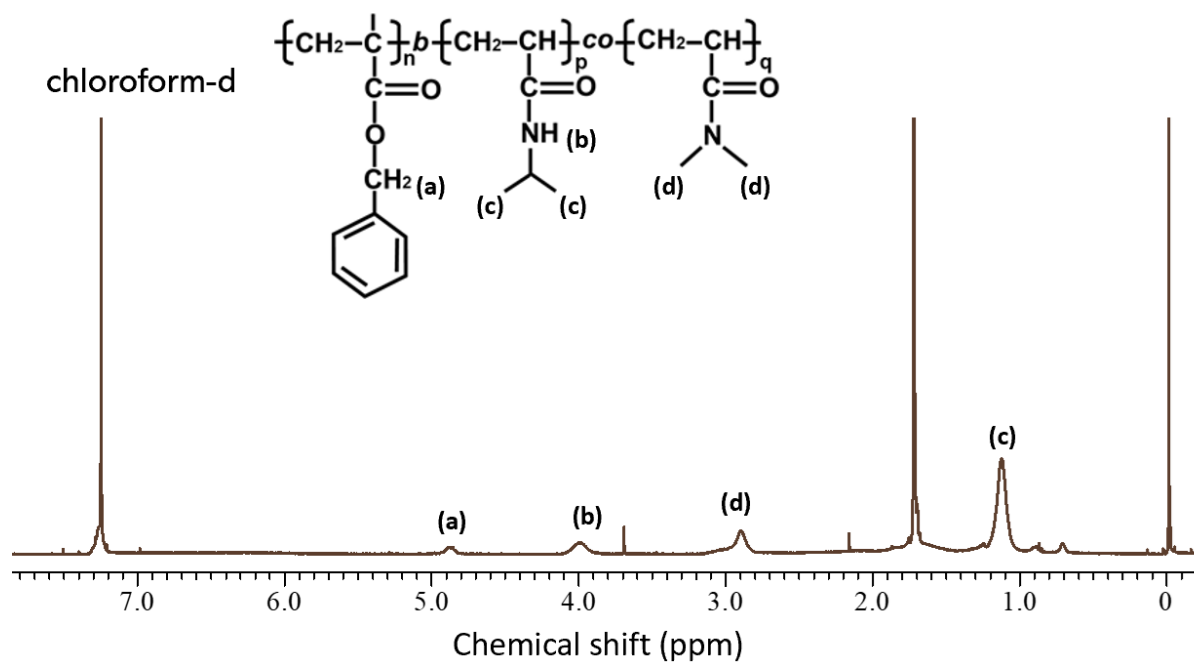


**Figure 2.6**  $^1\text{H}$  NMR spectrum of PBzMA-*b*-P(DMAAm-*co*-NIPAAm)

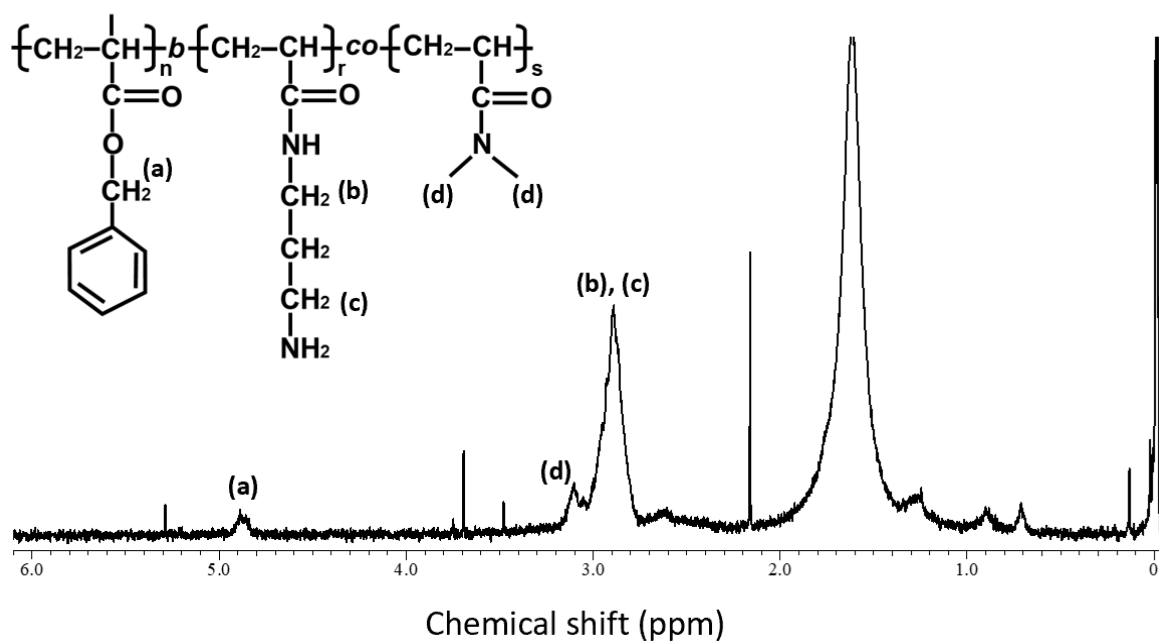


**Figure 2.7** <sup>1</sup>H NMR spectrum of PBzMA-*b*-P(NAPMAAm-*co*-NIPAAm)

### 2.3.2. Characterization of nanoparticle

PBzMA-*b*-P(NAS-*co*-DMAAm) and PBzMA-*b*-P(NIPAAm-*co*-DMAAm) were co-assembled in water via co-solvent evaporation method to form hetero-armed core shell nanoparticle. First, the reactivity of succinimide group on the corona-forming reactive chain was confirmed by mixing 5-amino fluorescein. After the reaction, fluorescent signal from the fluorescein molecule was clearly confirmed as below **Figure 2.8**. Thus, the succinimide on the corona of hetero-armed nanoparticle possessed the reactivity with primary amine.

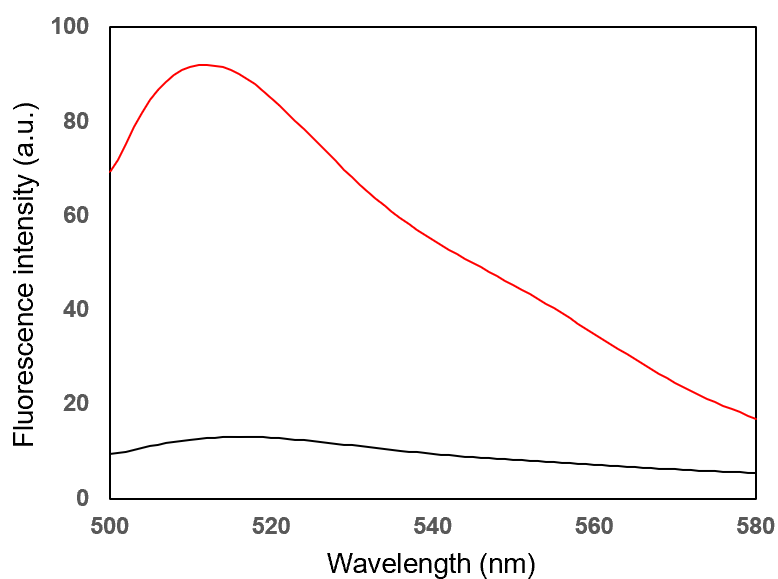


**Figure 2.8** Fluorescent spectra of PBzMA-*b*-P(DMAAm-*co*-NAS) in water before (black line) and after conjugating (red line) 5-aminofluorescein to NAS polymer.

In addition, the stability of the succinimide group in water was investigated (**Figure 2.9**). Although the succinimide group gradually decomposed in water, more than 95% of it remained after 1 day. Thus, the hydrolysis of the succinimide group was considered to be negligible for the duration of this experiment.

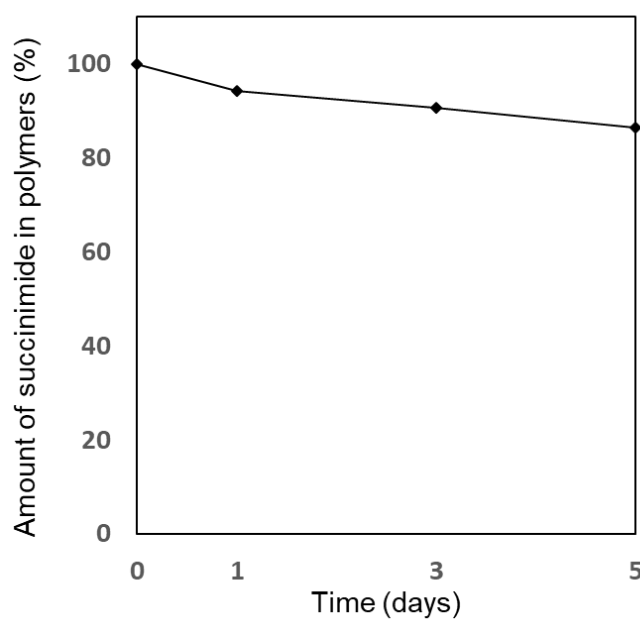


**Figure 2.9** Stability of succinimide group on PBzMA-b-P(NAS-co-DMAAm) in water. The amount of succinimide on the polymer was determined by  $^1\text{H}$  NMR.



PBzMA-*b*-P(NAS-co-DMAAm) and PBzMA-*b*-P(NIPAAm-co-DMAAm) were coassembled in water via a cosolvent evaporation method to form a heteroarmed core shell nanoparticle. We investigated the influence of the chain length of TR to prepare core-shell-type polymeric micelles. In the case of shorter TR chain with approximately 100 units, the micelle solution became opaque, and large aggregates were observed in DLS measurements (**Figure 2.10**). Therefore, a longer TR chain with 200 units was used to prepare a more stable polymeric micelle for further experiments.

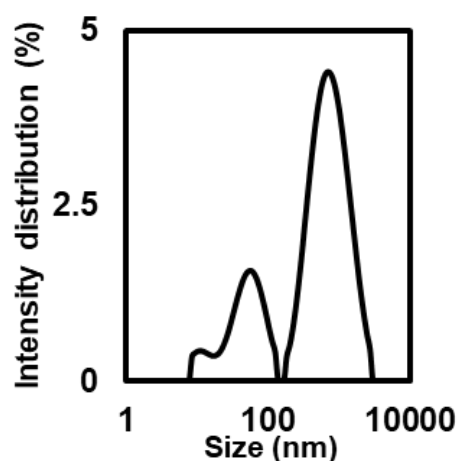


**Figure 2.10** Intensity vs average diameter of M(TR/NAS)[70/30] prepared from P(BzMA-*b*-P(NIPAAm-co-DMAAm) ([BzMA]/[NIPAAm]/[DMAAm] = 28/75/25 (unit)) and P(BzMA-*b*-P(NIPAAm-co-DMAAm) at 25 °C

*TR property of particle*

Subsequently, the optical transmittance changes of TR micelles, M(TR), was observed to confirm the phase transition temperature of TR polymer on nanoparticle (**Figure 2.11**). M(TR) showed the sharp phase transition at 39.7 °C. The phase transition temperature of M(TR) was higher than the that of PNIPAAm homopolymer micelles at 32 °C because of the introduction of hydrophilic DMAAm in TR segment.<sup>29</sup> The phase transition temperature of M(TR/NAS)[70/30] shift to 51 °C without showing any sudden transmittance change around 39.7 °C. Subsequently, the transmittance change of nanoparticle was observed in the presence of M(NH<sub>2</sub>). While M(TR) showed almost the same transmittance change behavior in the presence of M(NH<sub>2</sub>), M(TR/NAS)[70/30] showed decrease in the transmittance from 42 °C.

Heteroarmed TR polymeric micelles exhibited transmittance change at the higher temperature than homogeneous TR nanoparticle, M(TR). Our previous study reported the effect of the introduction of non-TR chain onto the TR polymeric micelles on TR behavior. According to the study, the hetero-armed TR polymeric micelles shift the cloud point of micellar solution due to the suppression of inter-micellar aggregation derived from hydrophobic interaction.<sup>26</sup> However, hydrophilic-hydrophobic phase transition change of TR chain occurs at the same temperature as the homogeneous TR polymeric micelle does. This indicated that the TR chain on M(TR/NAS)[70/30] started the phase transition from 39.7 °C, which was LCST of M(TR), even though the M(TR/NAS)[70/30] showed transmittance change at 51 °C. Therefore, succinimide on reactive chain appeared on the surface of on M(TR/NAS)[70/30] as the TR chain gradually shrunk from 39.7 °C. As the result, the succinimide group was allowed to contact with primary amine on M(NH<sub>2</sub>) to proceed coupling reaction from 39.7 °C, and then the transmittance change was observed due to the formation of aggregation between M(TR/NAS)[70/30] and M(NH<sub>2</sub>) from 42 °C.

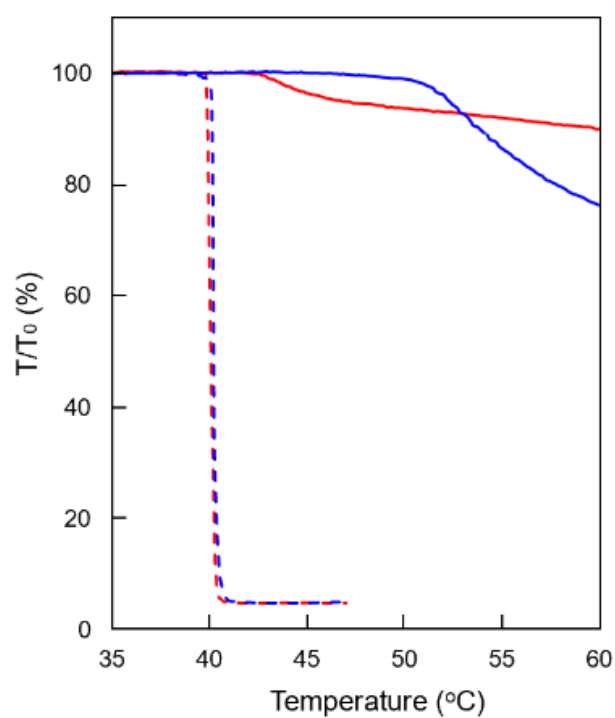


**Figure 2.11** Phase transition change of M(TR) (dotted-lines) and M(TR/NAS)[70/30] (solid lines) in the presence (red lines) and absence (blue lines) of M(NH<sub>2</sub>).  $T_0$  is the absorbance of the solution at 35 °C. Heating rate: 0.2 °C/min.

To examine the inter-micellar reaction between M(TR/NAS)[70/30] and M(NH<sub>2</sub>), the particle size change of hetero-armed nanoparticle was observed using DLS (**Figure 2.12**) and TEM (**Figure 2.13**). The M(NH<sub>2</sub>) exhibited unimodal peak and the volume average diameter was  $38 \pm 20$  nm in DLS histogram (**Figure 2.12 (A)**). The M(NH<sub>2</sub>) particles were observed as uniformly well-dispersed in TEM image as well (**Figure 2.13**).

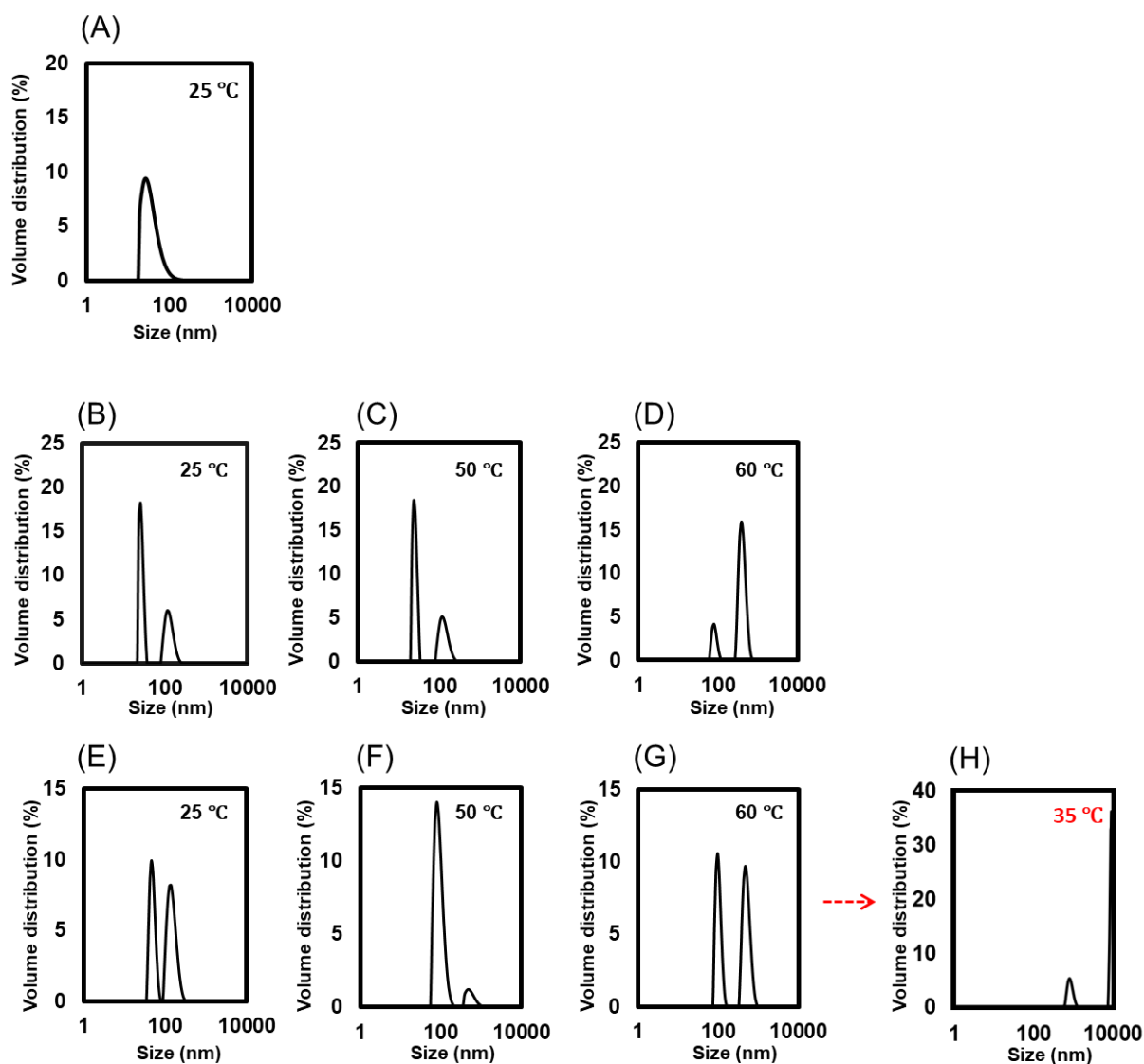


**Figure 2.12** The Particle size of (A) M(NH<sub>2</sub>) at 25 °C, M(TR/NAS) at (B) 25 °C, (C) 50 °C and (D) 60 °C. The particle size after mixing M(TR/NAS)[70/30] and M(NH<sub>2</sub>) at (E) 25 °C, (F) 50 °C, (G) 60 °C and after decreasing temperature below the LCST (H).

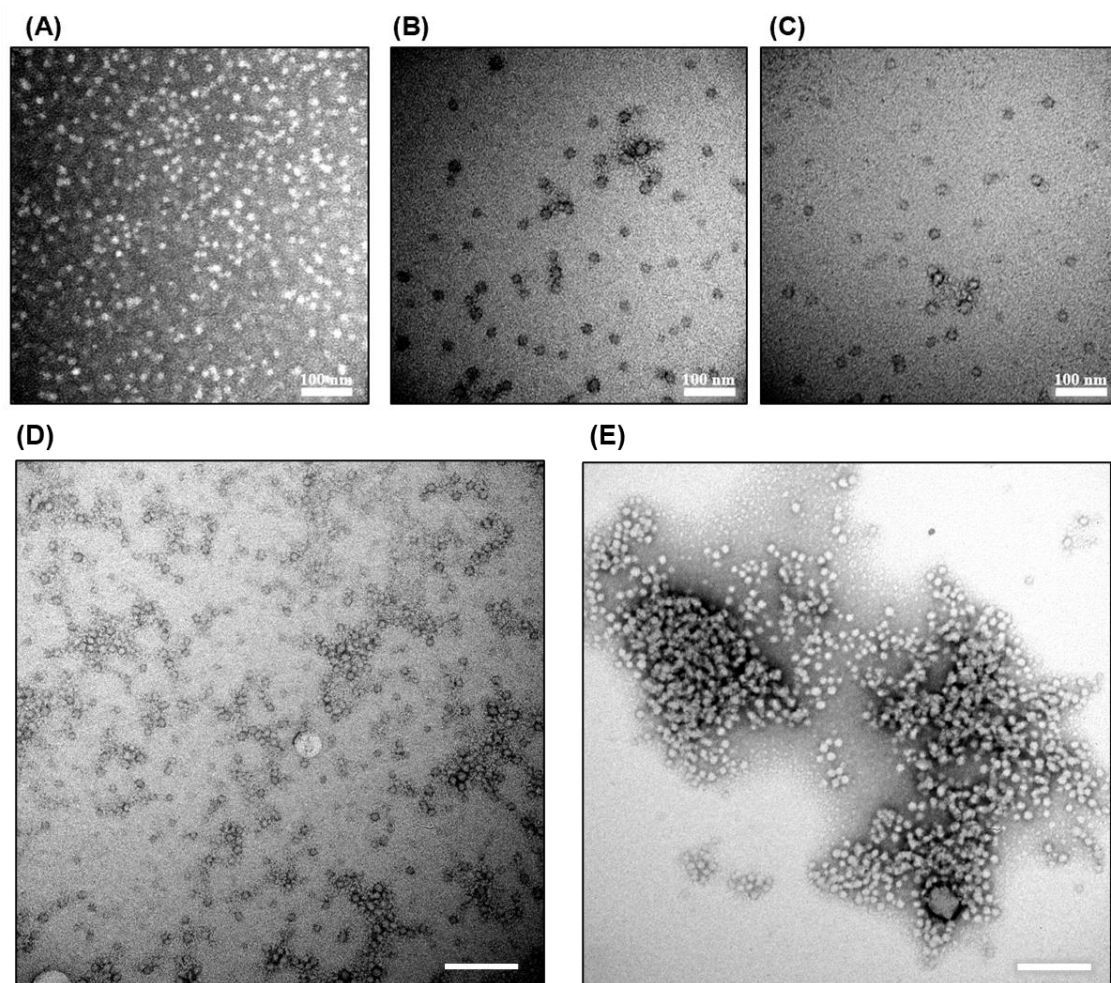


**Figure 2.13** TEM image of mixture of (A)  $M(NH_2)$ , (B)  $M(TR/NAS)[70/30]$  at 25 °C and (C)  $M(TR/NAS)[70/30]$  at 50 °C, and the mixture of  $M(TR/NAS)[70/30]$  and  $M(NH_2)$  at (D) 25 °C to (E) 50 °C. Scale bars: 200 nm.

The size of M(NH<sub>2</sub>) particle did not show any change by the temperature (data not shown). The M(TR/NAS)[70/30] showed bimodal peak at  $48 \pm 7$  and  $148 \pm 37$  nm at 25 °C. In the TEM image, most particles were observed as single particle, while some were observed as small inter-micellar aggregations (**Figure 2.12 (B)**). Thus, the small aggregation peak (the second peak in bimodal graph) detected in DLS was attributed to the inter-micellar aggregation. In addition, M(TR/NAS)[70/30] did not show any particle size changes upon temperature increasing above LSCT of TR polymer (39.7 °C) to 50 °C (**Figure 2.11**); however, size changes were observed upon increasing the temperature in the presence of M(NH<sub>2</sub>). When M(NH<sub>2</sub>) was added to the M(TR/NAS)[70/30], it showed bimodal peak at  $25 \pm 2$  and  $133 \pm 34$  nm below the LCST of TR chain. The second peak indicating small inter-micellar aggregation became large after the addition of M(NH<sub>2</sub>). Interestingly, at 50 °C where the UV transmission changes were observed in the presence of M(NH<sub>2</sub>), the single nanoparticle peak completely disappeared. In addition, the large submicron size aggregation (with a diameter of 730 nm) was detected in the mixture, while M(TR/NAS)[70/30] hardly showed size change at the same temperature range (25 °C to 50 °C) in the absence of M(NH<sub>2</sub>). This result also corresponded to the TEM image, where they showed the large inter-micellar aggregation when the temperature increased from 25 to 50 °C (**Figure 2.13 (D-E)**). When the temperature reached to 60 °C, the M(TR/NAS)[70/30] formed large aggregations of micelles. Only M(TR/NAS)[70/30] without M(NH<sub>2</sub>) also showed an aggregation peak, which was attributed to the TR aggregation as it was observed by UV transmission change above 51 °C. In addition, the submicron aggregation hardly dissociated upon lowering temperature below LCST (39.7 °C) again.

Below the LCST of TR chain, the volume distribution of inter-micellar aggregation continuously became larger in the mixture of M(TR/NAS)[70/30] and M(NH<sub>2</sub>). This result indicated that the interaction slightly occurred between M(TR/NAS)[70/30] and M(NH<sub>2</sub>) even below the LCST of TR chain. However, the particle size became significantly large after the

phase transition had taken place in the TR chain and then finally formed the huge aggregation. This strongly suggested that the inter-micellar reaction between succinimide on M(TR/NAS)[70/30] and primary amine on M(NH<sub>2</sub>) enhanced the formation of the large aggregation after the phase transition of TR chain. Because of the crosslinking formation through the stable covalent bond between the succinimide and amine groups, the inter-micellar aggregation in the mixture hardly dissociated once it formed and large aggregation peak was still remaining at lowering to 35 °C.

According to the results, the reaction between the succinimide group on hetero-armed nanoparticle and primary amine was accelerated by the phase transition of TR polymer on hetero-armed nanoparticle. Below the LCST of TR chain, the extended TR polymer chain covered outermost surface of nanoparticle and suppressed the contact of amine group on M(NH<sub>2</sub>) due to the exclusive volume effect of polymer chain. In contrast, TR chain gradually dehydrated and followed by increasing hydrophobicity above LCST. And then, corona-forming TR chain shrank so that the succinimide group allowed to expose on the surface of hetero-armed nanoparticle. As the result, the exposed succinimide group proceeded the reaction with amino group on the M(NH<sub>2</sub>) to form covalent bond between nanoparticles. Therefore, the aggregation formation in the mixture of M(TR/NAS) and M(NH<sub>2</sub>) hardly decomposed by temperature lowering below LCSR, while M(TR/NAS) aggregation, which was formed by physical hydrophobic interaction, showed reversibility by temperature change across the LCST.

### 2.3.3. Thermo-responsive hydrogel formation

Using high concentration M(TR/NAS) and M(NH<sub>2</sub>) solution, the TR hydrogel formation behavior was investigated. In particular, the ratio of TR and reactive polymer chain in hetero-armed micelle was varied to investigate the optimal number of succinimide group to form a stiff hydrogel by varying the temperature.



First, the controllability of the reaction was examined using polyallylamine, a linear-type amine polymer, instead of  $M(NH_2)$ . The reaction between  $M(TR/NAS)[70/30]$  and polyallylamine could not be controlled by the phase transition of the TR chain across the LCST. Even below the LCST of the TR chain, the reaction proceeded continuously to finally form a hydrogel (data not shown).

Subsequently, fluidity of the  $M(TR/NAS)$  and  $M(NH_2)$  was monitored at 25 and 50 °C which is summarized in **Figure 2.14**.  $M(TR/NAS)[70/30]$  exhibited a fluidic state regardless of the concentration change at 25 °C and showed no viscosity change at 50 °C. In contrast,  $M(TR/NAS)[50/50]$  and  $M(TR/NAS)[30/70]$  increased the viscosity of the solution as the concentration of micelles increased after mixing with  $M(NH_2)$  at 25 °C and showed no fluidity at the concentration higher than 11 and 9 wt%, respectively. Upon heating temperature at 50 °C, the fluidity of the solution became higher than that of at 25 °C and  $M(TR/NAS)[50/50]$  and  $M(TR/NAS)[30/70]$  became a stiff hydrogel at the concentration higher than 9 and 7 wt%. Therefore, in the presence of  $M(NH_2)$ ,  $M(TR/NAS)[50/50]$  and  $M(TR/NAS)[30/70]$  formed a hydrogel by controlling temperature across the LCST of TR chain at a concentration of 9-10 and 7–8 wt%, respectively. Based on the phase transition table, sol-gel transition map was depicted, representing a controllable area (**Figure 2.15**).

(A)

Concentration of M(TR/NAS) (wt%)	M(TR/NAS) [70/30]	M(TR/NAS) [50/50]	M(TR/NAS) [30/70]
13	F	S	S
12	F	S	S
11	F	S	S
10	F	F	S
9	F	F	S
8	F	F	F
7	F	F	F
6	F	F	F
5	F	F	F

F highly fluidic; flow in a inverted vial  
S less fluidic; not flow in a inverted vial

(B)

Concentration of M(TR/NAS) (wt%)	M(TR/NAS) [70/30]	M(TR/NAS) [50/50]	M(TR/NAS) [30/70]
13	F	S	S
12	F	S	S
11	F	S	S
10	F	S	S
9	F	S	S
8	F	F	S
7	F	F	S
6	F	F	F
5	F	F	F

**Figure 2.14** Phase transition table of Sol-Gel behavior after mixing of 10 wt% of M(NH<sub>2</sub>) with M(TR/NAS) solution at various concentration (5-13 wt%) at (A) 25 °C and (B) 45 °C

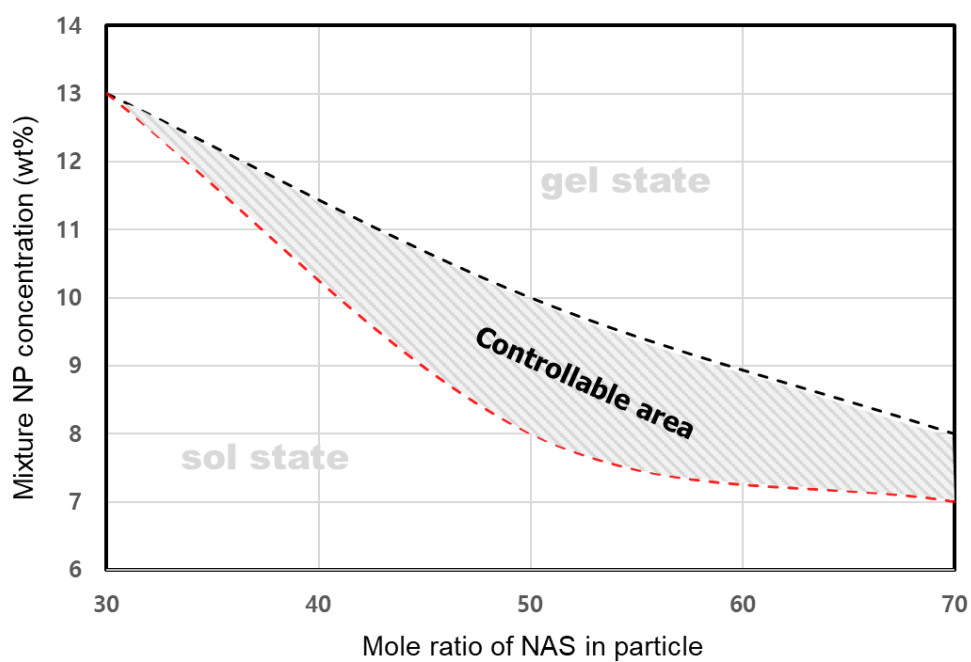


**Figure 2.15** Sol-Gel phase transition map of mixing of 10 wt% M(NH<sub>2</sub>) with M(TR/NAS) solution at various concentration (5-13 wt%) at (a) 25 °C (black line) and (b) 45 °C (red line).

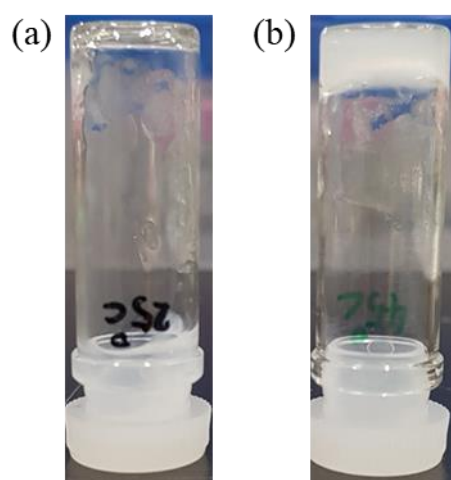


**Figure 2.16** Photo of gel formation at (a) 25 °C to (b) 50 °C in an inverted vial

To confirm the temperature responsive fluidity change of the solution, viscoelasticity of solution was studied by rheometer measurement (**Figure 2.17**).

Only the M(TR/NAS) solution showed very low  $G^*$  and no change in  $G^*$  value by temperature, which indicates that viscosity does not change by temperature. First, the M(TR/NAS) and M(NH<sub>2</sub>) were mixed using 10 wt% solution. The mixture of M(TR/NAS)[70/30] and M(NH<sub>2</sub>) gradually increased  $G^*$  and nearly plateau after 20 min at 25 °C. The temperature was subsequently increased to 45 °C; however, only a slight change in  $G^*$  value was confirmed. In contrast the mixture of M(TR/NAS)[50/50] and M(NH<sub>2</sub>) increased the  $G^*$  in response to temperature change and  $G^*$  value became 484 Pa after 20 min at 45 °C. The mixture of M(TR/NAS)[30/70] and M(NH<sub>2</sub>) increased  $G^*$  value to 264 Pa even at 25 °C and showed negligible temperature responsiveness at 45 °C (**Figure 2.17 (C)**).

Subsequently, the concentration effect on modulus change was evaluated using M(TR/NAS)[50/50] (**Figure 2.17 (D-F)**). At 25 °C, regardless of the concentration, the mixture showed similar  $G^*$  value. After heating up to 50 °C, the shear modulus became larger as the polymer nanoparticle concentration increased. However, low concentration of mixture did not increase the  $G^*$  at the high temperature which was similar result as M(TR/NAS)[70/30] was shown. Thus, the crosslinking formation efficiently occurred as the nanoparticle concentration increased.

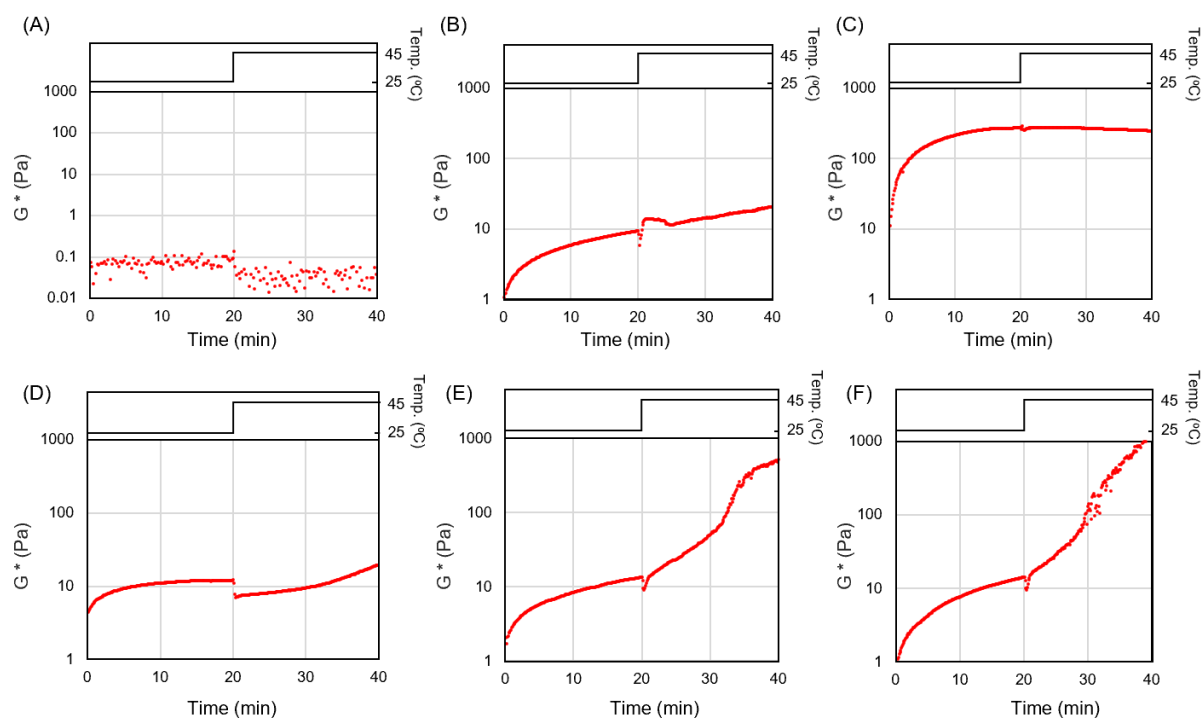


**Figure 2.17** Time sweep rheological measurement for Sol-Gel behavior of (A) M(TR/NAS)[70/30], 10 wt% of M(NH<sub>2</sub>) mixed with (B) 10 wt% of M(TR/NAS)[70/30], (C) 10 wt% of M(TR/NAS)[30/70], 10wt (D) 5 wt% of M(TR/NAS)[50/50], (E) 10 wt% of M(TR/NAS)[50/50], (F) 13 wt% of M(TR/NAS)[50/50] at 25 °C (0-20 min) and 45 °C (20-40 min).

The results indicated that the concentration of mixture and the composition of shell forming chain on hetero-armed micelles were important factors to optimized for achieving the responsiveness of  $G^*$  by the temperature signal. After mixing  $M(\text{TR}/\text{NAS})$  and  $M(\text{NH}_2)$ , increase in  $G^*$  value was observed at 25 °C, which was attributed to the partial reaction among the micelles as observed in DLS and TEM measurements.  $M(\text{TR}/\text{NAS})[70/30]/M(\text{NH}_2)$  and  $M(\text{TR}/\text{NAS})[50/50]/M(\text{NH}_2)$  showed similar  $G^*$  value, while  $M(\text{TR}/\text{NAS})[30/70]/M(\text{NH}_2)$  increased it continuously reached to more than 100 Pa. This indicated the surface of micelle was covered with corona-forming TR polymer when the composition of TR chain on the shell was more than 50%. In other words, the density of TR chain on corona was insufficient to reduce the contact of  $M(\text{NH}_2)$  by exclusive volume effect of TR chain when the composition of TR chain on hetero-armed micelles was reduced to 30%. Therefore,  $M(\text{TR}/\text{NAS})[30/70]/M(\text{NH}_2)$  showed uncontrollable increase in the  $G^*$  below the LCST of TR chain as the result of unavoidable crosslinking formation. In addition, the particle structure of the amine was essential to control the reaction by the covered TR chain because, compared to the spherical-type  $M(\text{NH}_2)$ , a linear-type polymer could easily penetrate the TR core and access the NAS unit on the reactive chain. Therefore, the exclusive volume effect of the polymer was considered as a key parameter to control the reaction between the succinimide and amine by the morphological change of TR chain on micelles.

After increasing temperature at 50 °C, the mixture showed different  $G^*$  change depending both on the concentration and composition of  $M(\text{TR}/\text{NAS})$ .  $M(\text{TR}/\text{NAS})[70/30]$  showed negligible TR  $G^*$  change, although the enhancement of reaction between the micelle was occurred as observed in DLS measurement. The similar tendency was observed in the low concentration of  $M(\text{TR}/\text{NAS})[50/50]$ . At this condition, the number of succinimide group was considerably lower than that of amine group on  $M(\text{NH}_2)$ , and thus the network formation was insufficient to increase the viscosity of mixture. In other words, increasing the amount of succinimide groups

was essential to form a stable hydrogel, and the ratio of the succinimide group to the amino group should be less than 9 to control the viscosity of solution by the temperature stimulus (**Table 2.3**).

**Table 2.3** Composition of polymer micelle

Code	Composition of polymer		Mixing condition for rheometer			G*	
	Reactive polymer	Thermo-responsive polymer	Concentration of M(TR/NAS) (wt%)	Concentration of M(NH <sub>2</sub> ) (wt%)	Molar ratio of succinimide and amino group in mixture	G* at 25 °C <sup>a</sup>	G* at 50 °C <sup>a</sup>
M(TR/NAS)[70/30]	3	7	10	10	1:14.5	8	18
			8	2	1:3.6	0.5	238
			10	2	1:2.9	0.9	247
M(TR/NAS)[50/50]	5	5	5	10	1:15.3	10	19
			10	10	1:7.7	12	484
			13	10	1:5.9	14	1108
M(TR/NAS)[30/70]	7	3	10	10	1:4.7	279	249

Consequently, the composition of shell-forming chain and concentration of each particle were related to the viscosity of the solution at low temperature, while the ratio of succinimide and amino groups was crucial to control the viscosity of the solution by temperature change.

According to the result of FT-IR analysis (**Figure 2.18**), the absorbance at approximately 1605 cm<sup>-1</sup>, attributed to the stretching vibration of C=O bonds in the amide, became stronger with the increase in the concentration of M(TR/NAS). This indicated that amide bonds were formed as a result of the reaction between the succinimide on M(TR/NAS) and primary amine on M(NH<sub>2</sub>). Interestingly, the mixture of 5 wt% M(TR/NAS) and 5 wt% M(NH<sub>2</sub>) showed almost the same intensity as the mixture of 5 wt% M(TR/NAS) and 10 wt% M(NH<sub>2</sub>). The result indicated that the number of amine groups on the M(NH<sub>2</sub>) was larger than that of the



succinimide groups on M(TR/NAS), as calculated. Therefore, the ratio of the succinimide and amine groups was considered important for the formation of the network structure.

Finally, in addition to the above discussion, the TR behavior of M(TR/NAS)[70/30] was observed by changing the concentration of M(NH<sub>2</sub>) to 2 wt% to optimize the ratio for developing hydrogel by heating (**Figure 2.19**). As the result, G\* value of mixture became less than 1 Pa which was almost the same as M(TR/NAS)[70/30] solution of *ca* 0.1 Pa. and the temperature responsiveness of G\* value was clearly observed by using 8 and 10 wt% of M(TR/NAS)[70/30] solution.

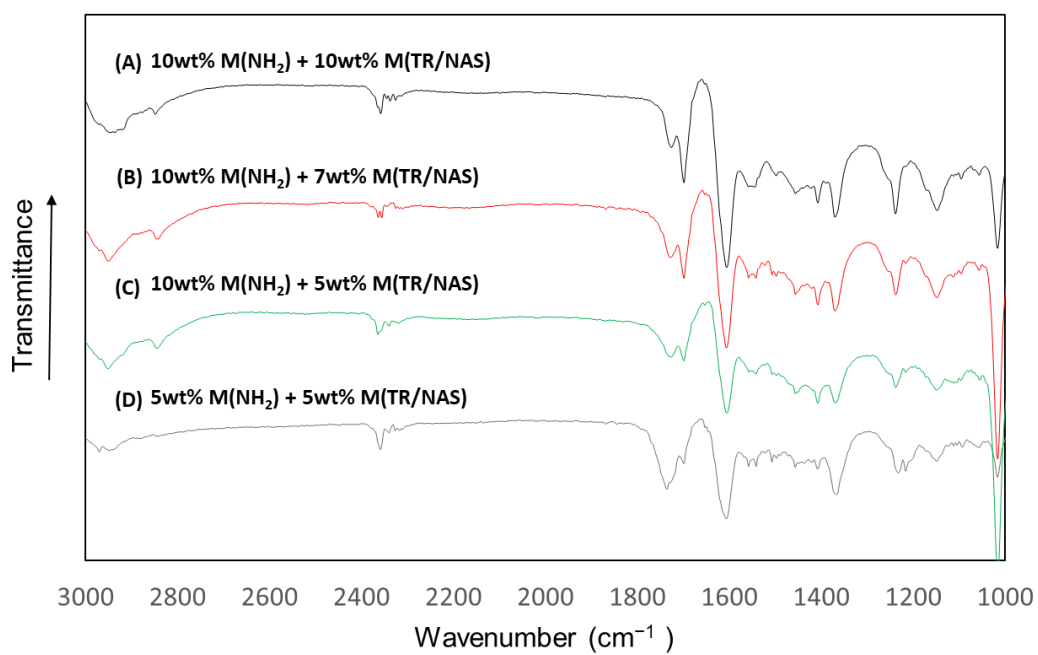


**Figure 2.18** IR spectra of mixtures of 10 wt%  $\text{M}(\text{NH}_2)$  and (A) 10 wt%, (B) 7 wt%, and (C) 5 wt% of  $\text{M}(\text{TR}/\text{NAS})$ , and (D) mixture of 5 wt%  $\text{M}(\text{NH}_2)$  and 5 wt%  $\text{M}(\text{TR}/\text{NAS})$ .

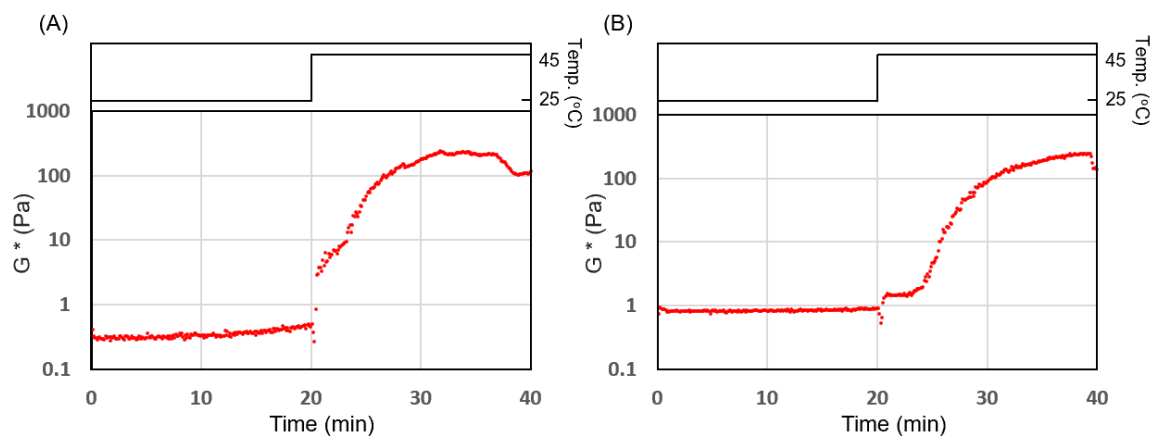


**Figure 2.19** Time sweep rheological measurement for sol-gel behavior of (A) 8 and (B) 10 wt% of M(TR/NAS)[70/30] and 2 wt% of M(NH<sub>2</sub>) at 25 °C (0-20 min) and 45 °C (20-40 min).

**Table 2.4** The ratio of succinimide and amine group ([Succinimide]/[amine] (mol/mol)) in the M(TR/NAS) and M(NH<sub>2</sub>) mixture. Concentration of M(NH<sub>2</sub>) is 10 wt%.

Concentration of M(TR/NAS) (wt%)	M(TR/NAS)[70/30]	M(TR/NAS)[50/50]	M(TR/NAS)[30/70]
5	29	15.3	9.4
6	24.2	12.8	7.8
7	20.7	11.0	6.7
8	18.1	9.6	5.9
9	16.1	8.6	5.2
10	14.5	7.7	4.7
11	13.2	7.0	4.3
12	12.1	6.4	3.9
13	11.2	5.9	3.6

## 2.4 Conclusions

In this study, we prepared a TR hetero-armed polymeric micelle using two different kinds of amphiphilic block copolymer possessing amino-reactive or TR segments. The reactivity of the succinimide group introduced on the shell of micelle was successfully controlled by thermally induced conformation change of the temperature-responsive polymer. The reaction between succinimide and amino group on the particles was significantly reduced when the outermost surface of micelles was covered with extended TR polymer below the LCST. After shrinkage of the TR polymer by heating, the succinimide group was exposed to the surface of micelles, and thus the coupling reaction between succinimide and amino group on the particles could rapidly proceed. By utilizing TR reactivity change property, the high-concentration nanoparticle solution could change the viscoelasticity and gelation was occurred only by temperature control across the LCST of the TR polymer. The hetero-armed TR polymeric micelle has potential for controlling the reaction of functional group through the morphological change of TR chain. Thus, this TR micellar system is promising for further uses for biomaterials. In particular, in situ gels for use as an embolization agent require injectability at temperatures within the physiological range. The hetero-armed TR polymeric micelle can potentially maintain its fluidity because of the shielding effect of the longer TR chain. In addition, the polymeric micelle can potentially be used for controlling a wide range of chemical reactions such as Michael addition for preparing TR responsive in situ hydrogels.

## 2.5 Reference

1. Zhou, F.; Chen, L.; An, Q.; Chen, L.; Wen, Y.; Fang, F.; Zhu, W.; Yi, T., Novel hydrogel material as a potential embolic agent in embolization treatments. *Sci. Rep.* **2016**, *6* (1), 32145.
2. Avery, R. K.; Albadawi, H.; Akbari, M.; Zhang, Y. S.; Duggan, M. J.; Sahani, D. V.; Olsen, B. D.; Khademhosseini, A.; Oklu, R., An injectable shear-thinning biomaterial for endovascular embolization. *Sci. Transl. Med* **2016**, *8* (365), 365ra156.
3. Hong, Y.; Zhou, F.; Hua, Y.; Zhang, X.; Ni, C.; Pan, D.; Zhang, Y.; Jiang, D.; Yang, L.; Lin, Q., A strongly adhesive hemostatic hydrogel for the repair of arterial and heart bleeds. *Nat. Commun.* **2019**, *10* (1), 1-11.
4. Li, L.; Yan, B.; Yang, J.; Huang, W.; Chen, L.; Zeng, H., Injectable Self-Healing Hydrogel with Antimicrobial and Antifouling Properties. *ACS Applied Materials & Interfaces* **2017**, *9* (11), 9221-9225.
5. Hennink, W. E.; van Nostrum, C. F., Novel crosslinking methods to design hydrogels. *Adv. Drug Deliv. Rev.* **2002**, *54* (1), 13-36.
6. Lee, B. H.; West, B.; McLemore, R.; Pauken, C.; Vernon, B. L., In-situ injectable physically and chemically gelling NIPAAm-based copolymer system for embolization. *Biomacromolecules* **2006**, *7* (6), 2059-2064.
7. Stenekes, R. J. H.; Hennink, W. E., Polymerization kinetics of dextran-bound methacrylate in an aqueous two phase system. *Polymer* **2000**, *41* (15), 5563-5569.
8. Yoshida, Y.; Kawahara, K.; Inamoto, K.; Mitsumune, S.; Ichikawa, S.; Kuzuya, A.; Ohya, Y., Biodegradable injectable polymer systems exhibiting temperature-responsive irreversible sol-to-gel transition by covalent bond formation. *ACS Biomater. Sci. Eng.* **2017**, *3* (1), 56-67.
9. Xu, J.; Liu, Y.; Hsu, S.-h., Hydrogels based on Schiff base linkages for biomedical applications. *Molecules* **2019**, *24* (16), 3005.
10. DeForest, C. A.; Polizzotti, B. D.; Anseth, K. S., Sequential click reactions for synthesizing and patterning three-dimensional cell microenvironments. *Nat. Mat.* **2009**, *8* (8), 659-664.
11. DeForest, C. A.; Anseth, K. S., Cytocompatible click-based hydrogels with dynamically tunable properties through orthogonal photoconjugation and photocleavage reactions. *Nat. Chem.* **2011**, *3* (12), 925-931.
12. Azagarsamy, M. A.; Anseth, K. S., Bioorthogonal click chemistry: An indispensable tool to create multifaceted cell culture scaffolds. *ACS Macro Let.* **2013**, *2* (1), 5-9.

13. Diryak, R.; Kontogiorgos, V.; Ghorri, M. U.; Bills, P.; Tawfik, A.; Morris, G. A.; Smith, A. M., Behavior of in situ cross-linked hydrogels with rapid gelation kinetics on contact with physiological fluids. *Macromol. Chem. Phys.* **2018**, *219* (8), 1700584.
14. Qu, J.; Zhao, X.; Ma, P. X.; Guo, B., pH-responsive self-healing injectable hydrogel based on N-carboxyethyl chitosan for hepatocellular carcinoma therapy. *Acta Biomater.* **2017**, *58*, 168-180.
15. Steele, A. N.; Stapleton, L. M.; Farry, J. M.; Lucian, H. J.; Paulsen, M. J.; Eskandari, A.; Hironaka, C. E.; Thakore, A. D.; Wang, H.; Yu, A. C.; Chan, D.; Appel, E. A.; Woo, Y. J., A biocompatible therapeutic catheter-deliverable hydrogel for in situ tissue engineering. *Adv. Healthcare Mater.* **2019**, *8* (5), 1801147.
16. Patenaude, M.; Campbell, S.; Kinio, D.; Hoare, T., Tuning gelation time and morphology of injectable hydrogels using ketone-hydrazide cross-linking. *Biomacromolecules* **2014**, *15* (3), 781-790.
17. Yan, S.; Wang, W.; Li, X.; Ren, J.; Yun, W.; Zhang, K.; Li, G.; Yin, J., Preparation of mussel-inspired injectable hydrogels based on dual-functionalized alginate with improved adhesive, self-healing, and mechanical properties. *J. Mater. Chem. B* **2018**, *6* (40), 6377-6390.
18. Jiao, Y.; Gyawali, D.; Stark, J. M.; Akcora, P.; Nair, P.; Tran, R. T.; Yang, J., A rheological study of biodegradable injectable PEGMC/HA composite scaffolds. *Soft Matter* **2012**, *8* (5), 1499-1507.
19. Cohen, S. G., The effects of temperature on the polymerization of styrene. *J. Am. Chem. Soc.* **1945**, *67* (1), 17-20.
20. Schild, H. G., Poly(*N*-isopropylacrylamide): experiment, theory and application. *Prog. Polym. Sci.* **1992**, *17* (2), 163-249.
21. Ma, Y.; Tang, Y.; Billingham, N. C.; Armes, S. P.; Lewis, A. L., Synthesis of biocompatible, stimuli-responsive, physical gels based on ABA triblock copolymers. *Biomacromolecules* **2003**, *4* (4), 864-868.
22. Sahu, A.; Choi, W. I.; Tae, G., A stimuli-sensitive injectable graphene oxide composite hydrogel. *Chem. Commun.* **2012**, *48* (47), 5820-5822.
23. Nakayama, M.; Okano, T., Multi-targeting cancer chemotherapy using temperature-responsive drug carrier systems. *React. Funct. Polym.* **2011**, *71* (3), 235-244.
24. Ponce, A. M.; Vujaskovic, Z.; Yuan, F.; Needham, D.; Dewhirst, M. W., Hyperthermia mediated liposomal drug delivery. *Int. J. Hyperth.* **2006**, *22* (3), 205-213.

25. Akimoto, J.; Tamate, R.; Okazawa, S.; Akimoto, A. M.; Onoda, M.; Yoshida, R.; Ito, Y., Reactivity control of polymer functional groups by altering the structure of thermoresponsive triblock copolymers. *ACS Omega* **2019**, *4* (15), 16344-16351.
26. Akimoto, J.; Ito, Y.; Okano, T.; Nakayama, M., Controlled aggregation behavior of thermoresponsive polymeric micelles by introducing hydrophilic segments as corona components. *J. Polym. Sci. A: Polym. Chem.* **2018**, *56* (15), 1695-1704.
27. Akimoto, J.; Lin, H.-P.; Li, Y.-K.; Ito, Y., Controlling the electrostatic interaction using a thermal signal to structurally change thermoresponsive nanoparticles. *Colloid. Surf. A* **2019**, *577*, 27-33.
28. Akimoto, J.; Nakayama, M.; Sakai, K.; Okano, T., Temperature-induced intracellular uptake of thermoresponsive polymeric micelles. *Biomacromolecules* **2009**, *10* (6), 1331-1336.
29. Takei, Y. G.; Aoki, T.; Sanui, K.; Ogata, N.; Okano, T.; Sakurai, Y., Temperature-responsive bioconjugates. 2. Molecular design for temperature-modulated bioseparations. *Bioconjug. Chem.* **1993**, *4* (5), 341-346.



---

## Chapter 3

### 3. Photo reactive polymers: PEG-based azide polymer for surface modification

---

#### 3.1 Introduction

Coating a material with a polymer alters its surface properties from those of the original material to those of the applied polymer. In addition, stimuli-responsiveness, superhydrophobicity, and ligands can be introduced through surface functionalization, which is readily achieved by simply introducing a functional polymer onto the material.<sup>1-3</sup> Functionalization of a surface can facilitate control of target-material interactions while suppressing non-specific interactions with the surface, thereby enhancing the signal to noise ratio in a variety of detection techniques.<sup>4</sup> Consequently, functional surfaces have been used in molecular detection and separation systems.<sup>5,6</sup>

Polymer-coated surfaces are prepared by introducing polymers onto surfaces through physical or chemical interactions. In particular, chemical modification through covalent bonding is beneficial when preparing stable polymer-coated surfaces. Generally, two techniques, namely the “grafting-from” and the “grafting-to” methods, are widely used to introduce a polymer onto a surface.<sup>7,8</sup> Recently, the grafting-from approach has been used to prepare well-regulated sophisticated surfaces that exhibit special functions by controlling the density of the polymer on the surface.<sup>9,10</sup> However, the grafting-from approach requires a specific functional group on the surface to propagate the monomer from the surface.

On the other hand, grafting-to is more convenient than grafting-from for immobilizing a polymer onto a surface, although there can be limited control over some properties, such as polymer density. The grafting-to approach conjugates a pre-synthesized polymer onto the surface using a coupling reaction or an activated species generated by external energy (e.g., heat, UV light, electron beam). In particular, polymers possessing reactive functional groups that are activated by external signals are highly useful when immobilized onto a material because they can directly form covalent bonds between the polymer and a wide variety of substrates.<sup>11-15</sup>

A photo responsive functional group in a photoreactive polymer is activated by exposure to light of a specific wavelength. Because physical shielding can be used to easily control the exposure location, a photoreactive polymer can be activated and immobilized in a predetermined area.

The phenylazide group is a well-known photoreactive functional group that is activated by UV light. After irradiation, the phenylazide group produces an active nitrene that forms covalent bond to a variety of materials.<sup>16, 17</sup> Our group and others have introduced phenylazide into various natural and synthetic polymers in order to control non-specific interactions between biomolecules and cells.<sup>13, 17-23</sup> Since radical polymerization is easy to perform, it provides useful access to synthetic polymers. In addition, polymer characteristics, such as chain length, composition, and functionality, are simply controlled by modifying the reaction conditions and through copolymerization. Unfortunately, polymers bearing phenylazide groups prepared by radical polymerization using acrylate or acrylamide monomers are highly hydrophobic due to the hydrocarbon-based backbone and the hydrophobic phenylazide groups. Consequently, phenylazide-introduced polymers become increasingly insoluble in aqueous media with increasing numbers of phenylazide groups. Consequently, the main chain of the polymer needs

to be constructed from monomers that are more hydrophilic in order to improve overall polymer hydrophilicity.

Ethylene glycol is the most popular hydrophilic main-chain monomer, and is widely used in the form of polyethylene glycol.<sup>24</sup> In particular, polyethylene glycol is highly hydrophilic and flexible, and can reduce non-specific interactions between biomolecules and cells.<sup>25</sup> Thus, the ethylene glycol structure is expected to increase the solubility of a polymer bearing hydrophobic phenylazide groups and improve surface properties when applied on a substrate.<sup>26</sup>

The furan group is a candidate photo responsive moiety that can be applied to polyethylene glycol; furans become involved in photo responsive reactions when combined with photosensitizers.<sup>27</sup> Furan-introduced polyethylene glycol has already been developed;<sup>28</sup> however, to the best of our knowledge, a furan-modified polymer has not been investigated as a photoreactive system.

In this study, we designed phenylazide-modified polyethylene glycols as photo-responsive polymers. The photoresponsivity of each polymer was investigated through its protein-adsorption and cell-adhesion properties following immobilizing onto various substrates. In addition, the function of the polymer was compared to that of a polyethylene-glycol-grafted polymer prepared by radical polymerization of a methacrylate monomer.

## 3.2. Materials and methods

### 3.2.1 Materials

Sodium azide, 4-(hydroxymethyl)phenylboronic acid, tetrabutylammonium bromide (TABA), epichlorohydrin, ethyl acetate, methanol, sodium bicarbonate, benzene, 50 wt% sodium hydroxide, copper (II) sulfate, methyltriphenylphosphonium bromide ( $[\text{MePPh}_3]^+\text{Br}^-$ ), *n*-

hexane, and *N,N*-dimethylformamide were purchased from FUJIFILM Wako Pure Chemical (Osaka, Japan). Lithium bromide, ethylene oxide (EO, 1.2 mmol/L toluene solution), and triisobutyl aluminium (*i*-Bu<sub>3</sub>Al, 1.0 mol/L toluene solution) were purchased from Tokyo Chemical Industry (Tokyo, Japan).

### 3.2.2 Instrumentation

<sup>1</sup>H NMR (400 MHz) spectra were recorded using a JNM-ECZ400R spectrometer (JOEL, Tokyo, Japan). Gel permeation chromatography (GPC) analysis was performed by a GPC system (Tosoh, Tokyo) with three columns (Shoedex KD802, KD804 and KD-806M) (Showa Denko, Tokyo, Japan) at 45 °C using *N,N*-dimethylformamide (DMF) containing 10 mmol/L lithium bromide as an eluent with a flow rate of 0.6 mL/min. IR spectra were recorded using an FT-IR spectrophotometer (FT-IR 4100, JASCO, Tokyo, Japan). Substrates were cleaned using a UV-ozone cleaner (ASM1101N, Asumi Giken, Tokyo, Japan)

### 3.2.3 Synthesis of 4-(hydroxymethyl)azidobenzene

The title compound was prepared using a copper(II) catalyst.<sup>29</sup> Sodium azide (3.9 g, 60 mmol), 4-(hydroxymethyl)phenylboronic acid (7.6 g 50 mmol), and copper(II) sulfate (800 mg, 5 mmol) were dissolved in methanol (300 mL) and the mixture was stirred for 24 h at room temperature. The solution was extracted with ethyl acetate and the extract was washed with saturated sodium bicarbonate solution. The organic phase was dried over anhydrous magnesium sulfate and the ethyl acetate was removed by evaporation using a rotary evaporator at 25 °C to afford a light-yellow solid. Yield 40%. <sup>1</sup>H-NMR (399 MHz, D<sub>2</sub>O): δ = 4.50 (d, *J* = 24.0 Hz, 2H), 6.98, 7.27, 7.30, 7.64 (d, *J* = 7.6 Hz, aromatic ring, 4H).

### 3.2.4 Synthesis of 4-(glycidyloxymethyl)azidobenzene (AzPheEO)

The title compound was prepared according to a previous report.<sup>30</sup> Epichlorohydrin (3.7g, 40 mmol) and 4-(hydroxymethyl)azidobenzene (3.0 g 15 mmol) were partitioned between 50 wt% sodium hydroxide (10 mL) and benzene (10 mL). After cooling to 4 °C, tetrabutylammonium bromide (as a phase-transfer catalyst) was added, and the mixture was stirred for 72 h at room temperature. The mixture was extracted with ethyl acetate and the extract was washed with saturated sodium bicarbonate solution. The organic phase was dried over anhydrous magnesium sulfate and the ethyl acetate was removed by evaporation at 25 °C to afford a yellow liquid. Yield: 76%. <sup>1</sup>H-NMR (399 MHz, CDCl<sub>3</sub>)  $\delta$  = 2.59 (dd,  $J$  = 2.8, 4.8 Hz, 1H, epoxy methylene), 2.77 (dd,  $J$  = 4.0, 4.8 Hz, 1H, epoxy methylene), 3.16 (m, methine, 1H), 3.80 (dd,  $J$  = 2.8, 12.0 Hz, -CH-CH<sub>2</sub>-O-CH<sub>2</sub>, 2H), 4.54 (d,  $J$  = 4.4 Hz, benzyl, 2H), 7.37, 7.05 (d,  $J$  = 8.8 Hz, aromatic ring, 4H).

### 3.2.5 Polymerization of AzPheEO with ethylene oxide

[MePPh<sub>3</sub>]<sup>+</sup>Br<sup>-</sup> (0.06 mmol) and AzPheEO were added to a Schlenk flask held under vacuum at 25 °C for 18 h. A solution of ethylene oxide and *i*-Bu<sub>3</sub>Al (0.6 mmol) were added to the flask at -30 °C under argon and the solution was stirred at 25 °C in the dark for 18 h. Methanol (1 mL) was added to the solution and the solvent was removed under reduced pressure. The crude compound was dissolved in acetone and the precipitate was collected by filtration. The solution was precipitated using hexane, and the precipitate was collected and dried under vacuum. The obtained polymer, poly(4-azidobenzyl glycidyl ether-*co*-ethylene oxide), is referred to as “AzPEG(x)”, where x is the phenylazide composition (mol%) as determined by <sup>1</sup>H NMR spectroscopy. The conditions for polymerization are summarized in **Table 3.1**.

**Table 3.1** Characterization of AzPEG

Code	Feed (mmol)		Polymer (unit ratio)	$M_n^b$	$M_w^b$	PDI <sup>b</sup>
	EO	AzPheEO	EO:AzPheEO ( <i>n:m</i> ) <sup>a</sup>			
AzPEG(1.2)	5.85	0.15	0.988 : 0.012	2570	4000	1.54
AzPEG(3)	5.7	0.3	0.97 : 0.03	2700	5600	2.27
AzPEG(9)	5.4	0.6	0.91 : 0.09	3900	7100	1.81
AzPEG(14)	5.1	0.9	0.86 : 0.14	5500	15000	2.72
AzPEG(30)	4.8	1.2	0.70 : 0.30	8400	44000	5.30

<sup>a</sup> *n* and *m* indicate the molar ratio of monomer in poly(ethylene oxide)<sub>*n*</sub>-*co*-(4-azidobenzyl glycidyl ether)<sub>*m*</sub> determined by <sup>1</sup>H NMR, <sup>b</sup> Determined by GPC

### 3.2.6 Photo-immobilization

The polymer was dissolved in a 1:1 (v/v) methanol/water solution. The solution was dropped onto a UV-ozone cleaned substrate and spin coated at 3000 rpm for 10 s. The substrate was dried in an oven at 50 °C for 1 h. A stainless-steel punch sheet with 500 μm holes (Yasutoyo Trading, Tokyo, Japan) was subsequently placed on the substrate and the surface was exposed to UV light at 45 mW/cm<sup>2</sup> (λ: 270 nm) for 10 s using a photo irradiator (L5662 UV spot light source, Hamamatsu photonics, Hamamatsu, Japan) at a distance of 10 cm from the substrate. The surface was then washed with water and then immersed in water for more than 2 d. The surface was then dried and the substrate was stored in a desiccator. The substrate was sanitized by exposure to UV light for 1 h prior to any cell-culture experiments.

### 3.2.7 Cell culturing

Mouse fibroblast (3T3) cells (Japanese Collection of Research Bioresources, Osaka, Japan) were cultured in Dulbecco Modified Eagle's Medium (Sigma-Aldrich, St. Louis, MO, USA) supplemented with 10% fetal bovine serum, as well as penicillin and streptomycin as antibiotics (Nakarai Tesque, Kyoto, Japan). The cells ( $1.0 \times 10^4$  cells/cm<sup>2</sup>) were seeded onto the substrate and incubated for 24 h, after which they were examined using a phase-contrast microscope.

### 3.2.8 Protein adsorption

A solution of Alexa488-conjugated albumin (Thermo Fisher Scientific, Waltham, MA, USA) was dropped onto the substrate and left for 1 h at 25 °C. The surface was washed three-times with Dulbecco's phosphate buffer saline. Fluorescence images were acquired using a fluorescence microscope (Olympus, Tokyo, Japan).

## 3.3 Results and discussion

### 3.3.1 Characterization of the photo reactive AzPheEO monomers

The photoreactive epoxide, AzPheEO, was synthesized by reacting epichlorohydrin with 4-(hydroxymethyl)azidobenzene to produce a yellow solid (**Figure 3.1**). <sup>1</sup>H NMR spectroscopy revealed signals clearly assignable to epoxy protons (2.59 and 2.77 ppm), benzylic protons (4.54 ppm), and aromatic protons (7.37 and 7.05 ppm) (**Figure 3.4**). In addition, the absorption band of the azido group was clearly observed at 2108 cm<sup>-1</sup> by FT-IR spectroscopy for both 4-(hydroxymethyl)azidobenzene and AzPheEO, with the original hydroxyl stretching band (3070–3500 cm<sup>-1</sup>) absent after reaction (**Figure 3.3**). On the basis of these results, we conclude that AzPheEO had been successfully synthesized.

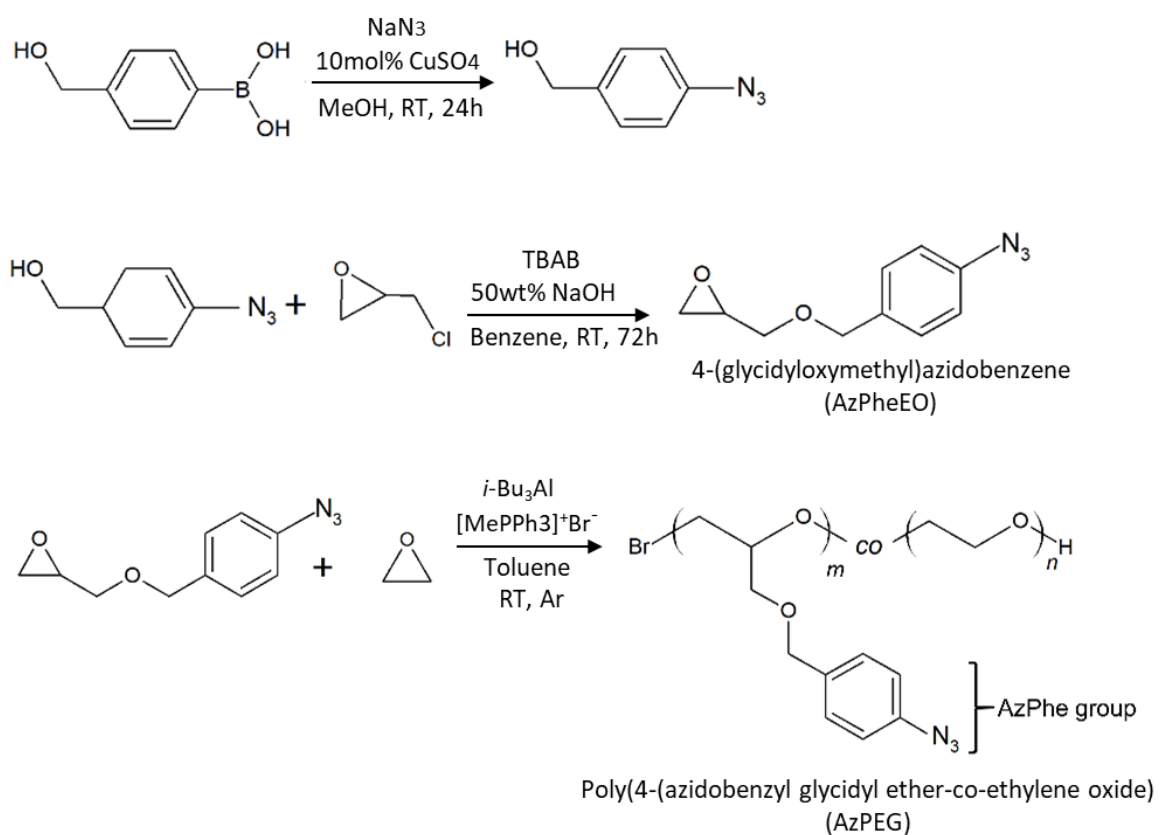


**Figure 3.1** Synthesis of photo reactive epoxy azido monomer (AzPheEO) and PEG-based photo reactive polymer (AzPEG)



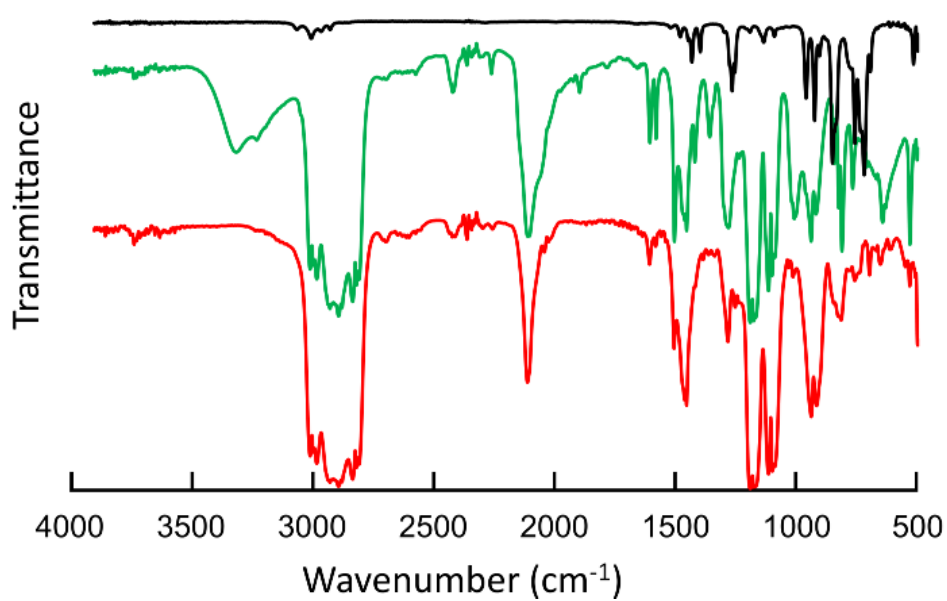


**Figure 3.2** FT-IR spectra of epichlorohydrin (black), 4-(hydroxymethyl)azidobenzene (green), and 4-(glycidyloxymethyl)azidobenzene (red).

### 3.3.2 Characterizing AzPEG polymers

AzPheEO was copolymerized with ethylene oxide by monomer-activated ring-opening polymerization using  $[\text{MePPh}_3]^+\text{Br}^-$  and *i*-Bu<sub>3</sub>Al as the initiator and monomer activator, respectively, to form polymers with various phenylazide unit contents (**Table 3.1**).<sup>31</sup> <sup>1</sup>H NMR spectroscopy revealed the complete absence of signals corresponding to the epoxy protons in the spectra of the products, while signals corresponding to the protons of the ethylenedioxy units (3.4-3.8 ppm) were clearly evident (**Figure 3.5**). The proportion of monomer units in each polymer was determined by comparing the integrated benzylic proton signal (2H, 4.5-4.6 ppm) in the spectrum of AzPheEO with those of the ethylenedioxy, ethylene, and methine protons. As shown in **Table 3.1**, the monomer-unit ratio in the synthesized polymer was regulated by the feed-monomer ratio.

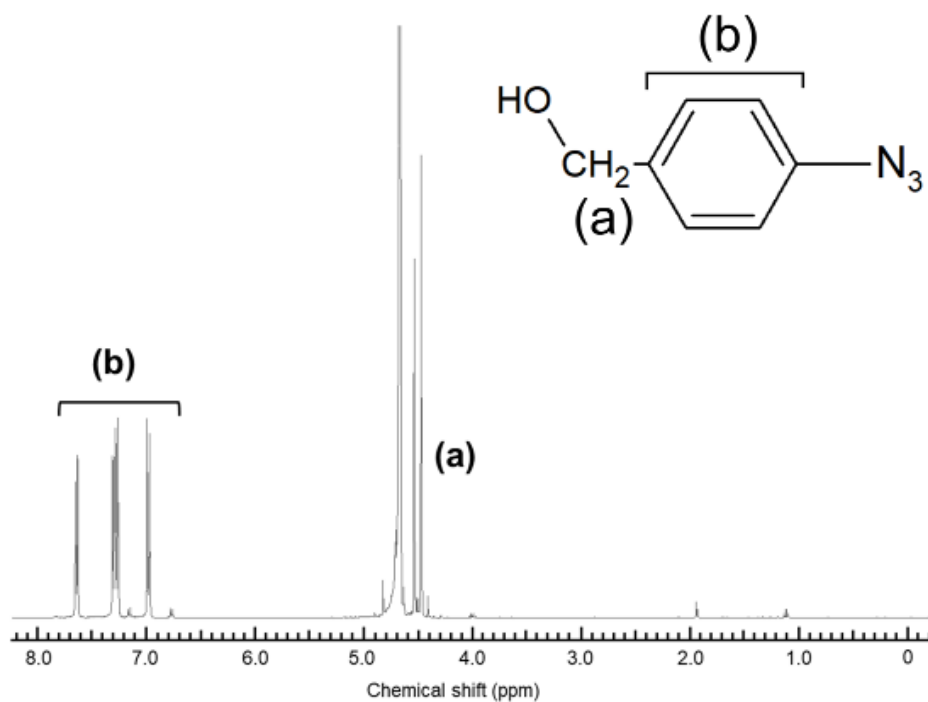


**Figure 3.3**  $^1\text{H}$  NMR spectrum of 4-(hydroxymethyl)azidobenzene (Solvent:  $\text{D}_2\text{O}$ ).

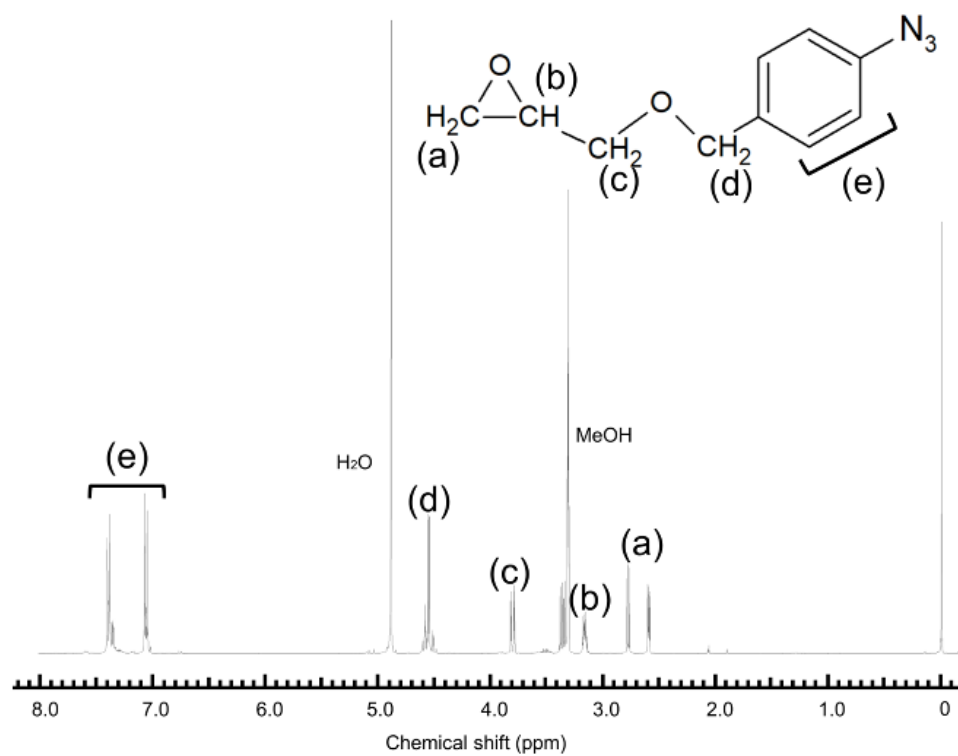


**Figure 3.4**  $^1\text{H}$  NMR spectrum of 4-(glycidyloxymethyl)azidobenzene (Solvent: methanol- $\text{d}_4$ )

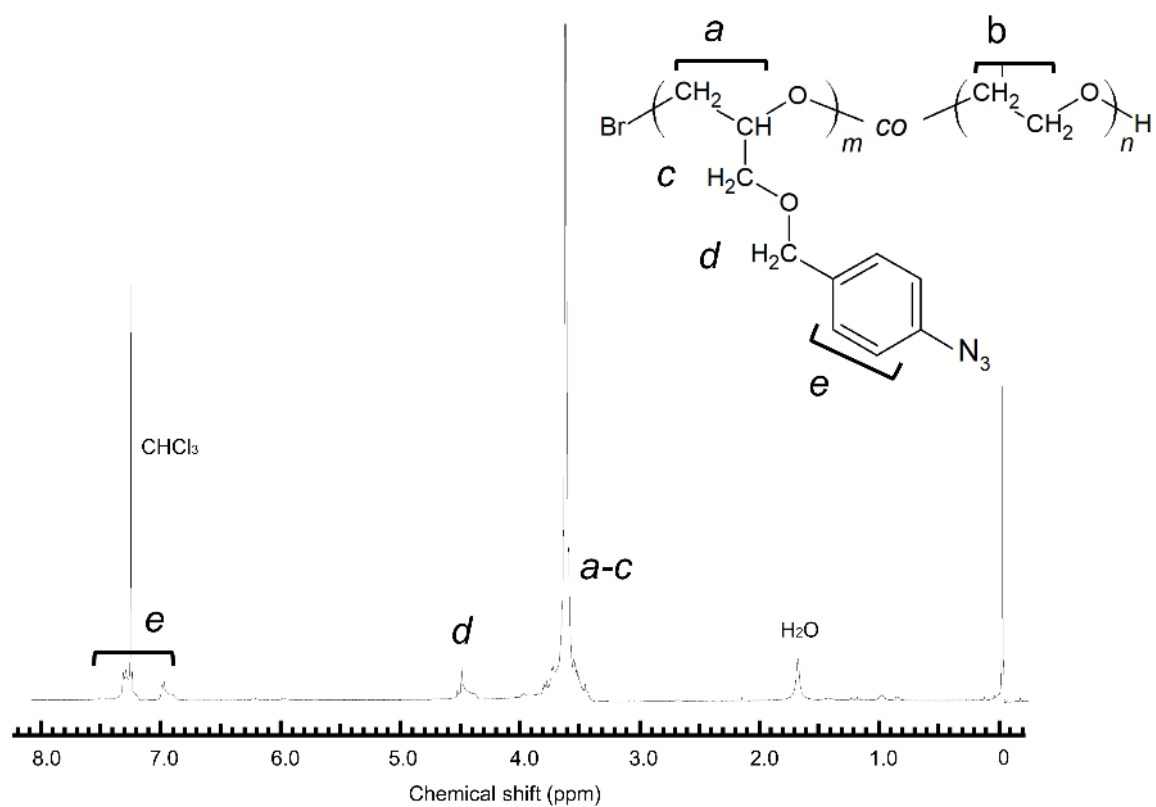


**Figure 3.5**  $^1\text{H}$  NMR spectrum of poly(4-azidobenzyl glycidyl ether-co-ethylene oxide) (AzPEG 9) (Solvent:  $\text{CDCl}_3$ ).

The presence of phenylazide groups in the polymer was also confirmed by UV-absorbance spectroscopy; the polymer exhibited an phenylazide-derived absorbance at 266 nm, similar to that of the azidobenzoic acid (**Figure 3.6**). FT-IR spectroscopy revealed that the prepared polymer clearly contains azide moieties, with the azide signal ( $2109\text{ cm}^{-1}$ ) increasing in intensity with increasing proportion of phenylazide unit in the polymer (**Figure 3.7**). On the basis of these results, we conclude that phenylazide units were successfully introduced on the side groups of the polyethylene glycol.

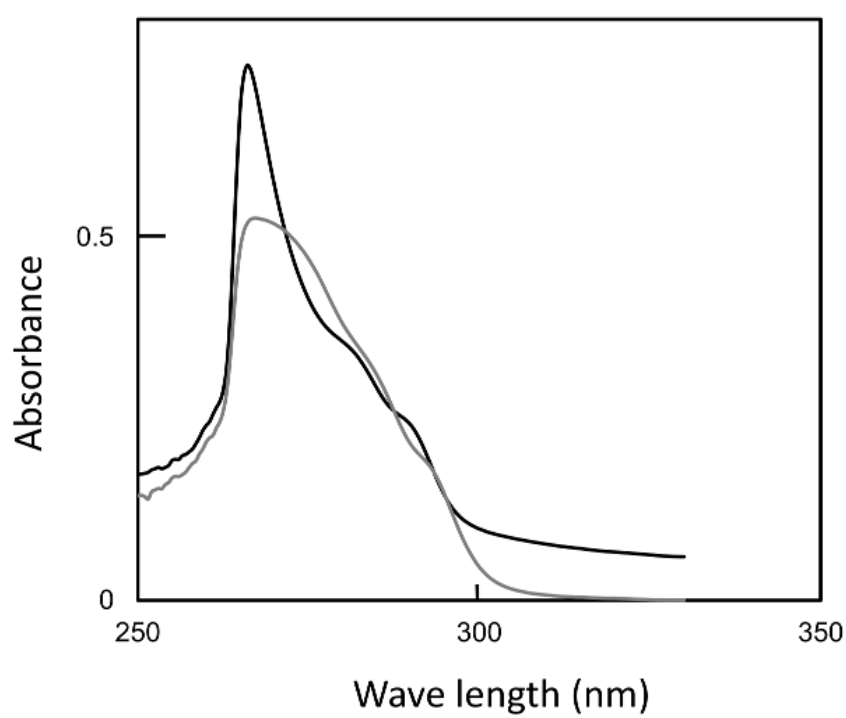


**Figure 3.6** UV absorbance spectra of AzPEG(9) (black) and azido benzoic acid (gray) in DMF.

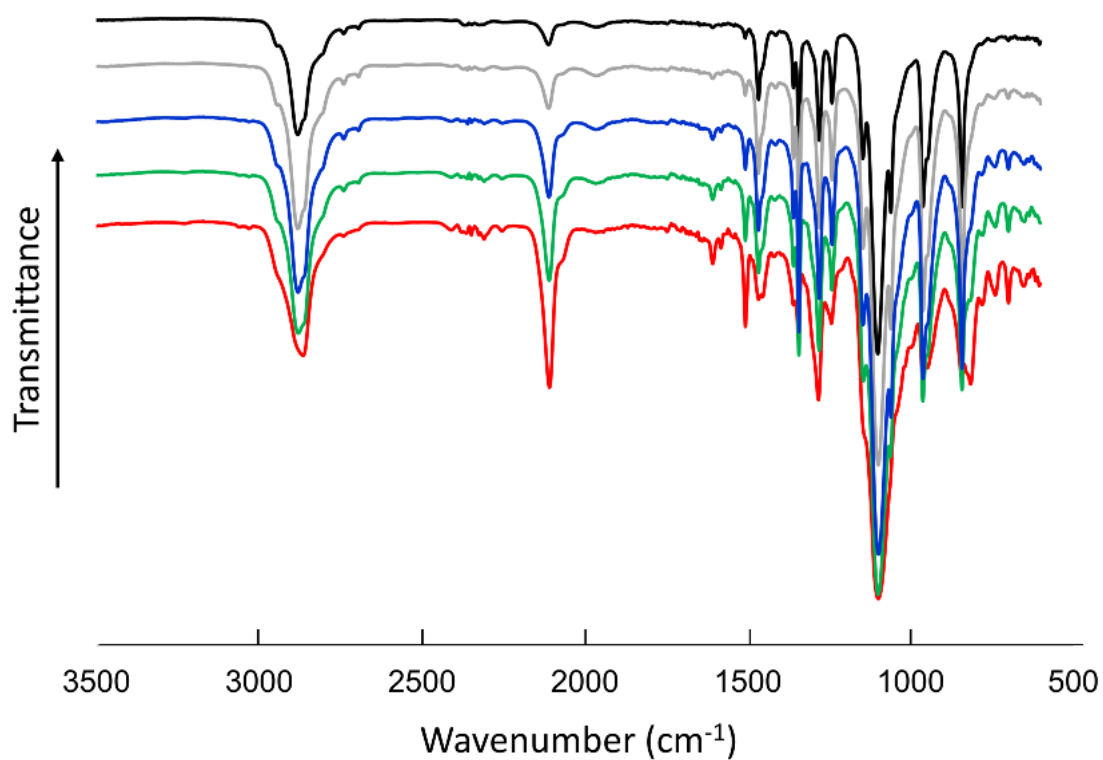


**Figure 3.7** FT-IR spectra of various poly(4-azidobenzyl glycidyl ether-co-ethylene oxide)s (AzPEG(1.2): black, AzPEG(3): gray, AzPEG(9): blue, AzPEG(14): green, and AzPEG(30): red).



The polymers were next subjected to gel permeation chromatography (GPC) (**Figure 3.8**). AzPEGs with small numbers of phenylazide units exhibited unimodal GPC traces; however, the polydispersity index of the AzPEG was observed to increase with increasing proportion of phenylazide group. In this study, we only used KD series columns to analyze the polymers. According to the manufacturer's information, KD series columns interact strongly with aromatic groups when DMF is used as the eluent. Hence, we speculate that the observed increase in polydispersity index is due to strong interactions between the column beads and the phenylazide groups of the polymers, resulting in increased GPC tailing and a (false) increase in the polydispersity of the polymer.

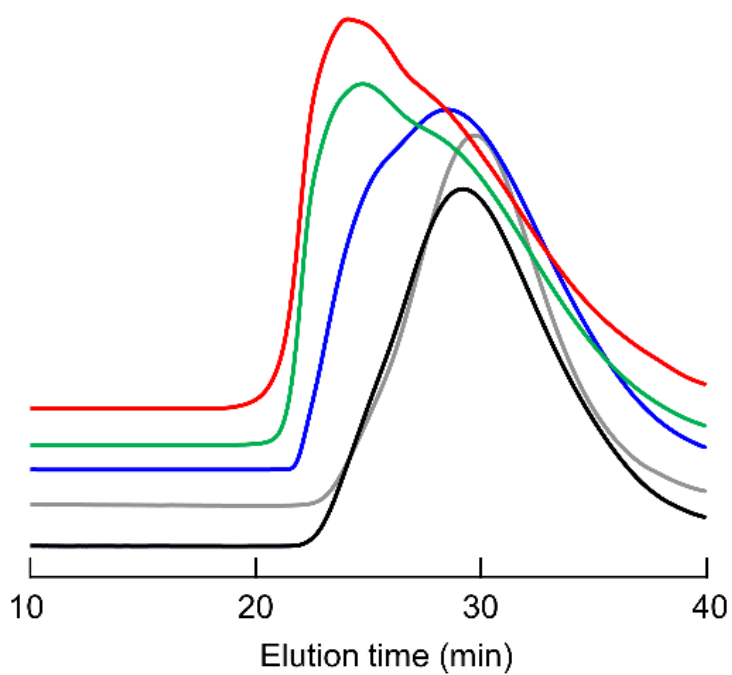


**Figure 3.8** GPC traces of AzPEG(1.2) (black), AzPEG(3) (gray), AzPEG(9) (blue), AzPEG(14) (green), and AzPEG(30) (red). Eluent: DMF containing 10 mmol/L LiBr.

Finally, we examined polymer solubility. AzPEG(1.2) and AzPEG(3) readily dissolved in water; however, polymer solubility was observed to decrease with increasing phenylazide content in the in AzPEG, with AzPEG(14) and AzPEG(30) hardly soluble in water. While AzPEG(14) dissolved in methanol and ethanol, AzPEG(30) hardly dissolved in any polar protic solvent; AzPEG(30) did dissolve in aprotic solvents, such as acetone.

**Table 3.2** Solubility of AzPEG polymers

Polymers	Solubility
AzPEG(1.2)	Water O
AzPEG(3)	Water O
AzPEG(9)	Water O
AzPEG(14)	Water X, Methanol O, Ethanol O
AzPEG(30)	Acetone O

### 3.3.3 Protein adsorption

The polymer solution was cast onto various substrates and photo-immobilized using a stainless-steel punched mask to localize the polymer-immobilized area on the surface. After exposure to UV light, the highly active nitrenes produced from the phenylazide moieties randomly attacked the polymer and substrate. As a result, a part of the AzPEG became conjugated to the silanol of the glass surface and was covalently immobilized on the substrate.<sup>13</sup> After applying the fluorescent protein (Alexa488-conjugated albumin) to glass, polycarbonate, and polystyrene plates, protein fluorescence was examined by fluorescence microscopy (**Figure 3.9**). Regardless of the type of plate, fluorescence was suppressed in the UV-exposed areas, while green fluorescence was observed in the surrounding regions. We speculate that the weak fluorescence on the glass substrate is due to low levels of protein adsorption because the glass substrate is more hydrophilic than the other substrates. We therefore conclude that AzPEG was successfully immobilized onto the surfaces through exposure to UV light, and that the immobilized AzPEG suppresses protein adsorption by the substrate. Hence, AzPEG is expected to exhibit strong antifouling properties due to the highly hydrophilic nature of the polyethylene glycol main chain.

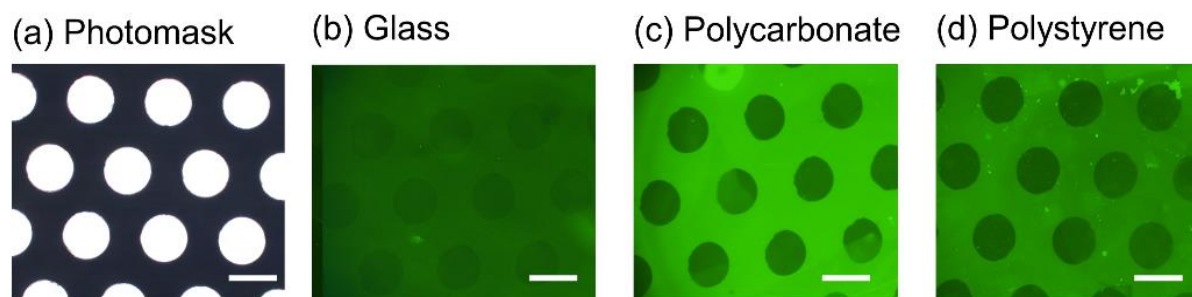


**Figure 3.9** (a) Phase contrast image of the photomask. Fluorescence microscopy images of AzPEG(3)-coated micropatterned substrates: (b) glass, (c) polycarbonate, and (d) polystyrene after adsorbing Alexa 488-conjugated albumin. Exposure times: (b) 1000, (c) 500, and (d) 500 msec. Scale bars: 500  $\mu\text{m}$ .

### 3.3.4 Cell adhesion

Cell adhesion onto AzPEG-coated glass was evaluated using 3T3 cells (**Figure 3.10-11**). A series of AzPEGs were spin-coated onto glass at different concentrations, and the polymers were immobilized at locations where the UV light passed through the stainless-steel punch sheet. After washing with water, 3T3 cells were cultured on the various coated surfaces for 24 h. The AzPEG(1.2)- and AzPEG(3)-immobilized glass showed cell adhesion at non-UV-exposed areas and suppression at the UV-exposed areas due to the introduction of hydrophilic PEG on the surface.<sup>23</sup> The non-cell-adhered pattern was almost identical to the hole pattern in the stainless-steel mask. However, cells were increasingly found in the UV-exposed areas at lower applied-polymer concentrations. In contrast, the AzPEG(9)-coated surface exhibited a clear cell pattern on the surface at low applied polymer concentrations, while cell adhesion at non-UV-exposed areas was also suppressed with increasing applied polymer concentration. Cell adhesion in the non-UV-exposed areas was completely suppressed on the AzPEG(14) immobilized surface regardless of the applied polymer concentration.

Subsequently, cell adhesion to a polystyrene surface was examined (**Figure 3.12**). Cell adhesion was suppressed on the UV exposed areas of the AzPEG(3)- and AzPEG(9)-coated surfaces. In addition, AzPEG(14) suppressed cell adhesion to the non-UV-exposed areas in a similar manner to the glass surface. In contrast, cells were confirmed to be adhered to the UV-exposed area of the AzPEG(1.2)-coated surface. Thus, the concentration of the polymer coating required to control cell adhesion was found to depend on the substrate.

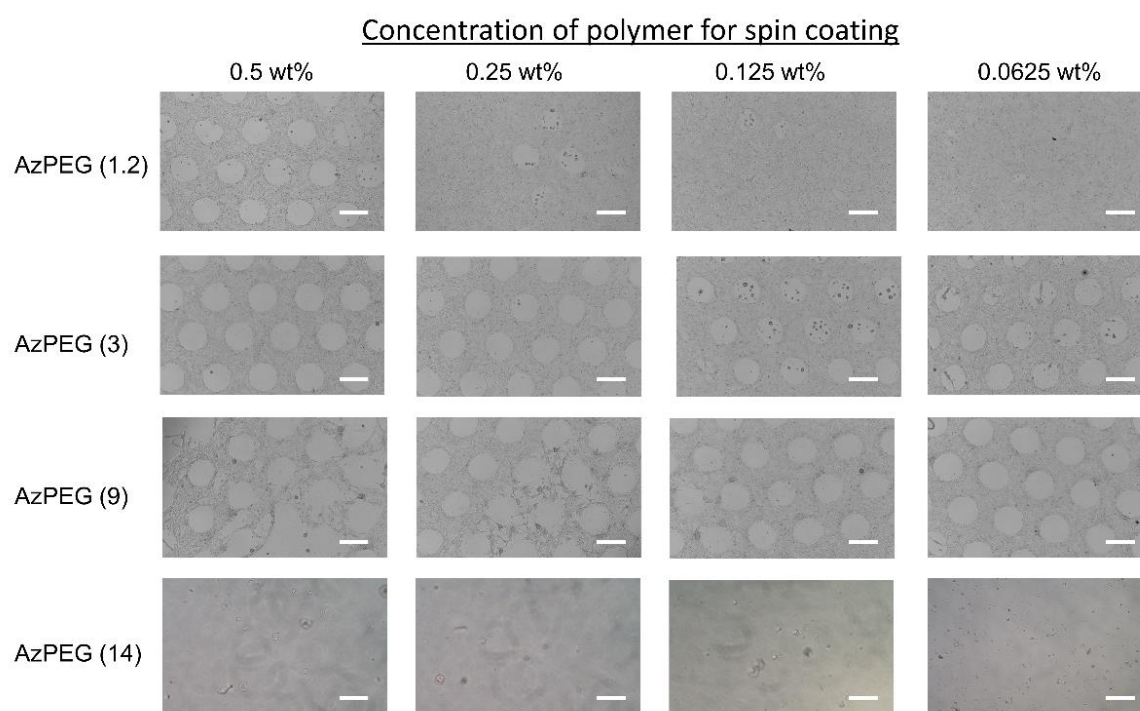


**Figure 3.10** Phase contrast images of 3T3 cultured on AzPEG-coated micro-patterned glass. Effect of composition: the surfaces were rinsed with water after photo-immobilization. Scale bars: 500  $\mu\text{m}$ .

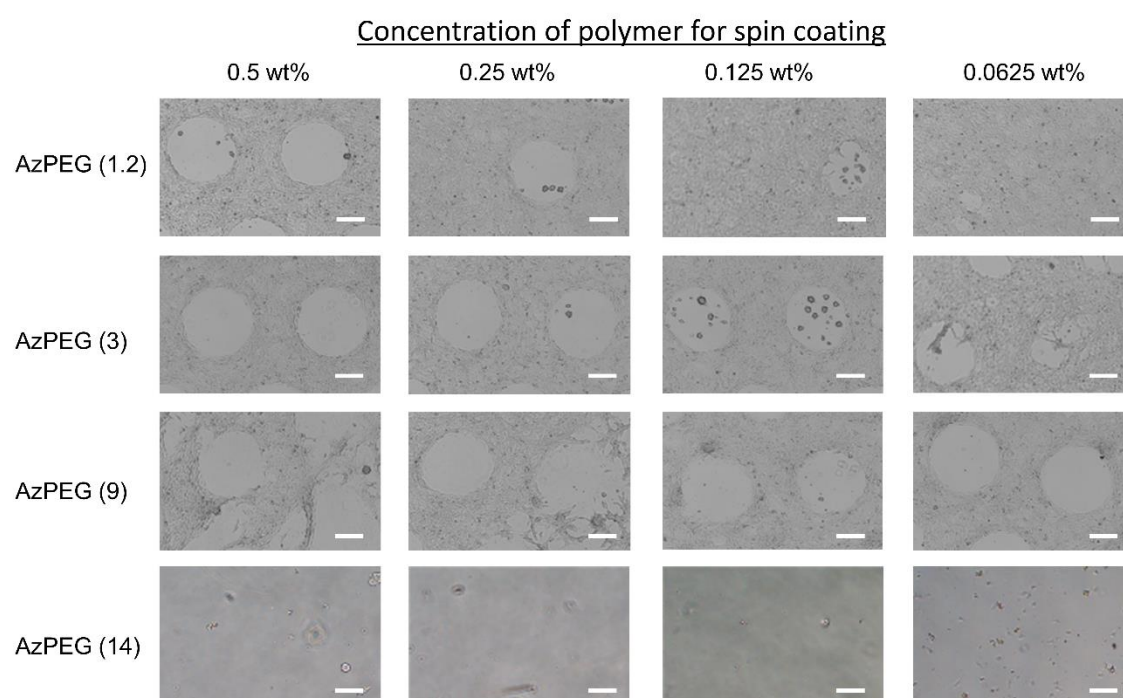


**Figure 3.11** Magnified image. Scale bar: 200  $\mu\text{m}$ .

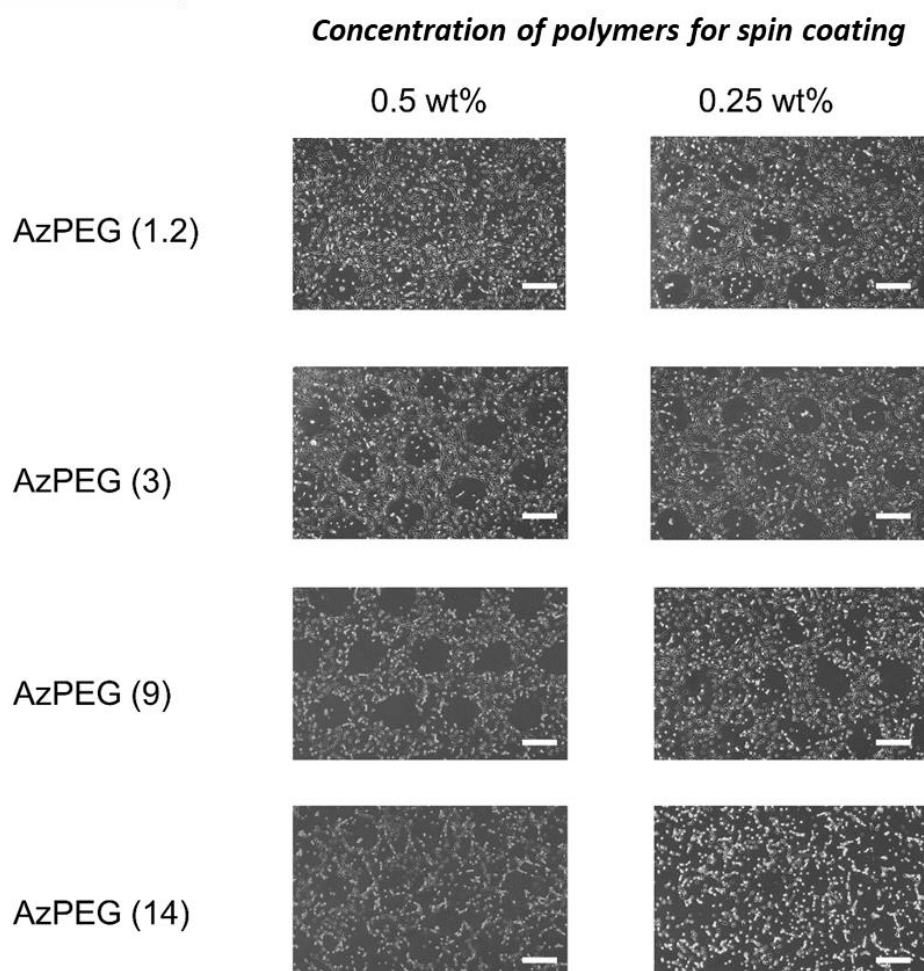


**Figure 3.12** Phase contrast images of 3T3 cultured on AzPEG-coated micro-patterned polystyrene dish. Seeding density:  $5.0 \times 10^3$  cells/cm<sup>2</sup>, Incubation time: 24 h. Scale bars: 500  $\mu$ m.



The surface conditions were investigated by FT-IR spectroscopy in order to examine the suppression of cell-adhesion observing in the non-UV-exposed areas. In this study, the surface was washed with water after photo-immobilization, and the polymer remaining on the surface was analyzed after washing with water in the absence of UV exposure. The AzPEG(3) was completely removed from the surface after washing with water (**Figure 3.13**). However, AzPEG(9) shows unwashed residues remaining on the surface when the water was used to wash. Subsequently, organic solvents were used to remove the polymer, and AzPEG(9) were completely washed using methanol and the FT-IR peak associated with the azide group was completely disappeared after washing (**Figure 3.14**). The AzPEG(14) were investigated using methanol and acetone however the AzPEG(14) could not completely removed from the surface even after washing with acetone, a rather good solvent. (**Figure 3.15**).

Cell adhesion was observed on the AzPEG(9) and AzPEG(14) surfaces by changing the rinsing protocol (**Figure 3.16-17**). When the substrate was rinsed with water, cell adhesion was clearly observed only at the low concentration, with cell adhesion suppressed at the high solution concentration of 0.5 wt%. On the other hand, cell adhesion was clearly observed on the surface rinsed with methanol, irrespective of the applied polymer concentration. In contrast, slightly improved cell adhesion was observed at the non-UV-exposed areas of the AzPEG(14) surface at low polymer concentration when washed with good solvents; however, cell adhesion was still suppressed due to polymer remaining on the surface. We conclude that, once adsorbed onto the substrate, the polymer becomes more difficult to remove with increasing phenylazide composition due to strong interactions between the phenylazide units in the polymer and the substrate. In addition, due to solubility issues, polymers with high azidophenyl contents are difficult to completely remove from the surface and are unsuitable for controlling cell adhesion.

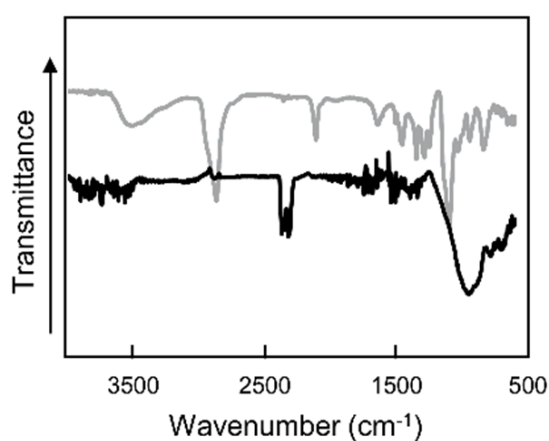


**Figure 3.13** FTIR spectra of AzPEG(3) coated glass surfaces before (gray line) and after rinsing (black line) with water.

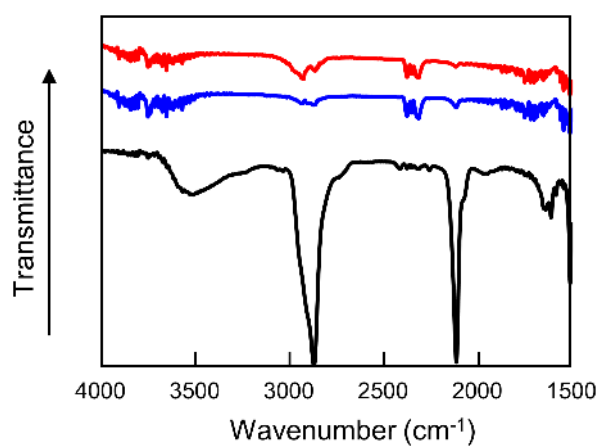


**Figure 3.14** FTIR spectra of AzPEG(9)-coated glass surfaces. Traces are before (black) and after rinsing with water (blue) and methanol (red).

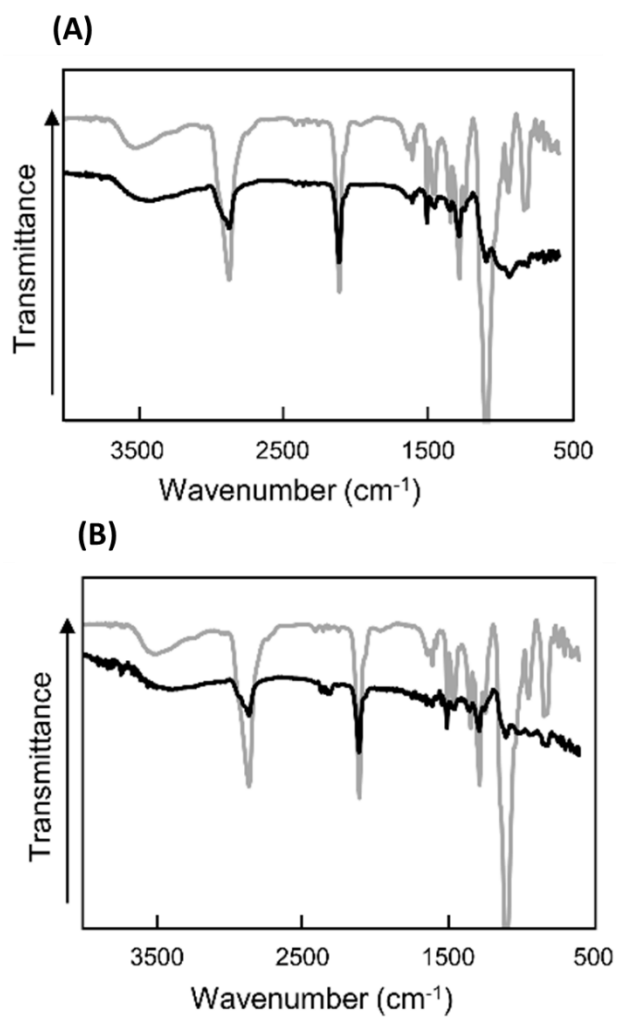


**Figure 3.15** AzPEG(14)-coated glass surfaces. Gray and black traces are before and after rinsing with (A) methanol, (B) acetone

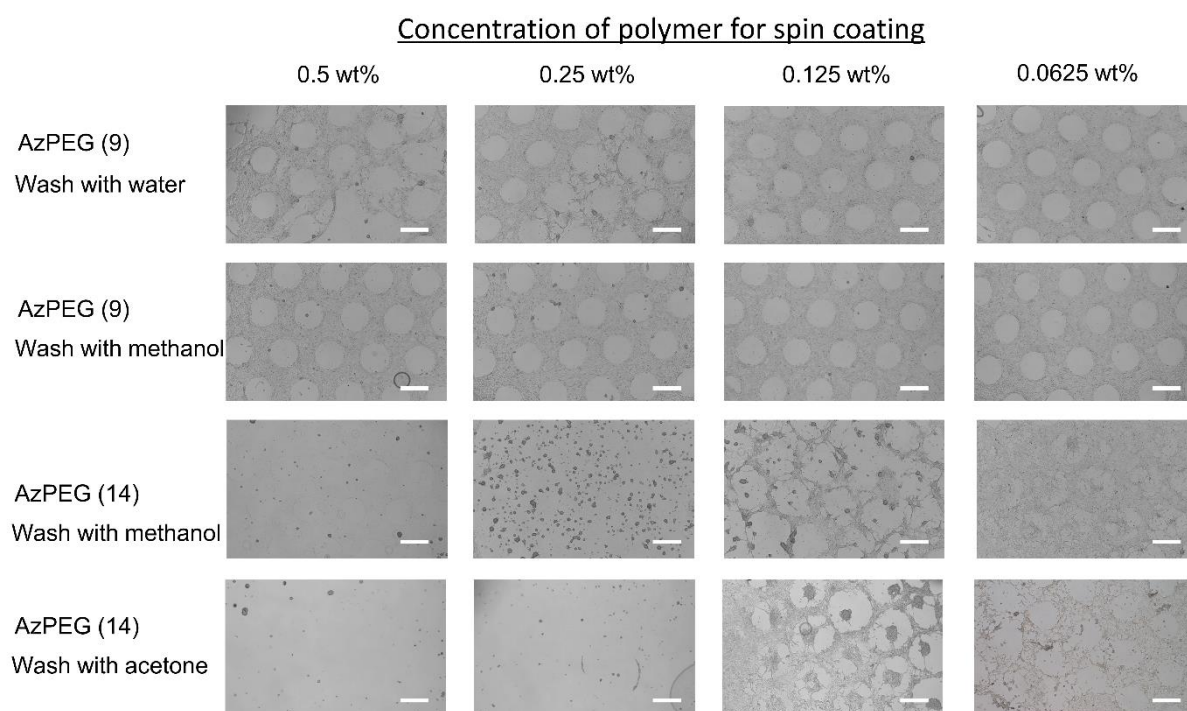


**Figure 3.16** Phase contrast images of 3T3 cultured on AzPEG-coated micro-patterned glass. The effect of washing solution: the surfaces were rinsed with water, methanol, or acetone after photo-immobilization. Scale bars: 500  $\mu\text{m}$ .

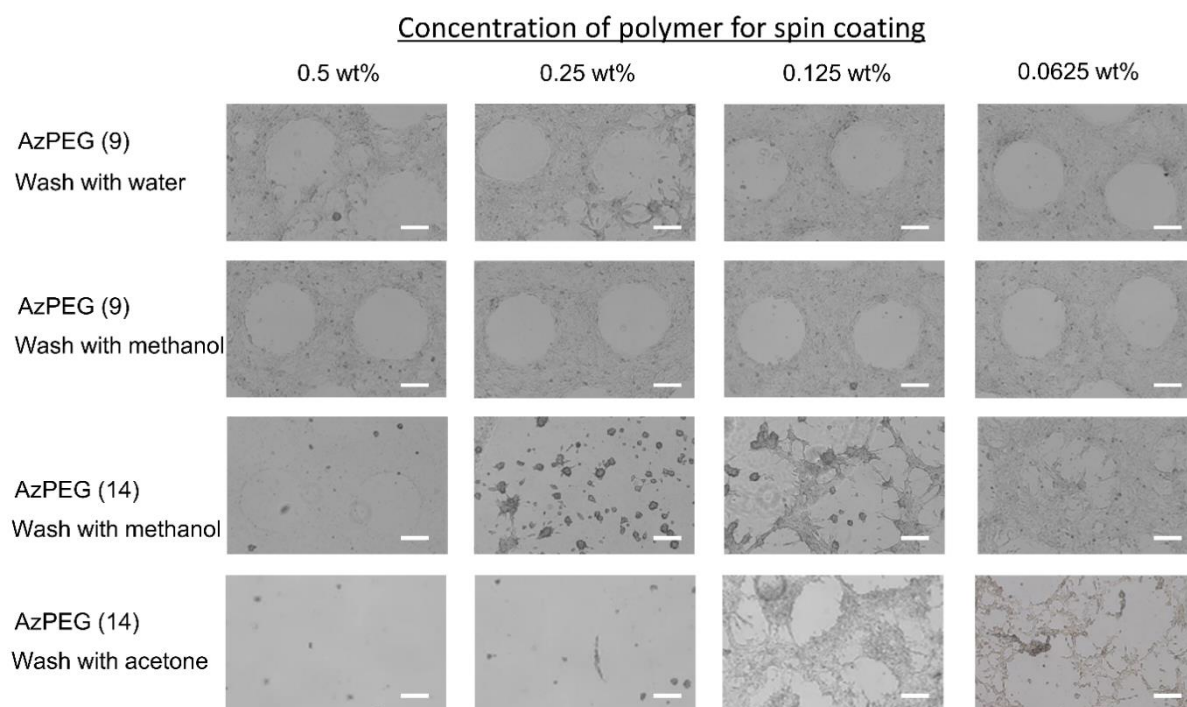


**Figure 3.17** Magnified image. Scale bar: 200  $\mu\text{m}$ .

Natural polymers (e.g., polysaccharides, proteins) and synthetic polymers (e.g., vinyl polymers) have been widely used to develop photoreactive polymers. Because the main chain of a vinyl polymer is composed of a hydrophobic alkylene chain, polymer solubility in water decreases with increasing number of hydrophobic units, such as azidophenyl units, in its side chains. In our previous study, we prepared poly(pentaethylene glycol methacrylate-*co*-azidophenyl methacrylate) as a photoreactive polymer.<sup>26</sup> Although the polymer dissolved in water, it hardly dissolved in protic solvents at a azidophenyl methacrylate composition in excess of 10% (data not shown).<sup>26</sup> In contrast, in this study, AzPEGs composed of less than 15% azidophenyl showed good solubilities in protic solvent, which is ascribable to the polyethylene glycol main chain. In addition, the molar number of azidophenyl units in a unit weight of AzPEG(9) was 1.5 mmol/g, which is more than five-times higher than that of poly(pentaethylene glycol methacrylate)<sub>0.9</sub>-*co*-poly(azidophenyl methacrylate)<sub>0.1</sub> (0.29 mmol/g). **Figure 3.18** shows the cell-adhesion behavior of a poly(pentaethylene glycol methacrylate)<sub>0.9</sub>-*co*-poly(azidophenyl methacrylate)<sub>0.1</sub>-treated surface, which shows a similar concentration dependence to that observed for the AzPEG(1.2)-immobilized surface. Because the azidophenyl units in AzPEG(1.2) are present at 0.19 mmol/g, immobilization efficiency appears to depend on the number of azidophenyl units in the polymer. Therefore, compared to other photoreactive polymers, AzPEG(1.2) is highly efficiently immobilized onto substrates and is soluble in protic solvents.

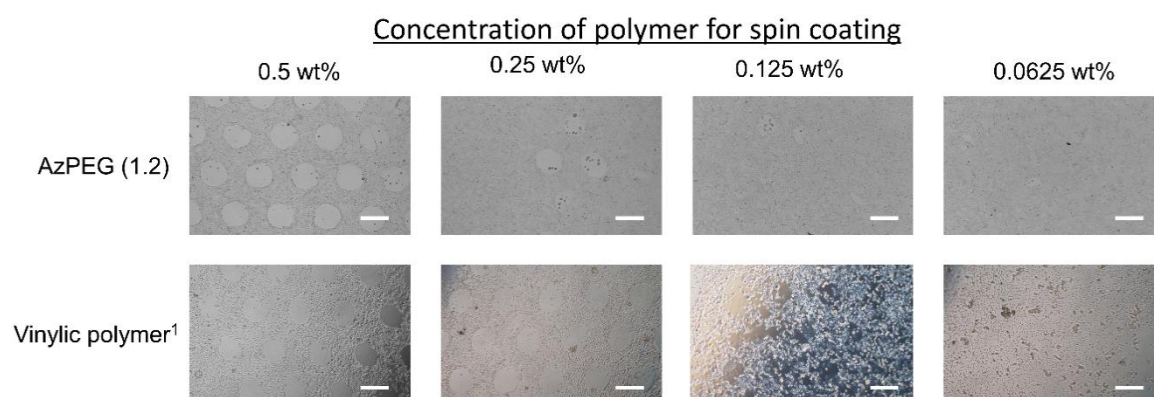


**Figure 3.18** Phase contrast images of 3T3 cultured on AzPEG(1.2)- and vinylic-polymer-coated micro-patterned glass. The surfaces were rinsed with water. The vinylic polymer is poly(pentaethylene glycol methacrylate)0.9-co-poly(azidobenzyl methacrylate)0.1. Scale bar: 500  $\mu m$ .

### 3.4 Conclusions

Ethylene-glycol-based photoreactive polymers were successfully synthesized using the AzPheEO monomer. The polymers were immobilized onto various substrates by exposure to UV irradiation, and suppressed non-specific adhesion of a protein to the substrate. In particular, the polymer possessing a low azidophenyl content was highly water solubility and suppressed cell adhesion. The advantage of the AzPEG polymer is that it contains more photoreactive functional groups on its side chains compared with an alkylene-main-chain polymer, while maintaining water solubility. Consequently, this polymer is expected to be used to immobilize bioactive molecules to substrates without the need for organic solvents. We expect that the highly reactive AzPEG will be used as a photo responsive antifouling agent.

### 3.5 References

1. Roach, P.; Shirtcliffe, N. J.; Newton, M. I., Progress in superhydrophobic surface development. *Soft matter* **2008**, *4* (2), 224-240.
2. Mendes, P. M., Stimuli-responsive surfaces for bio-applications. *Chem. Soc. Rev.* **2008**, *37* (11), 2512-2529.
3. Bes, L.; Angot, S.; Limer, A.; Haddleton, D. M., Sugar-coated amphiphilic block copolymer micelles from living radical polymerization: recognition by immobilized lectins. *Macromolecules* **2003**, *36* (7), 2493-2499.
4. Jiang, C.; Wang, G.; Hein, R.; Liu, N.; Luo, X.; Davis, J. J., Antifouling strategies for selective in vitro and in vivo sensing. *Chem. Rev.* **2020**, *120* (8), 3852-3889.
5. Nagase, K.; Okano, T., Thermoresponsive-polymer-based materials for temperature-modulated bioanalysis and bioseparations. *J. Mater. Chem. B* **2016**, *4* (39), 6381-6397.
6. Angenendt, P., Progress in protein and antibody microarray technology. *Drug Discov. Today* **2005**, *10* (7), 503-511.
7. Milner, S. T.; Witten, T.; Cates, M., Theory of the grafted polymer brush. *Macromolecules* **1988**, *21* (8), 2610-2619.
8. Zhao, B.; Brittain, W. J., Polymer brushes: surface-immobilized macromolecules. *Prog. Polym. Sci.* **2000**, *25* (5), 677-710.
9. Ohno, K.; Morinaga, T.; Koh, K.; Tsujii, Y.; Fukuda, T., Synthesis of monodisperse silica particles coated with well-defined, high-density polymer brushes by surface-initiated atom transfer radical polymerization. *Macromolecules* **2005**, *38* (6), 2137-2142.
10. Kuzmyn, A. R.; Nguyen, A. T.; Teunissen, L. W.; Zuilhof, H.; Baggerman, J., Antifouling polymer brushes via oxygen-tolerant surface-initiated PET-RAFT. *Langmuir* **2020**, *36* (16), 4439-4446.
11. Jiang, X.; Luo, J.; Yin, J., A novel amphipathic polymeric thioxanthone photoinitiator. *Polymer* **2009**, *50* (1), 37-41.
12. Wang, K.; Lu, Y.; Chen, P.; Shi, J.; Wang, H.; Yu, Q., Novel one-component polymeric benzophenone photoinitiator containing poly (ethylene glycol) as hydrogen donor. *Mater. Chem. Phys.* **2014**, *143* (3), 1391-1395.
13. Ito, Y.; Nogawa, M.; Takeda, M.; Shibuya, T., Photo-reactive polyvinylalcohol for photo-immobilized microarray. *Biomaterials* **2005**, *26* (2), 211-216.
14. Fong, D.; Lang, A.; Li, K.; Adronov, A., Visible light-mediated photoclick functionalization of a conjugated polymer backbone. *Macromolecules* **2020**, *53* (5), 1760-1766.



15. Zunker, S.; Ru"he, J. r., Photo-crosslinking of thioxanthone group containing copolymers for surface modification and bioanalytics. *Macromolecules* **2020**, *53* (5), 1752-1759.
16. Kallitsis, K.; Thuau, D.; Soulestin, T.; Brochon, C.; Cloutet, E.; Dos Santos, F. D.; Hadziioannou, G., Photopatternable high-k fluoropolymer dielectrics bearing pendent azido groups. *Macromolecules* **2019**, *52* (15), 5769-5776.
17. Ren, X.; Akimoto, J.; Miyatake, H.; Tada, S.; Zhu, L.; Mao, H.; Isoshima, T.; Müller, S.; Kim, S. M.; Zhou, Y.; Ito, Y., Cell migration and growth induced by photo-immobilised vascular endothelial growth factor (VEGF) isoforms. *J. Mater. Chem. B* **2019**, *7* (27), 4272-4279.
18. Sakuragi, M.; Tsuzuki, S.; Hasuda, H.; Wada, A.; Matoba, K.; Kubo, I.; Ito, Y., Synthesis of a photoimmobilizable histidine polymer for surface modification. *J. Appl. Polym Sci.* **2009**, *112* (1), 315-319.
19. Konno, T.; Hasuda, H.; Ishihara, K.; Ito, Y., Photo-immobilization of a phospholipid polymer for surface modification. *Biomaterials* **2005**, *26* (12), 1381-1388.
20. Ohyama, K.; Omura, K.; Ito, Y., A photo-immobilized allergen microarray for screening of allergen-specific IgE. *Allergol. Inter.* **2005**, *54* (4), 627-631.
21. Kim, E.-H.; Han, G.-D.; Noh, S.-H.; Kim, J.-W.; Lee, J.-G.; Ito, Y.; Son, T.-I., Photo-reactive natural polymer derivatives for medical application. *J. Ind. Eng. Chem.* **2017**, *54*, 1-13.
22. Buwalda, S.; Rotman, S.; Eglin, D.; Moriarty, F.; Bethry, A.; Garric, X.; Guillaume, O.; Nottelet, B., Synergistic anti-fouling and bactericidal poly (ether ether ketone) surfaces via a one-step photomodification. *Mater. Sci. Eng. C* **2020**, 110811.
23. Kang, I.-K.; Kim, G. J.; Kwon, O. H.; Ito, Y., Co-culture of hepatocytes and fibroblasts by micropatterned immobilization of  $\beta$ -galactose derivatives. *Biomaterials* **2004**, *25* (18), 4225-4232.
24. Herzberger, J.; Niederer, K.; Pohlitz, H.; Seiwert, J.; Worm, M.; Wurm, F. R.; Frey, H., Polymerization of ethylene oxide, propylene oxide, and other alkylene oxides: synthesis, novel polymer architectures, and bioconjugation. *Chem. Rev.* **2016**, *116* (4), 2170-2243.
25. Pasut, G.; Veronese, F. M., State of the art in PEGylation: the great versatility achieved after forty years of research. *J. Control. Release* **2012**, *161* (2), 461-472.
26. Ito, Y.; Hasuda, H.; Sakuragi, M.; Tsuzuki, S., Surface modification of plastic, glass and titanium by photoimmobilization of polyethylene glycol for antibiofouling. *Acta Biomater.* **2007**, *3* (6), 1024-1032.

27. Son, T. I.; Sakuragi, M.; Takahashi, S.; Obuse, S.; Kang, J.; Fujishiro, M.; Matsushita, H.; Gong, J.; Shimizu, S.; Tajima, Y., Visible light-induced crosslinkable gelatin. *Acta biomater.* **2010**, *6* (10), 4005-4010.
28. Barthel, M. J.; Rudolph, T.; Crotty, S.; Schacher, F. H.; Schubert, U. S., Homo- and diblock copolymers of poly (furfuryl glycidyl ether) by living anionic polymerization: Toward reversibly core-crosslinked micelles. *J. Polym. Sci A: Polym. Chem.* **2012**, *50* (23), 4958-4965.
29. Tao, C.-Z.; Cui, X.; Li, J.; Liu, A.-X.; Liu, L.; Guo, Q.-X., Copper-catalyzed synthesis of aryl azides and 1-aryl-1, 2, 3-triazoles from boronic acids. *Tetrahedron lett.* **2007**, *48* (20), 3525-3529.
30. Tonhauser, C.; Alkan, A.; Schömer, M.; Dingels, C.; Ritz, S.; Mailänder, V.; Frey, H.; Wurm, F. R., Ferrocenyl glycidyl ether: a versatile ferrocene monomer for copolymerization with ethylene oxide to water-soluble, thermoresponsive copolymers. *Macromolecules* **2013**, *46* (3), 647-655.
31. Carlotti, S.; Labbé, A.; Rejsek, V.; Doutaz, S.; Gervais, M.; Deffieux, A., Living/controlled anionic polymerization and copolymerization of epichlorohydrin with tetraoctylammonium bromide– triisobutylaluminum initiating systems. *Macromolecules* **2008**, *41* (19), 7058-7062.

---

## **Chapter 4**

### **4. Conclusions and future perspective**

---

#### **4.1 Conclusions**

This dissertation describes the development of polymeric materials based on thermal induced responsive and photo induced-reactive polymers. Newly designed functional polymers were synthesized and developed into polymeric materials that are regulated by external stimuli. The prepared functional polymers were provided their applicable uses for biomedical applications especially for in situ hydrogel and antifouling surface.

General introduction of stimuli responsive and reactive polymers is given in Chapter 1. The TR polymer and photo reactive polymers are defined, and their properties and mechanisms of each system are described in detail. In addition, the applications of stimuli induced reactive polymeric materials, in situ hydrogel and antifouling coatings, are described. Finally, the motivation, objectives and outline of this study are mentioned.

In Chapter 2, the design and synthesis of thermo-responsive polymer are addressed. It describes a preparation method of TR polymer and hetero-armed TR reactive nanoparticle in different ratio between two kinds of polymer is described. The reactivity of hetero-armed nanoparticle was well-controlled by temperature in the presence of external reactive molecules, which is the result of morphological change of nanoparticle induced by thermal stimulus. In addition, a crosslinked hydrogel can be developed by using a highly concentrated solution. The sol-gel change was confirmed by rheometric measurements.

---

In Chapter 3, the novel design and synthesis of photo-induced reactive polymers are described in detail. For the photo reactive polymer, a phenylazide-conjugated monomer was synthesized and then copolymerized with EO to obtain the PEG-based phenylazide-photo reactive polymer. The prepared photo reactive polymer sensitively responded and reacted by the UV irradiation due to phenylazide compounds introduced in the side chain of polymer. Regardless of the type of substrates, the polymer was well-coated on surfaces including glass, polystyrene, and polycarbonate. All the prepared coated pattern surface showed good suppression of protein adsorption and cell adhesion. The prepared PEG-based phenylazide photo reactive polymer showed better solubility and improvement in hydrophilicity compared to that exhibited by conventional phenylazide photo reactive polymer because of existence of PEG as main backbone chain.

Based on newly proposed polymeric materials, this dissertation concludes with the future applicable uses and providing a platform for fabrication of new materials based on stimuli-induced reactive polymers. This study takes the advantages of thermal and photo-induced systems which can be used for regulating the reactivity or interaction. Each system was demonstrated into the thermally responsive reactive nanoparticle for developing in situ hydrogel and the photo-induced reactive polymer for suppression of non-specific interactions. A simple thermal responsive system controlling the reactivity using a little tiny change in environmental condition provides a new aspect of hetero-armed polymeric micellar structure to control the chemical coupling reaction or in-situ gelation. Newly designed PEG-based phenylazide photo reactive polymer showed its simple ability of photo immobilization due to presence of the phenylazide groups. Even though large amount of the phenylazide group had been introduced into the side chain, the prepared photo reactive polymer showed good solubility in aqueous solution and protic solvents compared to the conventional phenylazide photo reactive polymers, which is attributed to the introduction of PEG as main backbone chain.

---

Therefore, it provides a better understanding for polymeric structures for improvements of hydrophilicity which will be advantageous to photo chemistry application including surface coating, immobilization, functionalization, and modification.

## **4.2 Future perspective**

This study shows that the stimuli-induced reactive polymers can be used for controlling the reactivities with the external molecules. Despite the advantages of the newly polymeric systems, each system still has some remaining discussing points and several additional studies.

For example, for the hetero-armed TR reactive particle, there are several factors that significantly affect the sol-gel behavior including structure of polymeric materials, length of TR polymeric chain, concentration of particle solution, pH of the system, and ratio of the TR polymer to reactive polymer in nanoparticles. The results of the study indicated that the ratio and the concentration of mixtures were key factors to optimize for controllable gelation by the temperature signal. In addition, the external particle shape (amine particle in this study) was also crucial to control the reaction, from the results of the experiments with a linear-type polymer (Polyallylamine). Therefore, the exclusive volume effect of the polymer turned out to greatly affect the controllability of the reaction between the succinimide and amine according to the morphological change of TR chain on micelles. Even though the thermally responsive reactive nanoparticles accelerated the reaction by temperature stimuli, more precise conditions need to be investigated to accurately control the reactivity of the particles. The system should be further studied by using different ratios, compositions, concentrations, chain lengths of TR polymers (200 units were used in this study) and even the shape/structure of the external reactive molecules.

---

The hetero-TR reactive particle has great potential to be applied as a stable and irreversible in situ hydrogel developed by chemically crosslinked structure. In situ gelation can be simply induced by body temperature after the gel precursor is injected in body. The proposed TR reactive particle possess the succinimide group as reactive sites and it reacts with the primary amine on counter particle to develop crosslinking networks. Proteins have many amino groups which can help the crosslinking formation or acceleration of reaction in body after injection. However, to apply the hetero-armed TR reactive polymer as injectable polymer for in situ hydrogel working in body system, cell cytotoxicity and biocompatibility experiments should be performed in advance to investigate effects of protein and other biomolecules on the gelation.

For the photo reactive polymer, the novel design of main backbone structure using PEG chains resulted in significant improvement in its solubility and hydrophilicity compared than that of the conventional phenylazide photo reactive polymer. However, when the azide components reach 15% of the total components, this polymer did not dissolve in protic solvents owing to strong hydrophobicity from structure of the phenylazide. Introducing another long PEG chain into side chain may be a possible solution for improving the overall solubility. Branched type of phenylazide PEG polymer is expected to have better antifouling property because branched PEG chain will be flexible so that it can show more resistance to fouling molecules. Also, it will show high solubility in water and organic solvent owing to PEG chains existing as main backbone chain and as brushes in the side chain of the polymer. In addition, the photoreactive polymers has more than two photo reactive groups in one chain in current structure. This may affect to thickness of the polymer coated surface because the crosslinking reaction may occur not only between the polymer chain and the surface but also between the polymeric chains themselves. Therefore, free end of PEG is favorable for preparing antifouling surface. The phenylazide-PEG photo reactive polymer has shown its potential uses for antifouling surface, and it will be highly useful for preparing polymer coated surface by utilizing photo reaction.

---

The approaches presented in this dissertation provides a better understanding on new functionalized polymeric materials with combination of stimuli-induced reactive system and will be very useful for developing new research branch with a wide range of practical applications. This study can be extended to other research fields including controlled drug delivery, embolization agents, biosensor, actuator, photo functionalized surface, microarray chips and diagnostic materials.

---

## List of publications

**So Jung Park**, Jun Akimoto, Naoki Sakakibara, Eiry Kobatake, and Yoshihiro Ito, Thermally Induced Switch of Coupling Reaction Using the Morphological Change of a Thermal responsive Polymer on a Reactive Heteroarmed Nanoparticle, *ACS Appl. Mater. Interfaces*. **2020**, 12, 43, 49165–49173

Jun Akimoto, **So Jung Park**, Sei Obuse, Masuki Kawamoto, Mika Tamura, Avanashiappan Nandakumar, Eiry Kobatake, and Yoshihiro Ito, Synthesis of Photoreactive Poly(ethylene oxide)s for Surface Modification, *ACS Appl. Bio Mater.* **2020**, 3, 9, 5941–5947



---

## Acknowledgements

I would like to express my gratitude to all those who supported me throughout my PhD program.

Foremost, I would like to express deep appreciation to my two advisors Dr. Yoshihiro Ito, from Nano medical engineering laboratory (NMEL) in RIKEN and Prof. Eiry Kobatake, from Tokyo Institute of Technology. I would like to thank to Prof. Eiry Kobatake for giving me an opportunity to study a graduate program in Tokyo Institute of Technology. Following his valuable guidance and insightful feedbacks, I would successfully finish my PhD program. Comprehensive advice, comments and supervision and generous supports helped me a lot until this works came to existence. Also, my sincere gratitude goes to supervisor in RIKEN, Dr. Yoshihiro Ito who guided me with continuous support on my research with enthusiasm, immense knowledge and sometimes with patience. His guidance helped me a lot in all the time of research and writing of this thesis. He was a great advisor as well as mentor who gave me motivation. It was a great honor to have opportunity to pursue the Junior Research Associate (JRA) program in NMEL during my PhD.

Besides, I specially thanks to Dr. Jun Akimoto who expertly guided me during my PhD course. He has devoted to supervising my research, from how to design the research topic, how to conduct experiments and analyze data results and how to write research articles. He provided me invaluable comments and the right direction when I encounter with difficulties during proceeding these projects and consequently leading me to successful completion my PhD program. His insightful feedback pushed me to sharpen my thoughts and improved in my research skills to become a higher level. It was my pleasure to work in his team for three years learning many things from work with him.

I am also grateful to my lab members in NMEL as well as other lab members in RIKEN for having active and aggressive discussions, the sleepless nights we were working together and for all the fun we have had in the last three years. Especially, to our chemistry team in NMEL whom never stopped challenging me and helping me develop the ideas through deep discussions in our group meeting every Friday. Also I thank to my colleague who previously worked in this lab for supporting me with research and experimental skills.

I am also deeply thankful to my thesis committee from the faculty of Department of Life Science and Technology: Prof. Kazushi Kinbara, Prof. Atsushi Maruyama, Prof. Hiroshi Tsutsumi, Prof. Masayasu Mie for their insightful comments and sharp questions. Their guidance greatly helped me to completing this PhD program.

Last but not the least, I thank to my family for supporting me spiritually and financially throughout my life and my dear friends in Korea who supported me a lot, especially to Dr. Juhyang Park who kept me going on research abroad.

This work was performed at NMEL Group in RIKEN and the Graduate School of Life Science and Technology of Tokyo Institute of Technology. I really appreciate for the financial support from RIKEN's junior research assistantship.